I. PRELIMINARY STUDIES IN THE APPLICATION OF A BALLISTIC PISTON TO INVESTIGATION OF CHEMICAL REACTION IN THE NITROGEN - OXYGEN SYSTEM

II. ISOBARIC HEAT CAPACITIES AT BUBBLE POINT OF PSEUDOCUMENE AND OF n-HEPTANE

Thesis by

Paul Francis Helfrey

In Partial Fulfillment of the Requirements

For the Degree of

Doctor of Philosophy

California Institute of Technology

Pasadena, California

1957

ACKNOWLEDGMENTS

It is a pleasure to acknowledge the guidance and friendly encouragement I have received from Professor William H. Corcoran, who directed the work described in the first part of this thesis. The ballistic piston project has been under the general direction of Professor Bruce H. Sage, and much is owed to his capable efforts. Professor Sage also directed the work described in Part II of this thesis. Dr. W. G. Schlinger shared responsibility for supervising the latter studies, and his helpful suggestions are greatly appreciated.

P. A. Longwell and N. P. Wilburn have also worked on the ballistic piston project in the course of their graduate studies. Their cooperation in the experimental work is gratefully acknowledged. They and many other students, especially C. J. Pings, Jr., and G. N. Richter, contributed valuable discussions. Professor William N. Lacey kindly reviewed the thesis, and made helpful comments.

I have received invaluable financial support in the form of California Research Corporation and Union Carbide and Carbon Fellowships, and Institute Scholarships.

Alethea Miller typed the manuscript, and Virginia Berry prepared inked drawings of most of the figures.

Finally I should like to thank my parents. Their encouragement and sacrifice have made my education possible.

ABSTRACT

I. An apparatus, in which gaseous samples may be subjected to rapid compression, is described. This "ballistic piston" offers a mechanically simple method of producing for a short time a very high temperature and pressure in a sample under study.

The results of preliminary studies on the nitrogen-oxygen system are presented. Appreciable yields of nitrogen dioxide, up to 3.3 mol per cent of the gas remaining after compression, were obtained. The conditions investigated involved calculated maximum temperatures as high as 13,000° R, and maximum pressures up to 30,000 psi. The maximum temperature and pressure achieved in each run were calculated on the basis of fairly simple assumptions. An increase in the yield of NO_2 with increasing maximum temperature and with increasing maximum pressure was noted.

Coefficients for a second order rate equation were tested by comparing predicted yields based on the coefficients with the observed yields. In the temperature range above 3500° R, rate coefficients not more than one-tenth as great as those obtained by extrapolation of existing data are indicated. The rate coefficients obtained are subject to much uncertainty because of the many simplifying assumptions made in treating the data. The results are discussed in the light of the limitations imposed by the assumptions.

II. As part of a long-term project for measurement of the heat capacities of hydrocarbons, the isobaric heat capacity at bubble point of 1,2,4,-trimethylbenzene (pseudocumene) was determined in the range 70-210° R. Using the same equipment, the same property was determined for n-heptane, a widely accepted standard for calorimetric work. The results are reported in a manuscript which includes results obtained by a later investigator on the project for 1,3,5-trimethylbenzene.

TABLE OF CONTENTS

PART I.

PRELIMINARY STUDIES IN THE APPLICATION OF A BALLISTIC PISTON TO INVESTIGATION OF CHEMICAL REACTION IN THE NITROGEN - OXYGEN SYSTEM

NOMENCLATURE

A cross sectional area of cylinder.

A pre-exponential factor in Arrhenius equation.

C_v isochoric heat capacity.

c a constant.

E internal energy.

E_a activation energy in Arrhenius equation.

F frictional force acting on piston.

f fugacity.

$f(G)$ a function of G.

$f(V^*)$ shorthand notation defined by equation 71.

G any property, specific

$\underline{G}$ any property, total.

$\tilde{G}$ any property, molal.

$\overline{G}$ any property, partial.

g acceleration due to gravity.

g_o standard value of g.

H enthalpy, $E + PV$.

i running index.

K equilibrium constant for chemical reaction.

k exponent in polytropic path for air.

k specific rate coefficient for chemical reaction.

k_d rate coefficient for decomposition.

k_f rate coefficient for formation.

k_{cc} rate coefficient for chemical reaction, with rates measured in terms of concentration, and with concentration as driving force.

k_{pp} rate coefficient for chemical reaction, with rates measured in terms of partial pressure, and with partial pressure as driving force.

l distance traversed by piston.

ln natural logarithm.

log logarithm to the base ten.

m mass.

m_p mass of piston.

N number of mols in system considered.

n number of components in system.

$\tilde{n}_i$ mol fraction of component i.

P pressure.

P_o initial pressure.

P* ratio of pressure to initial pressure.

p_i partial pressure of component i.

Q heat.

q heat, infinitesimal.

R molal gas constant.

r rate of chemical reaction.

r* rate of change of mol fraction of NO.

S entropy.

T absolute temperature.

T_o initial value of absolute temperature.

T_{o_s} standard initial temperature used in tabulation of functions.

T* ratio of temperature to initial temperature.

t temperature.

u velocity of piston, positive downwards.

u^* defined notation for $-\frac{dV^*}{d\theta}$.

V volume, specific.

V_o initial volume.

V^* ratio of volume to initial volume.

W work.

w work, infinitesimal.

w_p weight of piston.

x distance along path of piston, positive downwards.

Z compressibility factor, $P\tilde{V}/RT$.

β initial ratio of volume of air chamber to volume of sample chamber.

Δ increment.

Δ error in prediction; predicted final mol fraction NO_2 minus observed.

θ time.

ν_i activity coefficient, $\frac{f_i}{\pi_i P}$.

$\sum$ summation operator.

ϕ function defined by equation 40.

ψ function defined by equation 62.

f line integral, denotes integration along particular path.

Superscripts

o refers to component in the pure state.

$\sim$ denotes molal value of property.

$-$ denotes partial value of property.

Subscripts

A	refers to driving air.
a	refers to activities.
B	refers to sample.
d	refers to decomposition in chemical reaction.
f	refers to formation in chemical reaction.
i	refers to component i.
$\not{\phi}$	refers to substance in reference state.
o	refers to initial conditions.
p	refers to piston.
p	refers to pressure.
$\_$	denotes total value of property.

CONSTANTS

Molal gas constant, R.	1.98719	cal/(g mol ^{o}K)
	82.0567	(cm^3 atm)/(g mol ^{o}K)
	0.0820544	(liter atm)/(g mol ^{o}K)
	10.73147	(ft^3 psia)/(lb mol ^{o}R)
Standard gravitational acceleration, g_o.	980.665	cm/sec^2, be definition.
	32.1740	ft/sec^2, approximately.
Local gravitational acceleration, g.	979.572	cm/sec^2.
	32.1381	ft/sec^2.
Absolute zero of temperature	0^{o}	Kelvin
	-273.16^{o}	Centigrade
	0^{o}	Rankine
	-459.69^{o}	Fahrenheit

Atomic Weights		
Helium	4.003	
Nitrogen	14.008	
Oxygen	16	(exactly)

UNITS

English units were generally employed in recording data, such as pressures, temperatures, apparatus dimensions, etc. In using information from references, such as heat capacities, chemical rate coefficients, etc., the units given in the references have been freely employed. In substituting numerical values into equations, appropriate conversion factors were used to ensure consistency of units.

An extensive and authoritative list of constants and conversion factors is given by F. D. Rossini et al., in Selected Values of Physical and Thermodynamic Properties of Hydrocarbons and Related Compounds, API Research Project 44, Carnegie Press, Carnegie Inst. of Tech., Pittsburgh, Penn. (1953).

I. INTRODUCTION

In recent years there has been an increasing general interest in the behavior of systems at elevated temperature and pressure. Among the particular problems of great theoretical and practical importance is the fixation of nitrogen. This thesis reports exploratory studies in an investigation of the kinetics of the oxidation of nitrogen at high temperature and pressure.

Laboratory investigations of the physical and chemical properties of matter are able to cover only a limited range of conditions. The properties of materials of construction determine, in large measure, the maximum temperature and pressure which can be achieved in a static apparatus. If more extreme conditions are to be studied, means must be found for subjecting samples to conditions under which they are not at all in equilibrium with the containing vessel.

One possible procedure, useful for the study of gaseous systems, is to subject samples to compression which is so rapid as to be essentially adiabatic. In recent years, considerable effort has been devoted to the use of such processes, and it has been shown that very high temperature and very rapid changes in temperature may be obtained with fairly simple equipment.

The sample under investigation may be compressed either by the expansion of another gas, following rupture of a separating diaphragm, or by the movement of a piston.

In apparatus of the former type, rupture of the diaphragm results in the formation of a shock wave, which travels through the sample. With suitable initial conditions, a large temperature gradient will exist in the shock front, and rapid velocities of shock wave propagation may be attained. Among the recent applications of such "shock tubes" has been the study of very fast chemical reactions at moderate temperature, by Davidson and co-workers (1,2,3). A modified shock tube has been used by Glick, Squire, and Hertzberg (4) to investigate the rate of formation of NO at temperatures up to 3000° K.

The rapid compression of samples by movement of a free piston has been applied both to the study of PVT properties of gases and to the investigation of chemical reactions. Longwell (5) gives several references to such applications.

Ryabinin, Markevich, and Tamm (6) reported yields of as much as 1.6 per cent nitric oxide resulting from adiabatic compression of mixtures of nitrogen, oxygen, and argon. Maximum pressures and compositions of products were reported, but no attempt was made to determine reaction rates. The addition of the inert gas, argon, which has a relatively low molal heat capacity, permitted the attainment, for a given compression ratio, of much higher temperature than would have been possible with mixtures containing only nitrogen and oxygen.

The Chemical Engineering Laboratory at the California

Institute of Technology has undertaken an extensive program of research using an apparatus in which gaseous samples are rapidly compressed by the movement of a free piston. This "ballistic piston" equipment has been described by Longwell and Sage (7).

The first work done with the ballistic piston apparatus consisted of exploratory studies on several gaseous systems. Results of the earliest work on hydrocarbon systems have been described by Longwell (5), who was able to correlate the distribution of reaction products with the calculated reaction conditions, and in some cases to obtain effective rate coefficients for chemical reaction.

A study of the reaction between nitrogen and oxygen at high temperature and pressure was also undertaken, using the ballistic piston. This thesis is concerned with the exploratory work on this problem.

The preliminary experiments were intended to investigate the range of conditions which could safely be produced in the apparatus, to determine the range of conditions for which observable yields of nitrogen oxide could be obtained, and to attempt to determine the effects of various factors, such as maximum temperature and pressure, cooling rate, etc. on the yield.

It was hoped that even these early experiments might furnish some information on the rates of the chemical reactions involved. Much of this thesis is devoted to the pre-

diction of yields on the basis of various assumed chemical rate coefficients. The derivation of differential equations describing the behavior of the sample, and the procedures used in the numerical solution of the equations, are described in some detail.

At the time of the experimental work covered in this thesis, the apparatus had not been instrumented, and it was necessary to calculate pressure, temperature, and other variables of interest on the basis of assumed behavior. In order to concentrate effort on determining the effect of the assumed rate constant on the predicted yield, the simplest possible assumptions were made regarding the behavior of the apparatus and of the samples. The results obtained are therefore subject to considerable uncertainty, and should be regarded as provisional, until clarified by the results of future work.

Chemical Reaction

Nitrogen and oxygen combine reversibly to form nitric oxide, the overall reaction being

$$N_2 + O_2 \rightleftharpoons 2NO \qquad (1)$$

Because of the enormous requirements of modern industry and agriculture for fixed nitrogen, the oxidation reaction is of great practical as well as theoretical importance. In the early part of this century, reaction 1, occurring

at the high temperatures of the electric arc, was an important source of fixed nitrogen. This process has become relatively unimportant since the development of the synthetic ammonia process, which is much more economical (8).

The application of regenerative heat exchangers to the fixation of nitrogen has revived interest in the direct oxidation as an economical source of NO_2 and nitric acid (9,10,11). The reactions of NO are also of great importance in the field of propellant chemistry.

The equilibrium of reaction 1 and the rate of decomposition of NO were studied as early as 1906 by Nernst (12) and Jellinek (13). Values of the equilibrium constant and heat of formation for the ideal gas state, at temperatures up to 5000° K, are contained in the recent excellent tabulation by Rossini et al. (14). The equilibrium concentration of NO is very small at ordinary temperatures, but becomes appreciable at high temperatures. Despite its thermodynamic instability, NO decomposes extremely slowly at room temperature, and samples may be stored for years with no apparent decomposition.

Jellinek studied the decomposition of NO in the range 962 - 2023° K, and concluded that the reaction was second order in NO, although complicated by possible catalytic effects. He proposed that an empirical equation of the form $\log k = AT + B$ described the observed rate constants more satisfactorily than an equation of the form $\log k = -A/T + B$.

Wise and Frech (15) studied the decomposition of NO in a quartz reactor, in the range 870 - 1275° K. The decomposition was complicated by effects evidently catalytic in nature, especially at the lower temperatures. At higher temperature, the reaction appeared to be second order. For the homogeneous reaction, they proposed an Arrhenius equation for the temperature dependence of the rate constant; it was

$$K_2 = 3.1 \times 10^{15} e^{-\frac{82,000 \frac{cal}{g\,mol}}{RT}} \quad \frac{cc.}{g\,mol.\,sec.} \quad . \qquad (2)$$

Farrington Daniels (16,10) has discussed the conclusions drawn from extensive research on oxides of nitrogen. Decomposition of NO was studied using a special molybdenum electric furnace. At temperatures higher than 1400° C, the reaction appeared clearly second order in NO, although catalysis was found to be significant at lower temperature, and below 1000° C the reaction was of apparent zero order. Daniels proposed the equation

$$K = 1.64 \times 10^{11} e^{-\frac{69,500 \frac{cal}{g\,mol}}{RT}} \quad \frac{liter}{g\,mol\,sec} \qquad (3)$$

to describe the rate constant in the range 1450 - 1850° C. At the time of the work reported in this thesis, details of his experiments were not available. Another form of rate constant formula was later suggested by Daniels (17). The rate constant was described by

$$K = 1 \times 10^{9} \, e^{-\frac{69{,}500 \ \frac{cal}{g\,mol}}{RT}} \quad atm^{-1} \, sec^{-1} , \qquad (4)$$

also in the range 1450-1850° C.

Results obtained in pilot plant studies for the "Wisconsin Process" were quoted by Ermenc (11). Second order rate coefficients were determined for both the formation and decomposition of NO. Ermenc included graphs of log k vs. T for the range 3200-4400° F.

Glick, Squire, and Hertzberg (4) reported preliminary results from studies of the formation of NO in a shock tube. On the basis of assumed second order reactions, they determined rate constants in the range 2000-2500° K, and evaluated constants for an Arrhenius equation by least squares fit. The resulting equation was, for the decomposition rate coefficient,

$$K = 3.4 \times 10^{9} \, e^{\frac{40{,}000 \ \frac{cal}{g\,mol}}{RT}} \quad \frac{liter}{g\,mol\ sec} , \qquad (5)$$

although considerable scatter of the experimental points was noted.

Several observers have reported data which are not consistent with the assumption of a simple bimolecular mechanism. Zeldovich (18) studied the formation of NO in explosions with hydrogen and hydrocarbons as fuels. Analysis of the

data presents many difficulties, but Zeldovich was able to correlate the yields of NO with the amount of oxygen theoretically remaining after combustion of the fuel. He developed an expression for the temperature dependence of the second order decomposition rate coefficient,

$$k = 3 \times 10^{8} \; e^{-\frac{86{,}000 \; \frac{cal}{g\,mol}}{RT}} \qquad mm^{-1} \, sec^{-1}, \tag{6}$$

in which concentrations are expressed in millimeters of mercury at 17° C.

Further studies led Zeldovich to conclude that the bimolecular mechanism cannot be correct, because of the large collision cross sections required, and because of an increase in the apparent second order rate constant at low oxygen concentration. He proposed a chain mechanism involving O and N and discussed the corresponding rate equations, leading to the overall rate expression

$$\frac{d(NO)}{d\theta} = \frac{5 \times 10^{11} e^{-\frac{86{,}000 \; \frac{cal}{g\,mol}}{RT}}}{(O_2)^{\frac{1}{2}}} \left\{ (O_2)(N_2) \times e^{\frac{43{,}000 \; \frac{cal}{g\,mol}}{RT}} - (NO)^2 \right\}, \tag{7}$$

which was regarded as a satisfactory description of the observed results.

Vetter (19) studied the decomposition of NO in a flow reactor, at temperatures up to 1920° K. He calculated second order rate coefficients on the assumption of complete mixing

in the reactor. The apparent rate coefficients were larger for the runs in which oxygen had been added. The addition of nitrogen did not produce a similar increase, so Vetter concluded that it could not be explained by the effects of dilution. The calculated second order rate coefficients, at a given temperature, varied by as much as a factor of three, depending on the oxygen content of the system.

To explain the "oxygen effect," Vetter proposed a mechanism involving the reactions

$$NO + O \rightarrow N + O_2 \quad , \tag{8}$$

$$NO + N \rightarrow O + N_2 \quad , \tag{9}$$

$$NO + O \rightarrow NO_2 \quad , \tag{10}$$

$$O + NO_2 \rightarrow NO + O_2 \quad , \tag{11}$$

$$N + NO_2 \rightarrow 2NO \quad , \tag{12}$$

and their reverse steps. With suitable assumptions regarding the atomic species, this scheme, for the range of conditions covered, leads to a rate expression having the form

$$-\frac{d(NO)}{d\theta} = \frac{a(NO)^2(O_2)^{\frac{1}{2}} + c(NO)^3}{b(O_2) + (NO)} \quad . \tag{13}$$

Vetter determined values of a, b, and c for various temperatures, and in further discussion identified them with groupings of rate constants for the individual reactions. He considered the possibility that the simple bimolecular reaction $2NO \rightarrow N_2 + O_2$ also occurred, but was unable to reach any conclusions regarding its relative contribution.

Wise and Frech (20) also reported an increase in the rate of decomposition of NO in the presence of oxygen. To explain their observations, as well as those of Vetter, they proposed a chain mechanism initiated by

$$2NO \rightarrow N_2O + O \quad , \tag{14}$$

propagated by

$$O + NO \rightarrow N + O_2 \quad , \tag{15}$$

and

$$N + NO \rightarrow O + N_2 \quad , \tag{16}$$

and terminated by

$$O + O + M \rightarrow O_2 + M \quad . \tag{17}$$

On the basis of this mechanism, Wise and Frech deduced the rate equation

$$-\frac{d(NO)}{d\theta} = k_a(NO) + k_b\frac{(NO)(O)^{\frac{1}{2}}}{(NO)+(O_2)} \quad , \qquad (18)$$

and determined values of k_a and k_b from their data and those of Vetter.

The results of Wise and Frech (20) were criticized by Kaufman and Kelso (21), who were unable to duplicate the reported experimental results, and who also raised objections to the proposed mechanism. The situation is still the subject of controversy (22).

Kaufman and Kelso (23) discussed much of the available literature and reported their own results in the range 1123-1533° K. The decomposition of NO was studied in a quartz reactor. It was found that second order rate coefficients described the observed results well. A small decrease in apparent rate coefficient with increasing decomposition was interpreted as due to catalytic effects, but was cited as evidence against the oxygen effect reported by Vetter and by Wise and Frech. At temperatures above 1400° K, the second order rate coefficients were found to be independent of surface to volume ratio. Values determined from runs in which nitrogen or helium had been added in as much as 4:1 ratio to NO were substantially the same as those determined with pure NO.

The temperature dependence of the second order rate coefficient was given, in the range 1370-1535° K, as

$$K = 2.6 \times 10^{12}\, e^{-\frac{63.8\ \frac{Kcal}{g\ mol}}{RT}}\ \frac{cc.}{g.mol.\ sec.} \quad . \qquad (19)$$

Kaufman and Kelso also carried out experiments with added oxygen. No effect was observed at 1423° K, but a small increase in the apparent rate coefficient was noted at 1473° K. These authors suggested that much of the existing data could be represented by a rate expression of the form

$$-\frac{d(NO)}{d\theta} = k_a(NO)^2 + k_b(NO)(O_2)^{\frac{1}{2}} \quad . \qquad (20)$$

They used equation 19 as the representation of k_a and determined values of k_b from Vetter's data.

Equation 20 suggests that reaction between NO and atomic oxygen may be significant in the decomposition of NO. Kaufman and Kelso discussed several possible mechanisms for the formation of atomic oxygen.

The decomposition of NO is still the subject of active investigation by several of the workers cited (4,17,23). There is great need for further work, particularly to obtain data which are clearly applicable to the homogeneous reaction and not complicated by uncorrected catalytic effects. Effort is needed to establish firmly whether the "oxygen effect" reported by Vetter and by Wise and Frech is an essential feature of the homogeneous reaction, or whether it may be explained by errors in chemical analysis, catalytic reactions, or errors in treatment of data.

Summary of rate coefficients

Effective rate coefficients may be defined by the equation

$$-\frac{d(NO)}{d\theta} = k_{cc_d}(NO)^2 \quad , \tag{21}$$

which applies when the formation reaction is negligible.

As noted in the foregoing discussion, several authors have developed Arrhenius equations for k_{cc_d} to describe the temperature dependence of their rate coefficients. Graphs of these equations, over their respective temperature ranges, are shown in Figure 1. Selected experimental points from the results of Jellinek (13) and of Vetter (19) are included. Vetter's points from the experiments with high O_2/NO ratios are somewhat higher.

The mechanisms of the reactions among NO, O_2 and N_2 are by no means clearly established, and none of the existing work covers a range of conditions as wide as that encountered in the ballistic piston program. Hence it was felt that the first calculations should be based on the simplest mechanism for reaction 1, corresponding to bimolecular reaction in both directions. The predicted yields discussed in this thesis were all calculated on this basis. The rate coefficient formula of Daniels, equation 4, was chosen as the point of departure.

II. APPARATUS

The ballistic piston apparatus employed in these preliminary studies has been described in detail by Longwell and Sage (7). Because the description had not been published at the time of the preparation of this thesis, a description of the important features is given here.

Essential features.

The apparatus is shown schematically in Figure 2, and its general arrangement in the laboratory is indicated in Figure 3. It consisted essentially of a long, hollow, heavy-walled cylinder A, as shown in Figure 2, within which was the piston B. The piston divided the space within the cylinder into two sections, a sample chamber G and an air chamber H. Air was introduced into the chamber H through the valve C. The pressure in H was determined by means of the calibrated Bourdon gage E'. The samples were introduced into the chamber G through either or both of the valves K and U, and the pressure in the sample was measured by means of a mercury-in-glass manometer.

The annular space between the central section of the piston and the inner wall of the cylinder was connected through the valve L to a mechanical vacuum pump F. This feature of the equipment helped to prevent contamination of the samples by leakage of air from H past the O-ring seals J and J'.

In preparing for a run, a holding pin retained the piston in the position shown in Figure 2. When the initial conditions had been satisfactorily established, the valves C, L, K, and U were closed and the holding pin was sheared by rotation of the handle M. The initial air pressure in H was of the order of a thousand pounds per square inch, whereas the pressure in the sample chamber G was of the order of a hundred millimeters of mercury. Upon the shearing of the retaining pin, the piston accelerated rapidly downward, compressing the gas in G. Downward movement of the piston continued until the clearance between the lower face of the piston and the bottom of the cylinder was from 0.1 to 0.5 inch. Since the initial length of the sample space G was nearly 100 inches, the volumetric compression ratio was large, and the pressure in the sample at maximum compression was very high. This high pressure caused the piston to accelerate rapidly upward. After some oscillation the piston came to rest at a position such that the pressures in G and H were nearly the same. Samples of the gas in G were then withdrawn through the valve U.

Details of Construction.

The cylinder was constructed from two pieces of SAE 1040 steel tubing having a wall thickness of 1.5 inches. After the interior surface was machined, the cylinder was 3.000 inches in inside diameter with a variation of less than 0.001 inch. The two sections were joined as indicated in

Figure 4. Neoprene O-rings X and X' were used to seal the exterior of the cylindrical sections of the cylinder. At V and V', 1/4 inch buttress threads engaged the heavy collar. The short cylindrical sections W and W' served to hold the axes of the two sections in alignment. The bore of the cylindrical sections was enlarged approximately 0.001 inch over a region of about 0.2 inch from each end in order to avoid any possibility of impingement of one edge of the piston on the lip of the section as the piston entered the section.

Figure 5 shows details of the upper closure, which included the release mechanism previously mentioned. The jackscrew I, which was rotated by means of the handle M, pressed against the rod T which was attached to the upper end of the piston B. The upper end of the rod T was held in the sleeve P by means of the brass pin O. The pin O passed through hardened steel sleeves, provided in the steel sleeve P to permit shearing of the brass pin without deforming the soft steel assembly. Considerable downward force was exerted on the piston by the high pressure air in the space H, so that a shearing stress existed in the pin O. Appropriate rotation of the handle M caused the screw I to exert a downward force on the rod T and thus increase the shear in the pin O. In making a run, the handle M was turned until the pin O failed and the piston was free to move the cylinder. No difficulty was experienced with manual operation of this release mechanism with pres-

sures in the space H from 200 to 1500 pounds per square inch, and with brass pins of 3/8 inch diameter.

Figure 6 shows details of the assembly at the lower end of the cylinder. The piston B is shown entering the lowest section of the cylinder, which consisted of a cup in the upper end of the bottom closure Q. The closure Q was held in the sleeve R by the unsupported area seal S. A similar seal was provided at the juncture of the sleeve R with the lower of the two long sections of the cylinder.

Pressure in the sample was relatively high only near the end of the compression stroke; during the period of high pressure the sample was thus confined entirely within the cup in the bottom closure Q. Use of the cup thus minimized the difficulty of sealing the apparatus against leakage of sample. Also, erosion of the cylinder due to the action of hot, high pressure sample gases was localized in the closure Q, which is more easily repaired or replaced than the long sections of the cylinder. No apparent damage to the long sections had occurred after nearly a hundred runs, in which a variety of systems and a wide range of conditions were studied.

A valve U was provided in the lower part of the closure to permit withdrawal of a "product" sample after a compression cycle. This valve also was used to aid in introducing the sample before a run.

Measurements.

The pressure in the air chamber H of Figure 2 was measured by means of a calibrated Bourdon tube gauge. Uncertainty in the measurement of this pressure was of the order of one per cent or less. Temperatures of the air in the chamber H and of the sample in the chamber G were determined by means of mercury-in-glass thermometers with an uncertainty of 0.5° F. The bulbs of the thermometers were placed in wells located respectively in the threaded closure ring of the upper closure, shown in Figure 5, and in the threaded closure ring of the upper unsupported area seal in the sleeve R, shown in Figure 6.

The closest approach of the piston to the bottom of the cylinder was measured by means of lead crusher gauges. These consisted of lead shot for approaches closer than 0.075 inch, while taller gauges of roughly conical form were used when it was estimated that the piston would stop at a greater distance from the bottom. Following a run, the gauges were recovered and the appropriate dimension measured to within 0.0001 inch by means of a micrometer. When two gauges were used in the same run (usually they differed somewhat in initial height), they agreed in final height within the flatness tolerances of the piston head and bottom closure. The closest approach of the piston to the bottom of the closure is therefore believed known within 0.001 inch.

Auxiliary apparatus - Sample transfer system.

The system used to evacuate the sample chamber and to introduce sample is shown schematically in Figure 7. Pressures were measured by means of a mercury-in-glass manometer. The elevation of the mercury in the arms of the manometer was measured by means of a meter stick between the arms or, if greater accuracy was desired, by means of a cathetometer. The uncertainty in the measurement of the height of a mercury column by the latter means was 0.010 inch. A mercury diffusion pump discharging into a mechanical forepump was provided in order to evacuate parts of the system as desired. Samples were charged into the sample chamber of the apparatus by admitting in turn supplies of the desired components through the fitting provided in the valve block V_1. At the time of the experiments described in this thesis, the temporary system indicated in Figure 7 was connected to the "A" fitting of the valve block V_1. A permanent and more versatile sample transfer system was later constructed (7). The trap T_2 was immersed in a dry-ice-trichloroethylene bath to condense any water or other relatively non-volatile impurities present in the gas supplies. The trap T_1 was immersed in liquid nitrogen to prevent contamination of the vacuum pumps by corrosive materials when such materials were being handled.

By appropriate manipulation of stopcocks, one leg of the manometer could be connected to the sample chamber of the ballistic piston apparatus, and the other opened either

to the atmosphere or to the vacuum pumps. A McLeod gauge was provided to measure pressures in the very low range, and to check the attainment of a satisfactory "reference" vacuum.

Figure 8 is a photograph of the lower portion of the ballistic piston. The vacuum system and sample transfer system were located on the platform level, just below the mezzanine floor, and to the left of the row of pressure gauges which appears in the upper left corner of Figure 8. A platform hoist used in installing and removing the bottom closure appears in the lower center of Figure 8. The platform of the hoist is shown just below the lower closure. The cable leading from the bottom of the apparatus contains connections to electrical contacts in the bottom closure. The closure used in the experiments treated in this thesis was that indicated in Figure 6, and was not equipped with these contacts.

III. MATERIALS AND PROCEDURE

Substances used as sample components in this series of tests included nitrogen, oxygen, nitric oxide, and helium. The nitrogen was obtained from the Linde Air Products Company, and was reported to be 99.99 per cent pure. Mass spectrographic analysis of a sample indicated traces of oxygen and argon as impurities. The oxygen was also obtained from Linde Air Products. Mass spectrographic analysis of a sample indicated a trace of argon as impurity. The helium was obtained from the Air Reduction Pacific Company, and was reported to be 99.97 per cent pure. Mass spectrographic analysis indicated a trace of nitrogen. The nitric oxide was obtained from the Matheson Company, Inc., and was reported to be at least 98 per cent pure. No analysis of the nitric oxide was made. The impurities consisted of nitrogen and perhaps other oxides of nitrogen. The presence of as much as two per cent of such impurities would have little effect on the temperatures, pressures, and compositions calculated later.

As the components were introduced into the apparatus, they were passed at atmospheric pressure through a glass trap immersed in a dry-ice-trichloroethylene mixture. This procedure was intended to remove any moisture or other relatively non-volatile impurities. In these early runs, no further attempt was made to purify the gases introduced.

Experimental Procedure

Although the preparation of the equipment for a run was somewhat time-consuming, the procedure was rather simple, both in principle and operation.

The apparatus was cleaned by pulling swabs through the barrel, using solvents if necessary. The upper and lower closures were removed and cleaned separately. The barrel was coated with a lubricant by pulling a swab treated with the lubricant up and down through the barrel. "Molylube" (MoS_2) was used in most of the runs treated in this thesis. Graphite was used in a few runs in an attempt to determine the effect of the lubricant on the final products.

One or two lead crusher gauges of suitable height were placed in the bottom closure which was then installed. The piston was attached to the release mechanism by a shear pin and the assembly consisting of the piston and upper closure was installed.

The sample chamber G, shown in Figure 2, was then evacuated by opening the valves K and U to the vacuum pumps. The annular space around the central section of the piston was evacuated by the pump F.

The evacuation of the chamber was necessary, first, to remove air from the chamber so that a sample of the desired composition might be synthesized, and second, to check for leaks into the sample chamber. The lines connecting the vacuum pumps to the sample chamber were fairly long, and

of small diameter so that the evacuation of the relatively large sample chamber to a very low pressure proved rather time-consuming. In most cases, therefore, a "flushing" or "purging" operation was felt to be adequate. The chamber was evacuated to a pressure of less than one millimeter of mercury and then filled to about one atmosphere with one of the components of the desired sample. It was then again evacuated to a pressure of less than one millimeter of mercury and again filled to about one atmosphere with the same component. This procedure was repeated for a total of two or three cycles.

Synthesis of the desired sample then proceeded as follows. The sample chamber was filled with the first component to a pressure such that, when enough of the second component was added to bring the total pressure to one or two centimeters of mercury above the prevailing atmospheric pressure, the first and second components would be in the desired molal ratio. The pressure of the first component was measured by means of the manometer indicated in Figure 7, and the temperature of the lower portion of the apparatus measured by means of a mercury-in-glass thermometer as previously described. The valves K and U were then closed and the sample transfer system evacuated and filled with the second component to be added.

By appropriate manipulation of valves, the second component in the sample transfer system was kept at approximately atmospheric pressure, while being throttled into

the sample chamber through the valve K or the valve U. It was felt that, by this procedure, the lines up to the valves K and U would be filled with only the second component, and that none of the first would have a chance to flow or diffuse out of the sample chamber. The second component was added until the total pressure in the sample chamber reached the desired value, and the pressure and temperature were again measured. The valves K and U were then closed and the apparatus allowed to remain for a period of at least two hours to allow mixing of the component gases.

If a third component were to be added, the following precedure was used. The total pressure in the gas sample chamber, filled with the first and second components in the desired ratio, was reduced to a value such that addition of enough of the third component to give a total pressure slightly above atmospheric would result in a sample of the desired composition. The pressure was then measured, the valves K and U closed, and the transfer lines evacuated and then filled with the third component. The third component was then added in the same manner as described for the second component, and the temperature and pressure again measured.

If the component being added was of lower molecular weight than the gas already in the apparatus, it was added through the lower valve U; if of higher, through the upper valve K. It was hoped that this procedure would result in

better mixing of the sample in the cylinder, by convection. Another mixing period was allowed following addition of the third component. No systems of more than three components were studied, but the extension of the sample addition technique to somewhat more complex systems is obvious.

In most cases, a sample of the charge from the chamber G was then withdrawn and stored for analysis. Samples for analysis were stored in 500 cc. pyrex bulbs equipped with stopcocks and with taper joints. "Halocarbon" stopcock grease was used on the stopcocks and joints when NO_2 was expected in the sample.

Immediately before a run, the pressure of the charge in the chamber was reduced to the desired value by withdrawing some of the charge through the vacuum system. The pressure and temperature of the charge were again measured and the valves K and U closed.

Air from the laboratory high-pressure air supply was introduced into the chamber H to provide the desired pressure, which was measured by means of the Bourdon gauge previously mentioned. The vacuum pump F was operated until constancy of the gauge reading over a reasonable period indicated that the upper O-ring on the piston was sealing properly; the valve L was then closed and the pump F stopped. The valve C was then closed and the handle M turned to shear the brass pin holding the piston in place. After some oscillation, the piston came to rest. The air in H was blown down to atmospheric pressure and the upper closure removed. In most

cases, the position of the piston was then established by measurement relative to the top of the barrel. The valve U was opened, admitting gas into the transfer lines and the manometer, all of which had been evacuated. The pressure of the sample was measured, and the temperature of the lower end of the equipment again measured.

Volumes of the transfer lines and manometer had been established by a previous calibration. Using this calibration, the position of the piston, the pressure and temperature of the system, and chemical analysis of the samples, it was possible to calculate the quantity of "product" sample. Comparison with the quantity of "initial" charge indicated whether significant leakage into or out from the sample space had occurred. Following the measurements for the leakage check, the stopcocks to the previously evacuated sample bulb were opened and the sample bulb filled to about atmospheric pressure, if sufficient sample was available. A second product sample was usually taken, although the quantity of sample available was often such that the second sample bulb was filled to a pressure somewhat below atmospheric.

As soon as samples were collected, the piston was raised to the top of the barrel by admitting air from a 100 psig air supply through the valve U. The piston and lower closure were removed, the lead crusher gauges recovered and measured, and the equipment carefully cleaned. Usually the apparatus was promptly assembled for the next run. If no

runs were expected for several days, the upper and lower closures were installed, and the barrel evacuated. The long cylindrical sections, being of carbon steel, were subject to some corrosion if left exposed to the atmosphere for extended periods.

Chemical Analyses.

Mass spectographic analyses of the product samples and of most of the charge samples were obtained. For these preliminary runs on the nitrogen-oxygen system, it was felt that the expenditure of effort on the development of alternative analytical procedures was not justified.

Most of the analyses reported were performed by the Montebello, California, Laboratories of the Texas Company. A few were obtained from Consolidated Electrodynamics Corp. of Pasadena, California. The procedure of Friedel et al. (24) was followed. The accuracy of the analyses is discussed briefly in another section of this thesis.

Results of Tests.

The initial conditions of the various runs, the final heights of the lead crusher gauges, and the yields of NO_2 are given in Table I. The complete results of the mass spectographic analyses are given in Table II.

IV. CALCULATIONS

In order to test any given chemical rate equations against the results of experiment, it is necessary to use the rate equations to make predictions which can be compared with observed quantities. Typical experimental determinations of chemical reaction rates involve the study of systems which are at least very nearly isothermal, and often also isochoric or isobaric. Analysis of results of experiments in which the temperature, pressure, and volume of the reacting system vary radically during the course of the experiment presents correspondingly greater difficulties.

In attempting to use the ballistic piston as a tool for the study of chemical reaction rates, two major tasks arise. First, it is necessary to determine the conditions of the sample, viz. temperature, pressure, specific volume, composition, etc., as functions of time during the course of a run. Secondly, predictions based on various assumptions as to the reaction rates involved must be compared with the data from the experiment.

The objective of the experimental program is to perform as much as possible of the first task by providing measurements of the properties of the sample as functions of time, or at least measurements from which the desired properties may be calculated in a straightforward manner.

Long range plans for the ballistic piston project envisioned measurement of piston position and perhaps of other variables as functions of time. At the time of the exploratory measurements on the nitrogen-oxygen system, instrumentation for these measurements was not yet available. It was therefore necessary to estimate the condition of a sample during a run from a priori considerations.

Differential equations describing the motion of the piston and the behavior of the sample have been developed by Longwell and Sage (7), who made some numerical estimates of the effect of sample properties on position-pressure and position-time relationships. Longwell (5) made use of a "co-volume" equation of state to describe the behavior of the sample, and made use of experimental data on the position-time relation.

In this discussion, equations will be developed for the prediction of sample conditions on the basis of several simplifying assumptions. Equations in which the effects of reaction are neglected will be considered first, and used to calculate maximum temperatures and pressures for the various runs. Equations which take into account the effects of the reaction $N_2 + O_2 \rightleftharpoons 2NO$ will then be derived, retaining the other simplifying assumptions. Predictions of yields of NO_2, based on several assumed Arrhenius equations for the chemical rate coefficients, will be compared with the observed yields.

Equations of Motion.

The forces acting on the piston after it has been freed from the release mechanism include: 1) the pressure of the sample gas, acting over the lower face of the piston, 2) the pressure of the driving air, acting over the upper end of the piston, 3) the weight of the piston itself, 4) the frictional drag resulting from the contact of the piston and O-rings with the walls of the cylinder. If the pressures in the sample and in the driving air are assumed to be uniform, the acceleration of the piston is described by equation 22.

$$m_p \frac{d^2 x}{d \theta^2} = w_p + A P_A - A P_B - F. \qquad (22)$$

The meanings of the symbols used in equation 22 and in the other equations which follow are given in the nomenclature.

An expression equivalent to equation 22 is

$$m_p \frac{d u}{d \theta} = w_p + A P_A - A P_B - F. \qquad (23)$$

A differential equation involving energy terms may be obtained by considering the application of the forces in equation 23 over a distance dx.

$$m_p \frac{d u}{d \theta} dx = (w_p - F) dx + A P_A dx - A P_B dx. \qquad (24)$$

It is apparent that

$$A\,dx = d\underline{V}_A = -\,d\underline{V}_B \quad . \tag{25}$$

The left hand member of equation 24 may be rewritten as follows:

$$m_p \frac{d\,v}{d\theta}\,dx = m_p \frac{d\,v}{dx}\frac{dx}{d\theta}\,dx = m_p \frac{dx}{d\theta}\frac{d\,v}{dx}\,dx \tag{26}$$

$$= m_p\, v\, dv \quad .$$

Substitution of the appropriate terms from equations 25 and 26 in 24 gives

$$m_p\, v\, dv = (w_p - F)\,dx + P_A\, d\underline{V}_A + P_B\, d\underline{V}_B \quad , \tag{27}$$

which may be written as

$$m_p\, d\left(\frac{v^2}{2}\right) = (w_p - F)\,dx + P_A\, d\underline{V}_A + P_B\, d\underline{V}_B \quad . \tag{28}$$

Equation 28 might have been written directly from application of the principle of conservation of energy and from the assumptions made. The solution of equation 28 involves prediction of P_A and P_B as functions of x. Several simplifying assumptions were made to permit these predictions. While the resulting equations are only approximate, it was felt that more elaborate treatment was not justified, in view of the limited experimental data.

If it is assumed that no material leaks out from or into the sample chamber or the driving air chamber, that heat transfer to or from the walls may be neglected because of the short times involved, and that the expansions and compressions are reversible, the sample then follows an isentropic path. Neglecting changes in composition, i.e., neglecting chemical reaction, it may readily be shown that

$$\left(\frac{\partial T}{\partial \tilde{V}}\right)_{\tilde{S}} = \frac{-T\left(\frac{\partial P}{\partial T}\right)_{\tilde{V}}}{\tilde{C}_v} \quad . \tag{29}$$

If the sample is regarded as an ideal gas,

$$P\tilde{V} = RT \quad , \tag{30}$$

so that

$$\left(\frac{\partial P}{\partial T}\right)_{\tilde{V}} = \frac{R}{\tilde{V}} \quad . \tag{31}$$

Combination of equations 29 and 31 indicates that, for a perfect gas,

$$\left(\frac{\partial T}{\partial \tilde{V}}\right)_{\tilde{S}} = \frac{-T\frac{R}{\tilde{V}}}{\tilde{C}_v} \quad , \tag{32}$$

or

$$\left(\frac{\partial T}{\partial \tilde{V}}\right)_{\tilde{S}} = -\frac{P}{\tilde{C}_v} \quad . \tag{33}$$

Equation 32 may be rearranged to give

$$\frac{\tilde{C}_v}{R}\frac{dT}{T} = -\frac{d\tilde{V}}{\tilde{V}} \tag{34}$$

at constant $\tilde{S}$. Integration from the initial conditions to an arbitrary point gives

$$\frac{1}{R}\int_{T=T_o}^{T} \tilde{C}_v \, d\ln T = -\int_{\tilde{V}=\tilde{V}_o}^{\tilde{V}} d\ln \tilde{V} = \ln\frac{\tilde{V}_o}{\tilde{V}} \quad . \tag{35}$$

Since changes in the mass and composition of the sample have been neglected, the final term of 35 may also be written as ln $\frac{V_o}{V}$ or as ln $\frac{\underline{V}_o}{\underline{V}}$.

It will be useful to employ the dimensionless parameters defined by the following equations.

$$T^* = \frac{T}{T_o} \tag{36}$$

$$V^* = \frac{\underline{V}}{\underline{V}_o} = \frac{V}{V_o} = \frac{\tilde{V}}{\tilde{V}_o} \tag{37}$$

$$P^* = \frac{P}{P_o} \tag{38}$$

In terms of the dimensionless parameters, equation 35 becomes

$$\frac{1}{R}\int_0^{\ln T^*} \tilde{C}_v \, d\ln T^* = -\ln V^* \qquad (39)$$

(note that d $\ln T^*$ = d lnT).

Using the nomenclature developed by Longwell (5), the function ϕ is arbitrarily defined as

$$\phi = \frac{1}{\ln T^*}\int_0^{\ln T^*} \tilde{C}_v \, d\ln T^* \quad . \qquad (40)$$

The relation of equation 39 may be written in terms of this function as

$$\frac{\phi \ln T^*}{R} = -\ln V^* \qquad (41)$$

or, in exponential form,

$$T^* = V^{*-\frac{R}{\phi}} \quad . \qquad (42)$$

The ideal gas law, expressed in terms of the dimensionless variables, is

$$P^* V^* = T^* \, . \qquad (43)$$

Combination of equations 42 and 43 yields the isentropic relationship between P* and V*.

$$P^* = (V^*)^{-\left(\frac{R}{\phi}+1\right)} \quad . \tag{44}$$

Equations 42 and 43 were taken as descriptive of the isentropic temperature-volume and pressure-volume relationships in the sample. Similar equations might have been used to predict the behavior of the driving air. Instead, the polytropic path

$$P_A V_A^k = \text{constant} = P_{A_o} V_{A_o}^k \quad , \tag{45}$$

in which k is constant, was used to describe the expansion of the air. The use of data for the real gas, air, in the evaluation of k is described in Appendix I.

Substitution of equations 44, 37, 38, and 45 in equation 28 gives

$$m_p\, d\left(\frac{v^2}{2}\right) = (w_p - F)\,dx + P_{A_o}\left(\frac{V_{A_o}}{V_A}\right)^k d\underline{V}_A + P_{B_o}\left(\frac{V_{B_o}}{\underline{V}_B}\right)^{\left(\frac{R}{\phi}+1\right)} d\underline{V}_B \quad . \tag{46}$$

Integration of equation 25 gives

$$\underline{V}_A = \underline{V}_{B_o} - \underline{V}_B + \underline{V}_A \quad . \tag{47}$$

Substitution of 25 and 47 in 46 yields

$$m_p\, d\left(\frac{v^2}{2}\right) = (w_p - F)\,dx - P_{A_o}\left(\frac{V_{A_o}}{\underline{V}_{B_o} - \underline{V}_B + \underline{V}_{A_o}}\right)^k d\underline{V}_B + P_{B_o}\left(\frac{V_{B_o}}{\underline{V}_B}\right)^{\left(\frac{R}{\phi}+1\right)} d\underline{V}_B \quad . \tag{48}$$

Arbitrarily defining β by the relation

$$\beta = \frac{\underline{V}_{A_0}}{\underline{V}_{B_0}} \tag{49}$$

and substituting in 48 together with the following relation based on the definition of V_B^* ,

$$d\underline{V}_B = \underline{V}_{B_0}\, dV_B^* \tag{50}$$

we obtain

$$m_p\, d\left(\frac{v^2}{2}\right) = (\omega_p - F)\, dx - P_{A_0}\underline{V}_{B_0}\left(\frac{\beta}{1+\beta-V_B^*}\right)^k dV_B^* + P_{B_0}\underline{V}_{B_0}\, V_B^{*-\left(\frac{k}{\phi}+1\right)} dV_B^* \tag{51}$$

The terms T*, P*, V*, Ø, and other terms to be introduced later, will be used only in reference to the sample. These will be employed in subsequent equations without the subscript "B". Other properties, such as P, T, etc., will refer to the sample unless otherwise specified, and the subscripts will be used only where special emphasis is necessary.

Several terms in the integrated form of equation 51 will be derived in turn.

$$\int_{V_0^*}^{V^*}\left(\frac{\beta}{1+\beta-V^*}\right)^k dV^* = \beta^k \int_{V_0^*}^{V^*}(1+\beta-V^*)^{-k}\, dV^* \quad ; \tag{52}$$

$$\beta^{k}\int_{V_o^*}^{V^*}(1+\beta-V^*)^{-k}\,dV^* = \beta^{k}\left\{\left(\frac{-1}{1-k}\right)(1+\beta-V^*)^{1-k}\right\}\Bigg|_{V_o^*}^{V^*} . \quad (53)$$

Noting that $V_o^* = \frac{V_{Bo}}{V_{Bo}} = 1$, we have

$$\int_{1}^{V^*}\left(\frac{\beta}{1+\beta-V^*}\right)^{k} dV^* = \left(\frac{-\beta^{k}}{1-k}\right)\left\{(1+\beta-V^*)^{1-k} - \beta^{1-k}\right\} \quad (54)$$

or, rearranging,

$$\int_{1}^{V^*}\left(\frac{\beta}{1+\beta-V^*}\right)^{k} dV^* = \left(\frac{1}{k-1}\right)\left\{\beta^{k}(1+\beta-V^*)^{1-k} - \beta\right\} . \quad (55)$$

From equations 25 and 50,

$$dx = -\frac{V_{Bo}}{A}\,dV^* . \quad (56)$$

Integration of equation 56 gives

$$\int_{x_o}^{x} dx = -\frac{V_{Bo}}{A}\int_{1}^{V^*} dV^* = -\frac{V_{Bo}}{A}(V^*-1) . \quad (57)$$

The next term represents the work done on the sample.

$$\int_{1}^{V^*} V^{*-\left(\frac{R}{\phi}+1\right)}\, dV^* = \int_{1}^{V^*} V^{*-\frac{R}{\phi}}\, \frac{dV^*}{V^*} \quad . \tag{58}$$

Substituting appropriate terms from equation 42 in 58,

$$\int_{1}^{V^*} V^{*-\frac{R}{\phi}}\, \frac{dV^*}{V^*} = \int_{V^*=1}^{V^*} T^*\, d\ln V^* \quad . \tag{59}$$

From equations 34 and 37,

$$d\ln V^* = -\frac{\tilde{C}_v}{R}\, d\ln T^* = -\frac{\tilde{C}_v}{R}\, \frac{dT^*}{T^*} \quad . \tag{60}$$

Combination of equations 58, 59, and 60 results in

$$\int_{1}^{V^*} V^{*-\left(\frac{R}{\phi}+1\right)}\, dV^* = -\frac{1}{R}\int_{1}^{T^*} \tilde{C}_v\, dT^* \quad . \tag{61}$$

Using Longwell's nomenclature for another arbitrarily defined function, Ψ,

$$\Psi = \int_{1}^{T^*} \tilde{C}_v\, dT^* \quad , \tag{62}$$

the result expressed in 61 may be written as

$$\int_{1}^{V^*} V^{*-\left(\frac{R}{\phi}+1\right)}\, dV^* = -\frac{\Psi}{R} \quad . \tag{63}$$

We may now return to consideration of equation 51. Integrating both sides from initial conditions to an arbitrary point, substituting equations 55, 57, and 63 in the result, and assuming that the frictional drag on the piston is constant, we obtain

$$m_p \frac{v^2}{2} = \frac{V_{B_0}}{A}(\omega_p - F)(1 - V^*) + \frac{P_{A_0} V_{B_0}}{1-k}\left\{\beta^k (1+\beta-V^*)^{1-k} - \beta\right\} - P_{B_0} V_{B_0} \frac{\psi}{R} \quad . \tag{64}$$

From the definition of u and equations 25 and 37,

$$v = -\frac{V_{B_0}}{A}\frac{dV^*}{d\theta} \quad , \tag{65}$$

and hence

$$v^2 = \left(\frac{V_{B_0}}{A}\right)^2 \left(\frac{dV^*}{d\theta}\right)^2 \quad . \tag{66}$$

It will be convenient to introduce the notation

$$v^* = -\frac{dV^*}{d\theta} \quad . \tag{67}$$

Substitution of 66 and 67 in equation 64 and division of each term by $\frac{V_{B_0}}{A}$ gives

$$\frac{m_p V_{B_0}}{2A} v^{*2} = (\omega_p - F)(1 - V^*) + \frac{A P_{A_0}}{k-1}\left\{\beta - \beta^k (1+\beta-V^*)^{1-k}\right\} - A P_{B_0} \frac{\psi}{R} \quad . \tag{68}$$

Equation 68 describes the motion of the piston on the first downstroke. If an estimate of subsequent motion is desired, account must be taken of the effect of the friction term; the frictional force always acts to oppose the motion of the piston. With the sign convention chosen for the distance parameter x, equation 22 describes the motion of the piston when it is moving downward. When it is moving upward, the appropriate equation is

$$m_p \frac{d^2x}{d\theta^2} = \omega_p + F + A P_A - A P_B \quad , \tag{69}$$

and the equation corresponding to equation 51 is

$$m_p\, d\left(\frac{v^2}{2}\right) = (\omega_p + F)\, dx - P_{A_0} V_{B_0} \left(\frac{\beta}{1+\beta-V^*}\right)^k dV^* + P_{B_0} V_{B_0} V^{*-\left(\frac{k}{\phi}+1\right)} dV^* \quad . \tag{70}$$

Denoting terms involving V* as (V*), equations 51 and 70, respectively, may be written as

$$m_p\, d\left(\frac{v^2}{2}\right) = \omega_p\, dx - F\, dx + f(V^*)\, dV^* \tag{71}$$

and

$$m_p\, d\left(\frac{v^2}{2}\right) = \omega_p\, dx + F\, dx + f(V^*)\, dV^* \quad . \tag{72}$$

Denoting the terminal point of the i_{th} downstroke of the piston by x_{D_i} and the terminal point of the i_{th} upstroke by x_{U_i}, we may write integral forms of 71 and 72 for the various strokes. On the first downstroke

$$\int_0^{v^2} \frac{m_p}{2}\, d(v^2) = \omega_p \int_0^{x} dx - \int_0^{x} F\, dx + \int_1^{V^*} f(V^*)\, dV^* . \tag{73}$$

Applied at the terminal point, this becomes

$$\int_0^{v_{D_1}^2 = 0} \frac{m_p}{2}\, d(v^2) = \omega_p \int_0^{x_{D_1}} dx - \int_0^{x_{D_1}} F\, dx + \int_1^{V_{D_1}^*} f(V^*)\, dV^* \tag{74}$$

For the first upstroke

$$\int_{v_{D_1}^2 = 0}^{v^2} \frac{m_p}{2}\, d(v^2) = \omega_p \int_{x_{D_1}}^{x} dx + \int_{x_{D_1}}^{x} F\, dx + \int_{x_{D_1}}^{x} f(V^*)\, dV^* . \tag{75}$$

Addition of equations 74 and 75 results in

$$\frac{m_p}{2} \int_0^{v^2} d(v^2) = \omega_p \int_0^{x} dx - \int_0^{x_{D_1}} F\, dx + \int_{x_{D_1}}^{x} F\, dx + \int_1^{V^*} f(V^*)\, dV^* . \tag{76}$$

which, applied at the terminal point of the first upstroke, becomes

$$\frac{m_p}{2}\int_0^0 d(v^2) = w_p\int_0^{x_{v_1}} dx - \int_0^{x_{D_1}} F\,dx + \int_{x_{D_1}}^{x_{v_1}} F\,dx + \int_1^{V_{v_1}^*} f(V^*)\,dV^* \quad . \tag{77}$$

On the second downstroke,

$$\frac{m_p}{2}\int_0^{v^2} d(v^2) = w_p\int_{x_{v_1}}^{x} dx - \int_{x_{v_1}}^{x} F\,dx + \int_{V_{v_1}^*}^{V^*} f(V^*)\,dV^* . \tag{78}$$

Addition of equations 77 and 78 gives

$$\frac{m_p}{2}\int_0^{v^2} d(v^2) = w_p\int_0^{x} dx - \int_0^{x_{D_1}} F\,dx + \int_{x_{D_1}}^{x_{v_1}} F\,dx - \int_{x_{v_1}}^{x} F\,dx + \int_1^{V^*} f(V^*)\,dV^* \quad . \tag{79}$$

For constant F, this becomes

$$\frac{m_p v^2}{2} = w_p x + \int_1^{V^*} f(V^*)\,dV^* - F\left\{x + 2x_{D_1} - 2x_{v_1}\right\} \quad . \tag{80}$$

The extension of the technique used in obtaining equations 76 and 79 to subsequent motion is fairly obvious. Generalized equations in the form of 80 are, for the n^{th} downstroke,

$$\frac{m_p U^2}{2} = \omega_p x + \int_{\prime}^{V^*} f(V^*)\, dV^* - F\left\{ x + 2\sum_{i=1}^{n-1} x_{D_i} - 2\sum_{i=1}^{n-1} x_{U_i} \right\} , \tag{81}$$

and for the n^{th} upstroke,

$$\frac{m_p U^2}{2} = \omega_p x + \int_{\prime}^{V^*} f(V^*)\, dV^* - F\left\{ -x + 2\sum_{i=1}^{n} x_{D_i} - 2\sum_{i=1}^{n-1} x_{U_i} \right\} . \tag{82}$$

Evaluation of the integral term results in general equations analogous to equation 68; for the n^{th} downstroke,

$$\frac{m_p V_{B_0} U^{*2}}{2A} = \omega_p (1 - V^*) + \frac{A P_{A_0}}{R-1}\left\{ \beta - \beta^R (1 + \beta - V^*)^{1-R} \right\} - A P_{B_0} \frac{\psi}{R} - F\left\{ 1 - V^* - 2\sum_{i=1}^{n-1} V_{D_i}^* + 2\sum_{i=1}^{n-1} V_{U_i}^* \right\} , \tag{83}$$

and for the n^{th} upstroke,

$$\frac{m_p V_{B_0} v^{*2}}{2A} = \omega_p (1 - V^*) + \frac{A P_{A_0}}{R-1} \left\{ \beta - \beta^R (1 + \beta - V^*)^{1-R} \right\}$$

$$- A P_{B_0} \frac{\psi}{R} - F \left\{ 1 + V^* - 2 \sum_{i=1}^{n} x_{D_i} + 2 \sum_{i=1}^{n-1} x_{U_i} \right\} \tag{84}$$

An alternative approach to the derivation of equations 68, 83, and 84 is given in Appendix II.

Solution neglecting reaction.

Solution of the foregoing equations will yield approximations of the temperatures and pressures achieved in the various runs. These approximations will be considered next; in a later section, the derivation and solution of equations taking chemical reaction into account will be described.

The minimum volume of the sample, attained at the end of the initial downstroke of the piston, was determined from measurement of the heights of the lead crusher gauges. This volume corresponds to a piston velocity of zero, motion of the cylinder relative to its initial position being neglected. Equation 68 applied at this point becomes

$$0 = (\omega_p - F)(1 - V_{D_1}^*) + \frac{A P_{A_0}}{R-1} \left\{ \beta - \beta^R (1 + \beta - V_{D_1}^*)^{1-R} \right\} \tag{85}$$

$$- A P_{B_0} \frac{\psi}{R} ,$$

which may be solved for the effective frictional drag force F if Ψ can be established.

By definition,

$$\Psi = \int_{1}^{T^*} \tilde{C}_v \, d T^* \tag{62}$$

and

$$\phi = \frac{1}{\ln T^*} \int_{0}^{\ln T^*} \tilde{C}_v \, d \ln T^* \quad . \tag{40}$$

With the assumptions of ideal solution and perfect gases,

$$\tilde{C}_{v_i}^{\circ} = \tilde{C}_{v \neq i} \tag{86}$$

for the i^{th} component, and

$$\tilde{C}_v = \sum_{i=1}^{n} \tilde{n}_i \tilde{C}_{v_i}^{\circ} = \sum_{i=1}^{n} \tilde{n}_i \tilde{C}_{v \neq i} \quad . \tag{87}$$

Use of the outer equality of 87 in equations 62 and 40 respectively, leads to the relations

$$\Psi = \sum_{i=1}^{n} \tilde{n}_i \Psi_{i \neq} \tag{88}$$

and

$$\phi = \sum_{i=1}^{n} \tilde{n}_i \, \phi_{i\,\phi} \quad , \tag{89}$$

for a system of invariant composition.

From available data on the heat capacities (25,26), the functions Ψ and ϕ for the ideal gas state were evaluated for N_2, O_2, and NO by numerical integration of the defining equations 62 and 40. These evaluations were made relative to an arbitrary intial temperature T_{o_s} ($77^{\circ}F$), and values of the functions were tabulated over the range covered by the available data for $\tilde{C}_{v_\phi}$, i.e., up to $5000^{\circ}K$. For helium, the value of $\tilde{C}_{v_\phi}$ was taken as constant, equal to 3/2 R (27). For a constant heat capacity, it follows from the definitions that

$$\phi = \tilde{C}_v \tag{90}$$

and

$$\Psi = \tilde{C}_v \left(T^* - 1\right) \quad . \tag{91}$$

The calculation of Ψ and ϕ for mixtures was made from

the tabulated values for the pure components, by application of equations 88 and 89. If the initial temperature of the sample differed from T_{o_s}, the calculation of ψ and ϕ from the tabulated values involved only a simple correction. The pertinent equations for this small correction are derived in Appendix III.

When reaction is neglected, equation 42 describes the isentropic relationship between T* and V*. Since the minimum volume was known from measurement and ϕ was known as a function of T and hence of T*, equation 42 could be solved by trial and error for the value of T* corresponding to the minimum V*. This solution was usually made by guessing a value of ϕ, calculating T*, finding, from the tabulated values, a new ϕ corresponding to that T*, and calculating a new T*. Usually only a few trials were required.

Once the maximum value of T* was obtained from equation 42, ψ was obtained from equation 88 and the tabulated values for the pure components, and 85 was solved for F.

Calculation of the kinetic energy term involving u* may be made for other points along the path of the piston, from equation 68. The value of ψ is obtained by the procedure described for the minimum volume, and the value of F obtained from equation 85 is employed. As a somewhat simpler procedure, nominal values of T* rather than V* may be employed, so that trial and error solution of equa-

tion 42 is unnecessary. For points on the path beyond the first downstroke, equation 83 or 84 must be used in place of equation 68.

Writing u* as $-\frac{dV^*}{d\theta}$, equation 68 is a differential equation involving the variables V* and θ. Solution of this equation in a closed form has not been obtained. If the relation between V* and time is desired, it may be obtained by graphical or numerical integration, using the relation

$$\theta_2 - \theta_1 = \int_{V_1^*}^{V_2^*} \frac{1}{\frac{dV^*}{d\theta}} \, dV^* \qquad (92)$$

Results.

The "constant composition" approximations for the maximum temperature and pressure attained in each run are presented in Table III. The locations of the maximum points calculated in this manner are shown graphically in Figure 9.

In determining conditions for the series of runs, an attempt had been made to obtain several values of maximum partial pressure of oxygen at equal maximum temperatures, and several values of maximum temperature at roughly equal values of maximum partial pressure of oxygen. Figure 10 shows the quantity $P_{max}\,\tilde{n}_{O_2,o}$ plotted against the maximum temperature. Figure 11 is a similar plot of $P_{max}\,(\tilde{n}_{N_2,o}\,\tilde{n}_{O_2,o})^{\frac{1}{2}}$

as a function of maximum temperature; the quantity $(\tilde{n}_{N_2 o}\,\tilde{n}_{O_2 o})^{\frac{1}{2}}$ is more closely related to the potential for reaction than is $\tilde{n}_{O_2 o}$. The values of these pressure parameters are also given in Table IV.

The mass spectrographic analyses of the final samples are given in Table II. In Table IV, the yields of NO_2 are repeated, and several derived quantities are shown. The yield of NO corresponding to the observed yield of NO_2, the "inert free" yield of NO, and the quantity $\frac{\tilde{n}_{NO}^2}{\tilde{n}_{N_2}\,\tilde{n}_{O_2}}$ are given. It was felt that comparison of yields among the various runs would be more realistic on the "inert free" basis, i.e., with the diluent effects of helium and argon removed. In forming the parameter $\frac{\tilde{n}_{NO}}{\tilde{n}_{N_2}\,\tilde{n}_{O_2}}$, $\tilde{n}_{NO}$ was taken as the value corresponding to the observed yield of NO_2. The mol fractions $\tilde{n}_{N_2}$ and $\tilde{n}_{O_2}$ were calculated from this value of $\tilde{n}_{NO}$ and from the initial values $\tilde{n}_{N_2 o}$ and $\tilde{n}_{O_2 o}$ determined from pressure measurements. The formation of products other than NO was neglected.

The yield of NO is shown in Figure 12 as a function of the maximum temperature of the run. Figure 13 shows the yield on an inert free basis, again as a function of the maximum temperature. Because of the wide variation in the other factors influencing yield, little can be learned from this plot alone. Runs in which the maximum partial pressures of oxygen were roughly the same show an increase in yield with increasing maximum temperature.

In figure 14, the yield is shown as a function of the parameter $P_{max}\,(\tilde{n}_{N_2O}\;\tilde{n}_{O_2O})^{\frac{1}{2}}$. Since in the formation runs, the ratio of nitrogen to oxygen was always nearly 1:1, $P_{max}\,(\tilde{n}_{N_2O}\;\tilde{n}_{O_2O})^{\frac{1}{2}}$ was nearly the same as the maximum possible partial pressure of oxygen. Again, the wide variation in other factors makes interpretation difficult. The yield for runs with roughly equal maximum temperatures shows an increase with increase in the partial pressure function.

Inspection of the yields in conjunction with the extreme conditions as indicated in Figures 9, 10, and 11 leads to the conclusion that an increase in yield is promoted by increase in the maximum temperature attained, and by increase in the maximum pressure. This is to be expected; increase in the temperature, since the equilibrium constant becomes larger, leads to increase in the maximum amount of NO which can be formed. Higher temperature also means a probable increase in the reaction rate. Increase in the pressure means an increase in the potential for reaction, and hence promotes approach to equilibrium at the extreme conditions. The potential for reaction depends primarily on the chemical activities of the reacting species, but in runs in which equilibrium is closely approached at the highest temperature, higher total pressure will also promote greater yield of NO High maximum pressure results in rapid acceleration of the piston on the upward stroke, and hence in rapid cooling of the sample, tending to "freeze" the equilibrium approached at the highest temperature.

Table V gives the temperature at which the mol fraction of NO, equivalent to the observed yield of NO_2, would be at equilibrium. For each of the "formation" runs, this temperature is below the calculated maximum temperature of the run. To this extent, at least, the approximate temperatures are consistent with the observed yields.

Chemical reaction.

The effect of the formation or decomposition of NO will now be considered. Equations involving arbitrary changes in the fraction of NO present will be derived first, and the prediction of the extent of such changes will then be considered.

The first law of thermodynamics for a closed system may be written

$$d\underline{E} = \underline{q} - \underline{w} \quad , \tag{93}$$

which for an adiabatic system becomes

$$d\underline{E} = - \underline{w} \quad . \tag{94}$$

If only expansion work is involved, it may be evaluated for a reversible change in state as

$$\underline{w} = P d\underline{V} \quad . \tag{95}$$

Since $\underline{E}$ may be regarded as a function of the temperature and pressure of the system and of the amounts of the various components present, we may write

$$d\underline{E} = \left(\frac{\partial \underline{E}}{\partial T}\right)_{P,N} dT + \left(\frac{\partial \underline{E}}{\partial P}\right)_{T,N} dP + \sum_{i}^{n} \left(\frac{\partial \underline{E}}{\partial N_i}\right)_{T,P,N_j} dN_i , \tag{96}$$

where the subscript N_j indicates constancy of the number of mols of all but the i^{th} component. Since

$$\underline{E} = N\tilde{E} , \tag{97}$$

it is clear that

$$\left(\frac{\partial \underline{E}}{\partial T}\right)_{P,N} = N\left(\frac{\partial \tilde{E}}{\partial T}\right)_{P,N} \tag{98}$$

and

$$\left(\frac{\partial \underline{E}}{\partial P}\right)_{T,N} = N\left(\frac{\partial \tilde{E}}{\partial P}\right)_{T,N} \tag{99}$$

In considering chemical reaction, the assumption of ideal gas behavior will be retained. With this assumption,

$$\left(\frac{\partial \tilde{E}}{\partial T}\right)_{P,N} = \tilde{C}_v \tag{100}$$

and

$$\left(\frac{\partial \tilde{E}}{\partial P}\right)_{T,N} = 0 \qquad (101)$$

Also, by the definition of partial molal quantities,

$$\tilde{\tilde{E}}_i = \left(\frac{\partial E}{\partial N_i}\right)_{T,P,N_j} . \qquad (102)$$

Substitution of equations 98, 100, 101, and 102 in 96 gives

$$dE = N\tilde{C}_v dT + \sum_i^n \tilde{\tilde{E}}_i dN_i . \qquad (103)$$

We are primarily interested in the reaction

$$N_2 + O_2 \rightleftharpoons 2NO . \qquad (104)$$

Limiting consideration of variation in composition to that resulting from this reaction, it follows from stoichiometry that

$$dN_{N_2} = dN_{O_2} = -\frac{1}{2} dN_{NO} . \qquad (105)$$

Combination of equations 103 and 105 results in

$$d\underline{E} = N\tilde{C}_v\,dT + \left(\bar{\bar{\tilde{E}}}_{NO} - \tfrac{1}{2}\bar{\bar{\tilde{E}}}_{N_2} - \tfrac{1}{2}\bar{\bar{\tilde{E}}}_{O_2}\right)dN_{NO} . \quad (106)$$

The sample is assumed to be an ideal solution, so that

$$\bar{\bar{\tilde{E}}}_i = \tilde{E}_i^{\circ} , \quad (107)$$

and, since each component is regarded as a perfect gas,

$$\tilde{E}_i^{\circ} = \tilde{E}_{i\phi} \quad (108)$$

In view of these relations, equation 106 may be written

$$d\underline{E} = N\tilde{C}_v\,dT + \left(\tilde{E}_{\phi NO} - \tfrac{1}{2}\tilde{E}_{\phi N_2} - \tfrac{1}{2}\tilde{E}_{\phi O_2}\right)dN_{NO} . \quad (109)$$

By definition, the quantity in parentheses is $\Delta\tilde{E}_{f\phi\,NO}$, the standard molal energy of formation of NO, so the equation may finally be written as

$$d\underline{E} = N\tilde{C}_v\,dT + \Delta\tilde{E}_{f_\phi\,NO}\,dN_{NO} . \quad (110)$$

Since the total number of molecules in a system is not changed by the reaction indicated in equation 104, the product $\widetilde{PV}$ is not changed by the reaction at constant temperature in the ideal gas state. Therefore

$$\Delta \widetilde{E}_{f\phi\,NO} = \Delta \widetilde{H}_{f\phi\,NO} \quad . \tag{111}$$

Combination of equation 110 with equations 94 and 95 results in

$$P d\underline{V} = -N\tilde{C}_v dT - \Delta \widetilde{E}_{f\phi\,NO}\, dN_{NO} \quad , \tag{112}$$

which may be substituted in equation 28 to give

$$\frac{m_p}{2} d(v^2) = (\omega_p - F)dx + P_A d\underline{V}_A - N\tilde{C}_v dT - \Delta \widetilde{E}_{f\phi\,NO}\, dN_{NO} \, . \tag{113}$$

Using the same substitutions as before for P_A, $\underline{V}_A$, and x, and integrating, we obtain the following equation, similar to equation 64, but with the effect of reaction included.

$$\frac{m_p U^2}{2} = \frac{V_{Bo}}{A}(\omega_p - F)(1 - V^*) + \frac{P_{Ro} V_{Bo}}{R-1}\left\{\beta - \beta^R(1+\beta-V^*)^{1-R}\right\} \tag{114}$$

$$- \int_{T_o}^{T} N \tilde{C}_v \, dT \quad - \int_{N_{NO_o}}^{N_{NO}} \Delta \tilde{E}_{f_{\phi NO}} \, dN_{NO} \quad .$$

From equation 36,

$$dT = T_o \, dT^* \quad . \tag{115}$$

The number of mols of sample initially present may be obtained from

$$P_{Bo} V_{Bo} = N_{Bo} R T_{Bo} \quad ; \tag{116}$$

since the total number of mols does not change,

$$N = N_{Bo} \quad , \tag{117}$$

and the change in the number of mols of NO may be written as

$$\Delta N_{NO} = N \Delta \tilde{n}_{NO} = N_o \Delta \tilde{n}_{NO} \quad . \tag{118}$$

Substitution of equations 66, 67, 115, 116, 117, and 118 into 114 gives

$$\frac{m_p V_{B0}}{2A} v^{*2} = (\omega_p - F)(1 - V^*) + \tag{119}$$

$$\frac{A P_{A0}}{R-1}\left\{\beta - \beta^R (1+\beta-V^*)^{1-R}\right\}$$

$$- \frac{A P_{B0}}{R}\int_1^{T^*} \tilde{C}_v \, dT^* \quad - \quad \frac{A P_{B0}}{R T_{B0}}\int_{\tilde{n}_{NO_0}}^{\tilde{n}_{NO}} \Delta \tilde{E}_{f\,NO} \, d\tilde{n}_{NO} \quad .$$

Reaction Rate.

Determination of piston velocity from equation 119 requires a knowledge of the composition changes taking place. As mentioned in Section I, several mechanisms have been suggested for the reaction. The simplest involves only the single step indicated by equation 104, and it was felt that the hypothesis of this simple mechanism should be considered first.

The rate of reaction may be defined in terms of the rate of formation of NO in a closed, uniform system. Thus,

$$r = \frac{dN_{NO}}{V d\theta} \quad . \tag{120}$$

It must be emphasized that equation 120 applies to a system

in which the change in the number of mols of NO is due exclusively to reaction 104.

Other quantities related to the number of mols are often employed in describing the rate of chemical reaction. Frequently either the concentration or partial pressure of the component of interest is employed.

The rate of a chemical reaction is usually regarded as being proportional to some driving force. The constant of proportionality is known as the "specific rate constant" or "specific rate coefficient." In employing any given such coefficient, care must be taken that the coefficient be used only in conjunction with the corresponding driving force and proper defining rate equation.

In a closed, isochoric, isothermal system, the change in the partial pressure of NO is related to the rate defined by equation 120. For such a system, a rate equation corresponding to the mechanism indicated by equation 104 is

$$\frac{d p_{NO}}{d \theta} = K_{pp_f} p_{N_2} p_{O_2} - K_{pp_d} p_{NO}^2 \quad . \tag{121}$$

In writing the specific rate coefficients indicated in the above equation, the first subscript p indicates that the rate is measured in terms of the rate of change of the partial pressure of NO; the second, that partial pressures have been used as the "driving forces" for the reaction.

The subscripts f and d refer to formation and decomposition, respectively.

Using the assumptions of perfect gas behavior and ideal solution, we may write for the isochoric, isothermal system

$$\frac{d p_{NO}}{d\theta} = \frac{RT}{V} \frac{d N_{NO}}{d\theta} \tag{122}$$

or

$$\frac{1}{V} \frac{d N_{NO}}{d\theta} = \frac{1}{RT} \frac{d p_{NO}}{d\theta} \quad . \tag{123}$$

Combination of equations 123 and 121 yields

$$\frac{1}{V} \frac{d N_{NO}}{d\theta} = \frac{1}{RT} \left\{ K_{PP_f} p_{N_2} p_{O_2} - K_{PP_d} p_{NO}^2 \right\} \quad . \tag{124}$$

Since we have assumed that

$$p_i = \tilde{n}_i P \tag{125}$$

and

$$PV = NRT \quad , \tag{126}$$

we may write 124 as

$$\frac{1}{V}\frac{dN_{NO}}{d\theta} = \frac{RTN^2}{V^2}\left\{K_{PP_f}\tilde{n}_{N_2}\tilde{n}_{O_2} - K_{PP_d}\tilde{n}_{NO}^2\right\} . \qquad (127)$$

The rate of formation of NO, as defined by equation 120, has been related to partial pressures by considering a system in which the partial pressures are changed only by reaction 104, viz. an isothermal, isochoric system of ideal gases. The total rate of formation of NO in the system may be obtained by multiplying 127 by the volume of the system; thus

$$\frac{dN_{NO}}{d\theta} = \frac{RTN^2}{V}\left\{K_{PP_f}\tilde{n}_{N_2}\tilde{n}_{O_2} - K_{PP_d}\tilde{n}_{NO}^2\right\} . \qquad (128)$$

It must again be emphasized that this represents only the rate of change of N_{NO} due to reaction 104. In general, N_{NO} will be affected by other processes, such as material transfer into the system or other reactions. In this more general case, the contribution of reaction 104 to the total change of N_{NO} will still be given by equation 128, or the equivalent form based on 124.

Under the assumptions of no leakage, uniform conditions, and no other reactions, equation 128 describes the instantaneous rate of formation of NO in the ballistic piston apparatus. Since the total number of mols in the system is not changed by the reaction, equation 128 may be divided by N to give

$$\frac{d\tilde{n}_{NO}}{d\theta} = \frac{RTN}{V}\left\{K_{pp_f}\,\tilde{n}_{N_2}\,\tilde{n}_{O_2} - K_{pp_d}\,\tilde{n}_{NO}^{2}\right\} \tag{129}$$

or

$$\frac{d\tilde{n}_{NO}}{d\theta} = P\left\{K_{pp_f}\,\tilde{n}_{N_2}\,\tilde{n}_{O_2} - K_{pp_d}\,\tilde{n}_{NO}^{2}\right\} . \tag{130}$$

The term $\frac{d\tilde{n}_{NO}}{d\theta}$ will be designated as r*.

$$r^* = \frac{d\tilde{n}_{NO}}{d\theta} . \tag{131}$$

Using the definitions of P* and r*, 130 becomes

$$r^* = \frac{d\tilde{n}_{NO}}{d\theta} = P_{B_o} P^*\left\{K_{pp_f}\,\tilde{n}_{N_2}\,\tilde{n}_{O_2} - K_{pp_d}\,\tilde{n}_{NO}^{2}\right\} . \tag{132}$$

From the stoichiometry of the reaction,

$$\Delta \tilde{n}_{N_2} = \Delta \tilde{n}_{O_2} = -\frac{1}{2} \Delta \tilde{n}_{NO} \quad , \tag{133}$$

so that

$$\tilde{n}_{N_2} = \tilde{n}_{N_{2o}} + \frac{1}{2} \tilde{n}_{NO_o} - \frac{1}{2} \tilde{n}_{NO} \tag{134}$$

and

$$\tilde{n}_{O_2} = \tilde{n}_{O_{2o}} + \frac{1}{2} \tilde{n}_{NO_o} - \frac{1}{2} \tilde{n}_{NO} \quad . \tag{135}$$

Equations 134 and 135 may be substituted in equation 132 to give

$$r^* = \frac{d \tilde{n}_{NO}}{d \theta} = P_{B_o} P^* \left\{ K_{PP_f} \left(\tilde{n}_{N_{2o}} + \frac{1}{2} \tilde{n}_{NO_o} - \frac{1}{2} \tilde{n}_{NO} \right) X \right. \tag{136}$$

$$\left. \left(\tilde{n}_{O_{2o}} + \frac{1}{2} \tilde{n}_{NO_o} - \frac{1}{2} \tilde{n}_{NO} \right) - K_{PP_d} \tilde{n}_{NO}^2 \right\} \quad .$$

Solution of Equations

If conditions along the path of a compression and expansion of the sample were known, equation 136 could be integrated over the path to predict the amount of NO formed or decomposed. Actually, if both NO and O_2 are present at the end of a cycle, they will react almost quantitatively by the relatively slow reaction

$$2NO + O_2 \rightarrow 2NO_2 \qquad (137)$$

to give NO_2. The mol fraction of NO_2 corresponding to the yield of NO predicted by integration of equation 136 may be compared with the mol fraction of NO_2 indicated by the mass spectrographic analysis of a product sample. The comparison will afford a test of the possible validity of the rate coefficients used in integrating equation 136.

Since the variables in equation 136 are not known from measurements, they must be determined by simultaneous solution of the differential equations describing the system.

In order to proceed with this solution, the value of F must be known. A first approximation for F was obtained from the equations in which the effect of reaction was neglected. Equation 85 was solved for F, giving values varying over a wide range, and including negative values, as shown in Table III. Since negative values are clearly impossible physically, they indicate errors in the assumptions made to deduce equation 85. This equation was obtained

from equation 68 by setting u* equal to zero at the point of minimum sample volume. The resulting value of "nominal friction," F, reflects errors in the many assumptions made to derive equation 68; it should be regarded as an energy correction factor rather than as effective mechanical friction.

Taking the value of F obtained from equation 85 as a first approximation, values of u* may be obtained by solving equation 119 simultaneously with 136 and the differential relation between time and the dimensionless volume parameter V*. This latter relation is

$$d\theta = -\frac{1}{u^*}\, dV^* \qquad (138)$$

for $u^* \neq 0$.

Solution of equation 136 implicitly requires that values of k_{pp_f} and k_{pp_d} be available over the necessary temperature range, and that the composition be known. The mol fraction of NO must be obtained by integration of equation 136;

$$\tilde{n}_{NO} = \tilde{n}_{NO_o} + \Delta \tilde{n}_{NO} \qquad (139)$$

so that

$$\tilde{n}_{NO} = \tilde{n}_{NO_o} + \int_{\theta_o}^{\theta} r^* \, d\theta \quad . \qquad (140)$$

Solution of equation 119 will, in general, yield a value of zero for u* at a point V^*_B which differs from the measured minimum volume. It is therefore necessary to try a new value of F and again integrate equation 119, repeating with new values of F until the point of predicted zero piston velocity agrees with the observed minimum volume. The value of F obtained might be regarded as a second approximation to the effective friction, since reaction 104 is no longer neglected, as it was in deriving equation 85.

Method of Solution

Analytical solution of the equations taking reaction 104 into account has not been possible. Solution of equation 119 involves use of the results of 136 and 138, and use of equation 136 implicitly requires solution of equation 140. Thus, integration of either of the equations 119 or 136 over the path requires knowledge of the variables along the path, and this implies that the results of the integrations are already known.

It seemed natural, therefore, to turn to graphical or numerical methods of integration. The objection to the graphical approach is that it is impossible to plot points for a curve to be used in graphical integration unless the results of the integration are already known. Also, the wide range of variation of some of the variables makes graphical procedures unwieldy. It was decided to employ numerical methods in obtaining solution of equations 119

and 136.

Finite difference forms of several of the differential equations were therefore required.

Equation 28, which describes the motion of the piston, is

$$\frac{m_p}{2} d(v^2) = (\omega_p - F)\, dx + P_A\, d\underline{V}_A + P_B\, d\underline{V}_B \quad ; \tag{28}$$

substitution of equivalent terms from equations 25, 37, 38, 66, and 67 gives

$$\frac{m_p}{2}\left(\frac{\underline{V}_{Bo}}{A}\right)^2 d(v^{*2}) = \frac{\underline{V}_{Bo}}{A}(F - \omega_p)\, dV^* - P_A \underline{V}_{Bo}\, dV^* + P_{Bo} P^* \underline{V}_{Bo}\, dV^* \tag{141}$$

Division by $\frac{\underline{V}_{Bo}}{A}$ results in

$$\frac{m_p \underline{V}_{Bo}}{2A} d(v^{*2}) = (F - \omega_p)\, dV^* - A P_A\, dV^* + A P_{Bo} P^*\, dV^* \tag{142}$$

A finite difference equation may be written, corresponding to integration of equation 142:

$$\frac{m_p \underline{V}_{Bo}}{2A} \Delta(v^{*2}) = (F - \omega_p)\, \Delta V^* - A P_{A_{eff}}\, \Delta V^* + A P_{Bo} P_{eff}^*\, \Delta V^* \tag{143}$$

Equation 143 involves no loss of accuracy, as compared to equation 142; the difficulty in application of 143 is that it is not usually possible to determine the proper "effective" values of the variables. An approximate form may be written as

$$\frac{m_p V_{B_0}}{2A} \Delta(v^{*2}) \cong (F - w_p)\Delta V^* - A P_{A_{av}} \Delta V^* + A P_{B_0} P_{av}^* \Delta V^* , \tag{144}$$

where the "average" quantities, obtained by some fairly arbitrary procedure, are employed in place of the "effective" values defined by equation 143.

When the piston is near the bottom of its stroke, the sample pressure P_B is large. In this region, the weight of the piston, the frictional drag force, and the force exerted on the piston by the air in the upper chamber, are all fairly small compared to the upward force exerted by the sample gas. Hence an approximate equation describing the motion of the piston near the bottom of the cylinder may be written by eliminating the smaller terms of 144:

$$\frac{m_p V_{B_0}}{2A} \Delta(v^{*2}) \cong A P_{B_0} P_{av}^* \Delta V^* \tag{145}$$

which may also be written as

$$\frac{\omega_p V_{B_o}}{2Ag A P_{B_o}} \Delta(v^{*2}) \equiv P^*_{av} \Delta V^* \quad . \tag{146}$$

An equation relating temperature to volume along the adiabatic, reversible path assumed to apply in the sample is equation 112. In the derivation of this equation, the effects of reaction 104 had been considered.

$$P_B dV_B = -N\tilde{C}_v dT - \Delta \tilde{E}_{f\phi NO} dN_{NO} \quad . \tag{112}$$

Making the substitutions indicated by equations 38, 115, 116, 117, and 118, equation 112 may be written

$$P^* dV^* = -\frac{\tilde{C}_v}{R} dT^* - \frac{\Delta \tilde{E}_{f\phi NO}}{R T_o} d\tilde{n}_{NO} \quad . \tag{147}$$

A finite difference equation corresponding to integration of 147 is

$$P^*_{eff} \Delta V^* = -\frac{\tilde{C}_{v\,eff}}{R} \Delta T^* - \frac{\Delta \tilde{E}_{f\phi NO\,eff}}{R T_o} \Delta \tilde{n}_{NO} \quad ; \tag{148}$$

the approximate form, employing average values of the variables, is

$$P^*_{av} \Delta V^* \cong - \frac{\tilde{C}_{v\,av}}{R} \Delta T^* - \frac{\Delta \tilde{E}_{f\,NO\,av}}{R\,T_o} \Delta \tilde{n}_{NO} \quad . \tag{149}$$

Similar approximate equations may be obtained for other relationships. Thus, integration of equation 131 and use of an average value of the variable results in

$$\Delta \tilde{n}_{NO} \cong r^*_{av} \Delta \theta \quad , \tag{150}$$

and similar treatment of equation 67 yields

$$\Delta \theta \cong - \frac{\Delta V^*}{U^*_{av}} \quad . \tag{151}$$

Summary of Finite Difference Equations

The equations useful in numerical evaluation of conditions along the path of a compression-expansion cycle will be recapitulated here.

The equation relating change in the volume of the system to changes in the temperature and composition is

$$P^*_{av} \Delta V^* \cong - \frac{\tilde{C}_{v\,av}}{R} \Delta T^* - \frac{\Delta \tilde{E}_{f\,NO\,av}}{R\,T_o} \Delta \tilde{n}_{NO} \quad . \tag{149}$$

The equation relating change in the volume of the sample to change in the velocity of the piston near the bottom of the cylinder is

$$\frac{m_p V_{Bo}}{2A} \Delta(U^{*2}) \cong A P_{Bo} P_{av}^* \Delta V^* \tag{145}$$

or

$$\frac{\omega_p V_{Bo}}{2Ag} \frac{1}{A P_{Bo}} \Delta(U^{*2}) \cong P_{av}^* \Delta V^* \,. \tag{146}$$

The change in composition may be obtained from

$$\Delta \tilde{n}_{NO} \cong r_{av}^* \Delta \theta \,, \tag{150}$$

in which the time increment is given by

$$\Delta \theta \cong -\frac{\Delta V^*}{U_{av}^*} \,. \tag{151}$$

The chemical rate equation employed is

$$r^* = \frac{P}{P_o} P^* \left\{ k_{pp_f} \left(\tilde{n}_{N_2 o} + \frac{1}{2} \tilde{n}_{NO_o} - \frac{1}{2} \tilde{n}_{NO} \right) x \left(\tilde{n}_{O_2 o} + \frac{1}{2} \tilde{n}_{NO_o} - \frac{1}{2} \tilde{n}_{NO} \right) - k_{pp_d} \tilde{n}_{NO}^2 \right\} \quad (136)$$

P* may be obtained from

$$P^* V^* = T^* \quad (43)$$

once the volume and temperature have been related.

Relation of k_{pp_f} to k_{pp_d}

Since the net rate of reaction at equilibrium is zero, it can easily be shown that

$$k_{pp_f} = K_p k_{pp_d} , \quad (152)$$

in which K_p is the equilibrium constant for reaction 104. By definition, this relation must hold when the system is at equilibrium. Presumably, the rate coefficients are independent of the degree of departure of the system from equilibrium, so that 152 holds even if the system is not at chemical equilibrium.

In view of the assumption of ideal gas behavior, K_p is identical with K_a, the thermodynamic equilibrium constant written in terms of activities. Values of the equilibrium constant for the reaction

$$\frac{1}{2} O_2 + \frac{1}{2} N_2 \rightleftharpoons NO \qquad (153)$$

have been tabulated for temperatures up to 5000°K by Rossini et al. (14). The desired equilibrium constant for reaction 104 is just the square of the constant for reaction 153. Numerical values are included in Table VII.

Procedure Used in Numerical Solution of Equations

Details of the procedure which was used to obtain a prediction of the yield of NO will now be described.

Such a prediction implicitly involves knowledge of the effective chemical rate coefficients. The selection of particular values to be tested will be discussed later; the range was such that the general calculation procedure was the same in all cases.

Reaction 104 does not occur to an appreciable extent except at rather high temperature, corresponding to piston positions very near the bottom of the initial downstroke. Except in this region, therefore, the behavior of the system is described by equations 42 and 68, in which the effect of reaction is neglected.

Using the functions ϕ and Ψ for the initial composition, and using the value of F obtained from equation 85, equations 42 and 68 were solved at values of temperature in the range where the rate of reaction was expected to become appreciable. For the nominal value of temperature, solution of equation 42 gave the corresponding value of V*,

and solution of equation 68 gave the corresponding piston velocity. The chemical reaction rate, based on these values of temperature and volume, and on the initial composition, was computed by means of equation 136. By calculating corresponding values of temperature, volume, reaction rate, and piston velocity, for a few points, it was possible to establish a point in the downstroke above which the predicted change in composition was less than a preassigned small quantity.

For the portion of the stroke near the bottom of the cylinder, the sample temperature is high and the rate of chemical reaction is significant. In this region, values of the variables were established for several points by solution of the finite difference equations summarized on page 69 .

As described above, conditions were determined for the point before which no appreciable composition change occurred. Values of the variables at the end of a small increment in the volume parameter V* were then obtained by trial and error, using a general scheme which was the same for all succeeding volume increments.

Calculations were made in tabular form. A sample of the form employed is shown in Table VI, which presents an arbitrarily chosen segment of the calculations for Test 41, using the rate coefficient formula of Daniels (17), equation 4.

The order of calculations performed for a given increment was as follows:

1) A volume increment was chosen; its size was a compromise between conflicting requirements. The use of very small increments would require a great amount of labor to complete a prediction of final composition. The use of very large increments would lead to uncertainties in the results of the calculations, so large as to make comparison among different assumed rate coefficients difficult. In general, the size of the increment was chosen to keep the change in volume below ten per cent, and to keep the variation in the net rate of reaction less than fifty per cent. If the change in composition was very small, greater relative variation in the net reaction rate was allowed.

2) On the basis of experience with immediately preceding increments, a trial value of ΔT^* was chosen. It was merely an educated guess, and no formalized procedure may be given. The trial value of ΔT^* was added to the value of T^* at the beginning of the increment, to give a trial value of T^* for the end of the increment.

3) On the basis of the trial value of T*, it was possible to obtain by straightforward calculations:

   a) The temperature, T.

   b) The rate coefficients, k_{pp_d} and k_{pp_f}. The value of k_{pp_d} was computed from an equation of the Arrhenius type, $k_{pp_d} = A e^{-\frac{\varepsilon_a}{RT}}$. Corresponding values of k_{pp_f} had been calculated by means of equation 152 for the temperatures at which the equilibrium constant had been tabulated by Rossini (loc. cit.). Values at intermediate temperatures were interpolated, assuming straight line segments between the tabulated values on a log k_{pp_f} vs. 1/T plot.

   c) The pressure parameter, P*, by equation 43.

   d) The equilibrium mol fraction of NO, if desired. For each run, values of $\tilde{n}_{NO_{eq.}}$ were tabulated over the range of interest at 100°R intervals. Values at intermediate temperatures could be obtained by linear interpolation, with negligible error.

4) Using the value of P* obtained, it was possible to solve equation 146 for $\Delta(v^{*2})$. P^*_{av} was taken as the arithmetic average of the values at the beginning and end of the increment.

5) Taking u^*_{av} as the arithmetic mean of the values at the beginning and end of the increment, the time required for the incremental volume change was computed by means of equation 151.

6) On the basis of previous experience, a trial value of $\Delta \tilde{n}_{No}$ was chosen. Addition of this to the value of $\tilde{n}_{No}$ at the beginning of the increment gave the trial value of $\tilde{n}_{No}$ for the end of the increment. The rate parameter r* at the end of the increment was then calculated by means of equation 136.

7) From the values of r* at the beginning and end of the increment, r^*_{av} was calculated. In some of the first calculations performed, it appeared that the geometric mean gave somewhat better effective values than did the arithmetic mean, so the geometric mean was employed in subsequent calculations. The variation in r* was in general such that the difference between the two averages was small, and no further calculations relative to this question were made. In regions where r* was rapidly passing through zero as a result of shifting equilibrium, the arithmetic average was employed.

8) The value of $\Delta \tilde{n}_{No}$ was then calculated by means of equation 150.

9) The equation 149 was then solved for ΔT^*. In making this calculation, a constant value of $\Delta\tilde{E}_{f_{\phi NO}}$ was used, corresponding to a temperature near the region of most reaction. In most cases this was chosen as 4250° R. The variation of $\Delta\tilde{E}_{f_{\phi NO}}$ with temperature is not great, as shown in Table VII. Corresponding to the assumption of constant $\Delta\tilde{E}_{f_{\phi NO}}$, it was also assumed that $\tilde{C}_v$ was not changed by the reaction. For each Test, a plot of $\frac{\tilde{C}_v}{R}$ vs. T was prepared. The value of $\frac{\tilde{C}_v}{R}$ used in equation 149 was read from the plot at the average temperature of the increment.

10) The procedure outlined in steps 2 through 9 was repeated until the values of ΔT^* and $\Delta\tilde{n}_{NO}$ obtained in steps 9 and 8 agreed with the trial values used in steps 3 and 6. In general, if agreement was not obtained, the values from steps 9 and 8 were used as the new trial values, although in some cases better choices appeared. When agreement was obtained, the procedure was carried on to the next increment.

The conditions of the sample were "followed" by the above procedure until the indicated value of u* was zero, corresponding to minimum sample volume. In general, the value of V* at this point did not agree with the value measured by means of the lead crusher gauge. As mentioned

previously, it would have been possible to begin the finite difference calculations again with a new guess for F; however, the discrepancies in the minimum value of V* were not felt to be large enough to justify the additional labor involved. The conditions of the sample were therefore followed, by use of the same finite difference equations, along the first upstroke of the piston, from the point of calculated zero velocity to a point where the rate of chemical reaction became negligible. The corresponding value of $\tilde{n}_{NO}$ was taken as the yield of NO. It was assumed that the NO would be converted to NO_2 by reaction with excess oxygen.

In the calculations, the effect of compression-expansion cycles beyond the first was neglected. The difficulty of making quantitatively useful and reasonable assumptions regarding friction and heat transfer beyond the first cycle was felt to be insurmountable, on the basis of the data obtained.

Determination of Chemical Rate Coefficients

The difficulties inherent in attempting to establish rate coefficients from the experimental data obtained with the ballistic piston have been mentioned previously.

Briefly, there is no straightforward procedure which permits calculation of the desired coefficients from the experimental observations. It is necessary to hypothesize a reaction mechanism and the concommitant rate constants

and to calculate predictions of yields based on the assumed constants. If a given set of rate constants leads to accurate predictions for a wide range of experimental conditions, the constants may be accepted with some confidence. If no accurate predictions are obtained, a different set of constants must be tried. If accurate predictions are obtained for a very limited range of experimental conditions, the agreement must be regarded as fortuitous.

The time and facilities available permitted only a limited program of calculations. In setting up such a limited program, it is desirable to have in mind an outline for a more complete calculation scheme; a general program for evaluating the factors in an Arrhenius equation will be discussed briefly.

For the bimolecular mechanism corresponding to the chemical equation

$$N_2 + O_2 \rightleftharpoons 2NO \quad , \tag{104}$$

the simplifying assumptions made led to a rate expression in the form of equation 124.

$$r = \frac{1}{V}\frac{dN_{NO}}{d\theta} = \frac{1}{RT}\left\{K_{pp_f} p_{N_2} p_{O_2} - K_{pp_d} p_{NO}^2\right\} \tag{124}$$

Even assuming that the rate coefficients are inde-

pendent of composition and of pressure, it is still necessary to consider their variation with temperature. The simplest formula having wide general application is the Arrhenius equation, which for k_{ppd} may be written

$$k_{ppd} = A\, e^{-\frac{E_a}{RT}} \quad . \tag{154}$$

In order to evaluate the constants A and E_a from the experimental data, a procedure such as the following might be adopted.

For an assumed value of E_a, predictions of final compositions would be made for several runs, for each of several assumed values of A. By comparison of these predictions with the observed final compositions, a curve of some error parameter as a function of A would be obtained. The value of A corresponding to the minimum value of the error parameter would be taken as the "best" value of A for the assumed value of E_a.

A similar calculation would be carried out for each of several assumed values of E_a, and the minimum value of the error parameter obtained for each value of E_a would be plotted as a function of the value of E_a. The "correct" value of E_a would be that for which the error parameter was at its absolute minimum. The corresponding value of the pre-exponential factor A could be obtained from a curve of the "best" value of A as a function of assumed E_a, read

at the "correct" value of E_a.

For this combination of A and E_a, the error parameter would be zero if the assumed mechanism and rate constant formula were strictly applicable, if all the assumptions used in calculating predicted compositions were justified, and if there were no experimental errors. Such a situation would correspond to exact prediction for all runs. Because of the possibility of experimental errors in determinations of composition, and because of errors in the assumptions made in calculating the paths followed by the samples, exact agreement is most unlikely. A reasonably low minimum in the error parameter, with no unaccountably bad predictions, would be taken as justification for the assumed mechanism and rate constant formula. If no values of E_a and A could be found which yielded reasonable predictions of final composition for a wide range of conditions, it must be concluded that the rate constant formula or the assumed mechanism must be inadequate.

In this work, it has been necessary to predict piston velocity and sample conditions as functions of piston position, as outlined on page 72ff. Since the path predicted depends on the particular values of E_a and A chosen, a set of calculations must be carried out in detail for each combination of E_a and A. For example, it would not in general be possible to use the temperature-volume path calculated for one combination of E_a and A for any of the other combinations, but a new path must be obtained.

Choice of Rate Constants Tested

The calculation of the "best" values of E_a and A by the foregoing procedure would require much time. It was therefore decided to make predictions for a few selected values of the constants E_a and A and to see what conclusions might be drawn from the results.

It was decided to begin with one of the more promising of the existing rate constant formulas. Equation 4, developed by Daniels (17) from data in the range 1450-1850° C, was chosen. It will be renumbered here.

$$K_{pp_d} = 10^9 e^{-\frac{69{,}500 \text{ cal/gmol}}{RT}} \quad atm^{-1} sec^{-1} , \tag{155}$$

which may also be written

$$\log_{10} K_{pp_d} = 9 - \frac{2.734023 \times 10^4}{T, (°R)} \tag{156}$$

Using this equation for k_{pp_d} and following the procedure outlined on page 72 , predictions of final NO_2 yield were made for six of the experimental runs. The values of the friction factor F found by neglecting reaction were employed in predicting the piston velocities, and no corrections were made to get agreement of predicted and observed minimum vol-

umes.

The results are presented in Table VIII, where the observed yields are repeated for ease of comparison. Good agreement is achieved for only one of the six runs, Test 43. In two cases, 39 and the decomposition run, 45, the agreement appears very poor.

No calculations were made for Test 42; it was felt that because of the extremely high temperature reached, the assumption of no heat loss would lead to too great an error. No calculations were made for the final four runs, for which the mass spectrographic analyses showed some internal inconsistencies. From the six, for which calculations were made using equation 156, four were selected as representing a wide range of experimental conditions. Subsequent calculations were made for these four runs.

Variations of Rate Constant Formula

Once it had been decided that investigation of all possible combinations of E_a and A in the Arrhenius equation was too laborious, there were many possible choices for a limited program of calculations. It would have been possible to hold the value of E_a at the level suggested by Daniels, and investigate a few values of A, or several values of E_a might have been investigated, for the one value of A.

A still different approach was adopted, which, it was hoped, might yield clues to the order of magnitude of the

effective rate constant k_{pp_d} in the high temperature range.

This approach consisted of assuming that the factors in equation 155 adequately predicted the rate in the range $t \leq 1650^{\circ}$ C, and investigating the effect of varying E_a for higher temperatures. The temperature of 1650° C was the midpoint of the range for which equation 155 was proposed by Prof. Daniels. Its choice was somewhat arbitrary. Above 1650° C, the form of equation 154 was assumed to apply, with different values of E_a being tried. The corresponding values of A were computed such that the formulas would predict the same value of k_{pp_d} at 1650° C as given by equation 155. The values of E_a tested were 40,000 15,000, and zero. The corresponding Arrhenius equations were, in logarithmic form: for E_a = 40,000 cal/g mol,

$$\log_{10} k_{pp_d} = 5.647634 - \frac{1.573539 \times 10^4}{T, (^{\circ}R)} \qquad (157)$$

for E_a = 15,000 cal/g mol,

$$\log_{10} k_{pp_d} = 2.806645 - \frac{0.590077 \times 10^4}{T, (^{\circ}R)} \qquad (158)$$

for E_a = 0,

$$\log_{10} k_{pp_d} = 1.102052 . \qquad (159)$$

In each case, the corresponding units of k_{pp_d} are atm^{-1} sec^{-1}. The values of the rate coefficients given by each of the equations are tabulated for the temperature range of interest in Table VII. A logarithmic plot of the four equations is given in Figure 15.

In making a prediction of final NO yield for a run, the values of k_{pp_d} used, therefore, corresponded to two interesting straight line segments on a plot of log k_{pp_d} vs. $\frac{1}{T}$. In the range below 1650° C, equation 156 was used. In the range above 1650° C, the equation was either 156, 157, 158, or 159 as the case might be. Calculations were made for the four runs chosen, using the finite difference procedure described on page 72 . In all cases, the value of F obtained by neglecting reaction was employed, and no second approximation was made to get better agreement of predicted and observed minimum volume.

It was realized that, because of the arbitrary choice of equation 155 below 1650° C and the use of the two-slope representation of log k_{pp_d} vs. $\frac{1}{T}$, the "best" value of E_a above 1650° C would have no great significance as an indication of the "true" activation energy. It was hoped, however, that some idea of the magnitude of k_{pp_d} as a function of temperature might be obtained.

The results of the calculations are given in Table VIII, and the values of several error parameters are shown in Table IX.

It would not be feasible to include the details of all of the finite difference calculations used in obtaining the predictions listed in Table VIII. An effort has been made to summarize several significant points in Table X. This table includes the extreme conditions predicted in each calculation, an indication of the range of variables over which reaction is predicted to be significant, and an indication of the region in which the predicted composition begins to depart markedly from the equilibrium composition.

In an effort to show some of the other important relations indicated by the calculations, Tables XI through XVIII and Figures 16 through 30 were prepared. The predictions based on equation 156 and on equation 159 are given. These two represent, respectively, the highest and the lowest values of k_{pp_d} for a given temperature and were therefore selected as illustrations. In the tables, the predicted temperatures, net reaction rates, mol fractions of NO, and times are given for several values of the volume ratio V*. Some of the relations indicated in the tables are shown graphically in Figures 16 through 30.

In Figure 16, the volume-time relations in the region of interest are shown, based on the use of equation 156. The shapes and relative positions of the various tests on this plot would be similar for the other rate equations although small variations would occur.

The relation of temperature to volume, as predicted using equation 156, is shown in Figure 17 for the four runs. The differences between the compression and expansion paths are due to the effect of the energy of the chemical reaction. This effect is especially pronounced in the case of Test 45. Similar asymmetry is exhibited in the temperature-time relations shown in Figure 18.

The predicted chemical rates and compositions are indicated in Figures 19 through 30. The use of the rate constants indicated by equation 156 results in general in a path which approaches the equilibrium composition closely near the bottom of the compression stroke. The approach to equilibrium is pronounced for the runs reaching higher temperature. As shown in Figure 29, the system in Test 41 follows the equilibrium composition over a large portion of the temperature range, if the rate constants are as high as indicated by equation 156. The use of the much smaller constants indicated by equation 159 results in prediction of much greater departure of the system from chemical equilibrium.

The predicted net rate of reaction at a point depends on many factors. These include the temperature, pressure, and composition of the sample. The degree of approach to equilibrium is very important, and since the temperature is changing, the equilibrium mol fraction of NO is itself changing with time. The predicted composition depends upon the path up to the point in question. The figures

cited above show that, when plotted as a function of a single variable, such as temperature or time, the rate presents a picture which is by no means simple.

It can be appreciated, therefore, that it is difficult to predict the final composition for a run without going through a detailed calculation of the entire path.

Other Calculations

Although it still appeared difficult to draw definite conclusions regarding the rate constants from the results of the finite difference calculations, it seemed clear that generally better predictions may be obtained by the use of rate constants somewhat smaller than those given by equation 156. This observation suggested other calculations which could be relatively easily performed.

The equation for the rate of change of the mol fraction of NO was

$$r^* = \frac{d\tilde{n}_{NO}}{d\theta} = P_{B_o} P^* \left(k_{ppf} \tilde{n}_{N_2} \tilde{n}_{O_2} - k_{ppd} \tilde{n}_{NO}^2 \right) \qquad (132)$$

As has been observed, the integration of this equation is complicated by several factors. P* and the k's at any point are functions dependent on the previous path. Probably the most troublesome effect arises from the reversibility of the reaction; unless the system is far from equilibrium, the terms in the braces in equation 132 are

comparable, and for close approach to equilibrium they are very large compared to the difference between them.

However, if the rate constants used are fairly low, the system may be well away from equilibrium at the highest temperature achieved in a run. Should the predicted composition cross the equilibrium composition at a lower temperature on the expansion stroke, the net rate will be low at that point. Such a situation is illustrated in Figures 27, 28, 29, and 30 for the predictions based on the low rate coefficients of equation 159.

For such circumstances, a fair approximation to the total change in the mol fraction of NO may be obtained by neglecting one of the terms in braces in equation 132. Thus, for the formation runs, in which the initial sample contains nitrogen and oxygen,

$$\Delta \tilde{n}_{NO} = \int r^* d\theta \cong \frac{P}{B_o} \int P^* k_{PP_f} \tilde{n}_{N_2} \tilde{n}_{O_2} d\theta \quad . \tag{160}$$

The mol fractions of nitrogen and oxygen do not change greatly, so the use of average values will contribute an error certainly less than ten per cent. Using average values, equation 160 may be written

$$\Delta \tilde{n}_{NO} \cong \frac{P}{B_o} \left(\tilde{n}_{N_2} \tilde{n}_{O_2} \right)_{av} \int P^* k_{PP_f} d\theta \quad . \tag{161}$$

A similar expression may be written for runs in which the initial sample contains NO rather than oxygen.

$$\Delta \tilde{n}_{NO} \cong -\frac{P}{B_0}\left(\tilde{n}_{NO}^2\right)_{av} \int P^* K_{PP_d}\, d\theta \,. \tag{162}$$

In this case, the variation in $\tilde{n}_{NO}$ is likely to be significant, perhaps by a factor of 2 or 3, so that the choice of the average is more critical.

The integral $\int P^* K_{PP_f}\, d\theta$ or $\int P^* K_{PP_d}\, d\theta$ may be evaluated with fair accuracy even if the details of the path are not precisely known. Because of the influence of reaction energy on the predicted temperature, the details of the pressure-temperature and time-temperature relations cannot be determined in advance of determination of the composition-temperature relation. However, for a given temperature, the corresponding pressure and piston velocity can be estimated with fair accuracy, certainly within 5 or 10 per cent, by using the values from a previous finite difference calculation, or perhaps by using the path calculated neglecting the effect of reaction entirely.

The main difficulty lies in predicting the maximum temperature attained. Because the piston velocity is low in the region of maximum temperature and the time in a given temperature interval therefore relatively long, most of the change in composition will occur near the

maximum temperature.

By suitable choice of a path from among those indicated by the previous finite difference calculations, it should be possible to obtain a fair approximation to the temperature-pressure and temperature-time relations, without performing the laborious numerical integrations for each rate constant formula.

The advantage of the calculations based on equations 161 and 162 and making use of previously determined temperature-pressure and temperature-time relations, is as follows. It becomes rather simple, for a given value of E_a, to determine the corresponding pre-exponential factor, A. Using equation 154, the Arrhenius equation, as the description of k_{ppd} , and making use of equation 152, equation 161 may be written as

$$\Delta \tilde{n}_{NO} \equiv \frac{P}{B_o}\left(\tilde{n}_{N_2}\,\tilde{n}_{O_2}\right)_{av} \int P^{*} K_p\, k_{ppd}\, d\theta \tag{163}$$

or

$$\Delta \tilde{n}_{NO} \equiv \frac{P}{B_o}\left(\tilde{n}_{N_2}\,\tilde{n}_{O_2}\right)_{av} \int P^{*} K_p\, A\, e^{-\frac{E_a}{RT}}\, d\theta \tag{164}$$

or

$$\Delta \tilde{n}_{NO} \equiv P_{B_o} \left(\tilde{n}_{N_2}\, \tilde{n}_{O_2}\right)_{av} A \int P^* e^{-\frac{E_a}{RT}} K_p \, d\theta \,. \tag{165}$$

For the "decomposition" runs, equation 162 may be written as

$$\Delta \tilde{n}_{NO} \equiv -P_{B_o} \left(\tilde{n}_{NO}^{\,2}\right)_{av} A \int P^* e^{-\frac{E_a}{RT}} \, d\theta \,. \tag{166}$$

In both cases, the change in the mol fraction of NO is seen to be directly proportional to the pre-exponential factor A. Thus, for a given value of E_a, the value of A may be calculated for any run from the observed change in the fraction of NO.

The neglect of the reversibility of the reaction and the use of temperature-pressure and temperature-time relations not exactly in correspondence with the predicted composition may lead to some error. Even so, it was felt that values of A in error even by as much as a factor of 2 or 3 would be useful in the attempt to estimate effective rate constants in the temperature region up to 5000° R.

Procedure for Calculations Neglecting Reverse Reaction

Values of activation energy reported in the literature are all fairly high. The value of 69,500 cal/g mol suggested by Daniels seems fairly representative. Calculations were therefore based on the use of the rate equa-

tion 156, and were made for three runs, Tests 36, 39, and 45. Unless the rate constants were extremely small, the samples in test 41 would approach equilibrium at the maximum temperature, so that in this case calculations based on neglect of reversibility would not be useful. In the other cases corresponding values of pressure, temperature, and time were taken from one of the sets of numerical integrations previously described. In each case, the set chosen was that for which the final yield of NO was closest to the observed value. Thus, for Tests 39 and 45, the path obtained by use of equation 159 was used, and for Test 36, the path based on equation 158 was used.

For each of the values of the volume ratio V* used in the previous numerical integration, the value of k_{pp_d} was calculated from equation 156, or the value of k_{pp_f} was calculated as described on page 75 . From this value of k_{pp} and the values of P* and θ obtained in the previous numerical integration, a plot of $P^* k_{pp}$ vs. θ was prepared. By graphical integration, the integral $\int P^* k_{pp} \, d\theta$ was evaluated.

For purposes of illustration, the calculations for Test 36 are shown in Table XIX, in somewhat abridged form, and in Figure 31. The curves for the other tests are similar.

The results for the three tests considered are given

in Table XX. The results for the decomposition run, Test 45, seem to indicate a smaller value of A than do the results of the formation runs, 36 and 39.

V. DISCUSSION

The results of the finite difference calculations based on equations 156-159 have been summarized in Tables IX and X. The results of the calculations based on an activation energy of 69,500 cal/g mol and neglecting the effects of reverse reaction have been given in Table XX.

Errors

In attempting to interpret the foregoing results in terms of possible values of k_{ppd}, it is desirable to keep in mind the limitations imposed by errors in the many simplifying assumptions made, and by possible errors in the data used. No precise calculations of these errors were made, but, for most of the assumptions, the magnitude of the errors introduced can be estimated.

Probably the most serious error in prediction of composition from a given Arrhenius formula arises from error in the predicted temperature. For a reasonable activation energy, say 30,000 to 70,000 cal/g mol, the rate constant is a strong function of temperature, and errors of a few per cent in temperature may mean large errors in the values of the rate constants.

An important source of error tending to make the calculated value of temperature too high is the neglect of heat loss. The paths to which the samples were subjected

were so complicated that it is hard to make realistic estimates of this effect. Some very rough estimates of energy loss were made assuming radiation to be the chief mechanism. More recently, estimates have been made on the basis of new experimental measurements (28).

Because the maximum temperatures were so high, it seemed reasonable that radiation was an important mechanism for energy loss. Upper limits to the amount of energy lost by radiation were estimated by considering transfer between black surfaces having, respectively, the temperatures of the gas and of the walls. For a run with maximum temperature near 5000° R, the energy lost by radiation should not have exceeded five per cent of the energy put in by compression, even if the effective emissivity of the gas was almost unity. The actual emissivity of a sample was probably much less than 1.0. The effective emissivity of NO for the conditions of interest may be as high as 0.3 (29,30), while nitrogen, oxygen, and helium have very low emissivities (31). The effective emissivities of the samples may have been increased by the presence of small amounts of substances such as NO_2 and perhaps CO_2 and SO_2, but the concentrations of these substances cannot be reliably estimated.

In recent experiments with the ballistic piston apparatus (28), the rise in temperature of a small, thin disc

mounted in the bottom of the cylinder was observed. Preliminary analysis of the results was made for a series of runs in which the initial samples contained 40 mol per cent nitrogen, 20 per cent oxygen, and 40 per cent helium. Depending on the conditions of the runs, the heat lost to the bottom of the cylinder and to the lower face of the piston varied from about five per cent to about thirteen per cent of the energy put in by compression of the sample. Some additional energy was undoubtedly lost to the vertical walls of the cylinder, but this has not been measured. In some other runs in which the initial samples contained only nitrogen and helium, so that less radiation would be expected, the heat loss appeared generally less but was still significant, so mechanisms other than radiation may be important in determining the total heat loss.

In order to investigate the effects of error in temperature for a reasonable value of the activation energy, calculations were made based upon the paths obtained in the numerical integrations in which an activation energy of 40,000 cal/g mol had been used above 1650° C. It was desired to consider the effects of heat loss, but detailed estimation of this energy loss was regarded as impossible. A somewhat arbitrary device was adopted, which would give results qualitatively similar to the effects of heat loss. The calculations for each run were based on the numerical integrations already carried out, in which heat loss had been neglected. The position-time relation determined in

the previous integration was retained. For each point on the compression stroke, a new value of the temperature was taken, equal to 90% of the value obtained in the previous calculations. For points on the expansion stroke, a new value was obtained by subtracting from the old value, ten per cent of the maximum value obtained in the previous calculations.

Using the previous position-time relation and these new values of temperature, final NO mol fractions were calculated by numerical integration of equation 136. The values of k_{pp_d} and k_{pp_f} were obtained from equations 157 and 152 using the "new" temperature. As in the previous numerical integrations, a trial-and-error solution over each increment was necessary to determine the composition, since the rate is a function of the composition.

The results of these "decreased temperature" calculations are shown in Table XXI. The effect of reducing the predicted temperature is striking in some cases, especially Test 39. In others, notably Test 41, almost no change in the predicted final mol fraction of NO occurs.

An explanation of the differences in behavior may be seen by reference to Figure 32, which shows qualitatively the predicted mol fractions as functions of temperature for two hypothetical runs in which the maximum temperatures achieved are, respectively, rather high and relatively low.

In the high temperature run, if the predicted maximum temperature is arbitrarily reduced to, say, ten or fifteen

per cent below that first calculated, the new maximum temperature will still be within the range for which the rate constants are very large. The predicted composition at the new maximum temperature will still fall nearly on the equilibrium curve, although at a lower point. In the temperature region in which the predicted composition begins to depart from the equilibrium curve, there will be some differences due to changes in the pressure-temperature and time-temperature relations, but these will be small, especially if the predicted composition has followed the equilibrium path over a large temperature range. The predicted final mol fraction may well be nearly the same as calculated for the original high maximum temperature.

In the low temperature run, most of the change in composition takes place in a very small temperature range near the maximum temperature. For this run, a reduction of ten or fifteen per cent in the predicted maximum temperature will mean a large change in the maximum values attained by the rate coefficients.

The reduction in pressure at the point of maximum compression will be of the same order as the reduction in maximum temperature, i.e. ten or fifteen per cent. The length of time for which the piston is near the bottom of the cylinder will be increased, but by a small relative amount (roughly proportional to the inverse one-half power of the relative reduction in pressure). The compo-

sition was assumed to be well below equilibrium in the region of appreciable rate, so the effect of the reverse reaction will be small. For the low temperature run, therefore, the yield of NO will be roughly proportional to the value of k_{pp_f} at the bottom of the stroke of the piston, so that a change of ten or fifteen per cent in the predicted temperature may well result in a change by a factor of ten in the predicted yield.

The foregoing consideration of the behavior in a "high temperature" run, and of that in a "low temperature" run, shows why it is reasonable that, for a given rate coefficient formula, the predicted yields in some runs may be affected very little by errors of ten or fifteen per cent in calculated temperature, while in other runs the effect may be very large. If the maximum temperature of a run is between the extremes considered, the predicted composition will approach equilibrium at the maximum temperature but will not follow the equilibrium curve over a large temperature interval. In such a case, the effect on predicted yield of reducing the predicted temperature will be intermediate, as determined by the conditions of the run considered.

In computing the volume-temperature relations along the isentropic path assumed, it was assumed that the samples were perfect gases. A consideration of generalized compressibility factors based on the law of corresponding

states (32) indicates that, although the maximum pressure achieved in a typical run was very great, the corresponding temperature was so high that the compressibility factor would not have been more than about ten per cent in excess of unity, even at the extreme conditions. Over most of the path, the departure from ideal gas behavior would have been less. In the case of the high-pressure run, Test 36, departure from ideal behavior may have been as much as twenty per cent in the compressibility factor, at the extreme conditions. Similar estimates of the departure from ideal gas behavior were obtained using the co-volumes tabulated by Longwell (5).

Departure from perfect gas behavior is reflected in errors in the calculated temperature. If chemical reaction is neglected, the isentropic temperature volume derivative may be written in terms involving the compressibility factor as

$$\left(\frac{\partial T}{\partial V}\right)_S = \frac{-P\left(1 + \frac{T}{Z}\left(\frac{\partial Z}{\partial T}\right)_V\right)}{C_v\Big|_{P=0} + \int_{V=\infty}^{V} \frac{P}{Z}\left\{2\left(\frac{\partial Z}{\partial T}\right)_V + T\left(\frac{\partial^2 Z}{\partial T^2}\right)_V\right\} dV} \quad . \tag{167}$$

Rough estimates based on compressibility factors determined from published virial coefficients (33) indicate that this derivative, for the real gases at typical extreme conditions, may exceed the ideal gas value by as much as ten per cent. Since it will be closer to the ideal gas value over much of the path, the error in the

maximum temperature, calculated from the observed compression ratio, will be somewhat less, perhaps about five per cent.

The determination of the equilibrium mol fraction of NO for a given temperature may be in error as a result of the assumption of ideal gas behavior. Some idea of the magnitude of the error involved may be gained by considering an ideal solution of the real gases involved. With this assumption the thermodynamic equilibrium constant for reaction 104 may be written as

$$K = \frac{f_{NO}^2}{f_{N_2}\, f_{O_2}} = \frac{\tilde{n}_{NO}^2\, f_{NO}^{\circ 2}}{\tilde{n}_{N_2}\, \tilde{n}_{O_2}\, f_{N_2}^{\circ}\, f_{O_2}^{\circ}} = \frac{\tilde{n}_{NO}^2\, \nu_{NO}^{\circ 2}}{\tilde{n}_{N_2}\, \tilde{n}_{O_2}\, \nu_{N_2}^{\circ}\, \nu_{O_2}^{\circ}}, \qquad (168)$$

where the fugacities and mol fractions are those existing at equilibrium.

The relative error in the determination of the equilibrium mol fraction of NO, caused by assuming ideal gas behavior, will be roughly proportional to the difference between $\left(\frac{\nu_{NO}^{\circ 2}}{\nu_{N_2}^{\circ}\, \nu_{O_2}^{\circ}}\right)^{\frac{1}{2}}$ and unity. Inspection of the generalized fugacity chart (32) shows that this error is small, since $\nu_{NO}^{\circ 2}$ is not much different from $\nu_{N_2}^{\circ}\, \nu_{O_2}^{\circ}$. The error introduced may be as much as one or two per cent, at typical extreme conditions. This uncertainty in the equilibrium mol fraction of NO at the extreme conditions is very small compared to that resulting from the fact that the maximum

temperature is not precisely known.

In all of the calculations in this thesis, it was assumed that the only chemical reaction of significance was the formation of nitric oxide from the elements. It is possible, and even likely, that other reactions did occur. The mass spectrographic analyses of the product samples indicated the presence of CO_2, SO_2, and N_2O in various samples. The SO_2 may have resulted from oxidation of the "molylube" used to lubricate the cylinder. This lubricant contained a fraction of one per cent of carbon as an impurity, hardly enough to account for the amount of CO_2 reported. The CO_2 may have resulted in part from oxidation of the steel of the apparatus or from oxidation of the neoprene O-ring. It is possible that some of the mass peak reported as CO_2 really represented N_2O. Very probably it merely resulted from oxidation of residual carbon on the filament of the mass spectrograph apparatus (24). The water reported in several of the samples is undoubtedly an error in the analyses.

None of the compounds mentioned above appeared in large concentration, so their influence on the predicted composition is not significant. However, because of the high unit energies involved, the formation of even a small amount of any of these compounds would have a significant effect on the temperature of the sample.

Other reactions which would have slight effect on the

composition but considerable effect on the temperature of the sample include ionization and dissociation. The extent of ionization is probably small (34), but the extent of dissociation may be significant. Formation of equilibrium amounts of O and N (35), at the maximum temperature of a typical run, would require sufficient energy so that the temperature calculated neglecting this effect might be high by as much as ten per cent. An attempt to correct the calculated temperature and composition, taking ionization and dissociation into account, would require information as to the rates of these reactions, as well as the existing information on the equilibrium behavior.

The formation of NO_2 from NO and oxygen is among the reactions neglected. Actually there may be some oxidation of NO, even at the highest temperatures of the runs.

Equilibrium constants for the reaction

$$NO_2 \rightleftharpoons NO + \frac{1}{2} O_2 \qquad (169)$$

were determined in the classical experiments of Bodenstein et al. (36). Values for even temperatures have been calculated from this data by Giaque and Kemp and are summarized by Yost and Russell (37). The equilibrium constant is given as

$$K_p = \frac{P_{NO} P_{O_2}^{\frac{1}{2}}}{P_{NO_2}} \qquad (170)$$

The equilibrium ratio of NO_2 to NO depends on the partial pressure of oxygen. Rearrangement of equation 145 to solve for this ratio gives

$$\frac{P_{NO_2}}{P_{NO}} = \frac{P_{O_2}^{\frac{1}{2}}}{K_p} \quad . \tag{171}$$

For each of the runs under consideration, approximate values of this ratio were estimated for the temperature region of interest. The pressure-temperature relation was taken from the finite difference calculations based on equation 156. A constant mol fraction of oxygen, as large as was to be expected in the range, was used. Values of K_p were extrapolated from the values given by Yost and Russell. Consideration of available heat capacity data (25,26) indicates that the extrapolated values of K_p are not seriously in error. The estimated equilibrium ratios of NO_2 to NO are shown in Figure 33. It is seen that, in the temperature range in which the rate of the primary reaction is believed to be significant, the fraction of NO oxidized to NO_2 is not large, even if the equilibrium amount of NO is formed.

No data on the rate of oxidation of NO is available for the temperature range of interest. The rate of oxidation at somewhat lower temperatures was studied by Bodenstein and Lindner (36), and found to be of third order. More recent studies have proposed mechanisms not involving third order

reactions (38,39), but the empirical third order rate constants of Bodenstein seem to give reasonable prediction of observed rates, especially outside the very low pressure range (39,40). Rate constants were extrapolated from the data of Bodenstein, as recalculated by Yost and Russell (37), and were used to estimate the rates of conversion of NO to NO_2. It appears that, for Test 36, the ratio of NO_2 to NO should be nearly the equilibrium value, but that, for the other tests, it may be somewhat less.

Below about 3000° R, the equilibrium ratio of NO_2 to NO increases rapidly with decreasing temperature, even at low pressure. If, in later studies, it should develop that the rate of the primary reaction, equation 104, is significant even below 3000° R, the formation of NO_2 will have to be taken into account.

As a result of neglect of the formation of NO_2 at high temperature, the predicted final yields of NO_2 will be slightly too low. If more precise estimates of the temperature become possible, it will be desirable to consider the formation of NO_2. While the influence of this reaction on the predicted composition is its most important effect, the energy liberated by the exothermic oxidation of NO will have a small effect on the calculated temperature. For present purposes, the fraction of NO converted to NO_2 is small enough, even if equilibrium is reached, so that the conclusions regarding the order of magnitude of the rate

constant are not affected by neglecting formation of NO_2.

The possibility of catalyzed reactions was ignored in the calculations. It seems almost certain that the steel of the piston and cylinder remained so cold that even catalytic reaction would be most unlikely at the walls. However, finely divided particles of the lubricant used to coat the cylinder might well become dispersed throughout the sample and become relatively hot.

Tests 50 and 51 were made in an attempt to investigate the possibility of catalytic effects. Except that graphite was used, instead of "molylube," as the lubricant, an attempt was made to duplicate the conditions of Test 43. The first attempt, Test 50, resulted in a minimum volume somewhat smaller than desired; on the basis of experience with this test, Test 51 was run and calculated extreme conditions nearly in agreement with those of Test 43 were obtained.

The yields of NO_2 from these tests, using graphite, were much smaller than was the yield in Test 43. At first glance, it might appear that the catalytic effects were very significant. Unfortunately, the mass spectrographic analyses for the later tests were not obtained from the same source as was that for Test 43. The later group showed some internal inconsistencies, and may be subject to question. Difference in lubricating effectiveness may partially explain the difference in yields. From the calculated "friction" values for Tests 43 and 51

(Table III), it appears that graphite is a substantially better lubricant. It is thus a possibility, although remote, that only one stroke of the piston was significant in influencing composition in Test 43, but that in Tests 50 and 51, later "bounces" of the piston produced temperature high enough to cause decomposition of NO in the sample.

Leakage of the sample past the leading edge of the piston and past the O-ring seal cannot be precisely calculated as a function of piston position, and was neglected. On the first run, Test 36, erosion of the piston head indicated some flow of hot, expanding gases out of the sample chamber. The piston head used in this run was discarded, and a new head, having a somewhat tighter fit in the cylinder (clearance about .001 inch) was made from stainless steel. Only a small amount of erosion of this new piston head occurred, although several runs were made using it.

The use of the annular space around the middle of the piston and the use of an O-ring seal at each end of the piston made it very unlikely that the driving air could leak into the sample during a run, but such leakage may not be entirely impossible.

In some of the runs, the piston position and corresponding sample pressure were measured after the run, as well as before. The net molal leakage from the sample could be calculated from this information after the product

composition was determined, assuming no solid or liquid products had been formed. The results for some of the runs are shown in Table XXII. The net loss indicated is generally less than five per cent. It is subject to some uncertainty since it depends on knowledge of the product composition; the formation of solid or liquid products would be interpreted as leakage.

The error introduced by neglecting leakage depends somewhat on the details of leakage rate as a function of piston position, but the figures for net losses give an idea as to the magnitude of the error.

Another assumption which is not strictly correct is that the samples remained uniform. Since the maximum velocities attained by the piston were well below sonic velocity, it is probable that no shock waves or significant pressure gradients existed in the sample. Since the heat lost may have amounted to something like ten per cent of the energy added by compression, it is possible that appreciable thermal gradients existed. It was felt that the combined effects of conduction, radiation, and turbulence were too complicated to admit useful estimates of the magnitude of non-uniformity in temperature. In calculating compositions from a given rate constant formula, no attempt was made to consider non-uniformity in temperature. The possibility of errors from this source should be borne in mind.

In all of the predictions of final composition, it was assumed that only one stroke of the piston was significant in determining the composition. As has been mentioned earlier, it is to be expected that the piston will reverse its direction of motion several times before coming to rest. It is possible that, in each of several successive compressions of the sample, its temperature would be raised to a level high enough to cause reaction.

It was felt that the effects of friction, heat loss, side reaction, etc., were so complicated that no quantitatively useful results could be obtained by continuing the numerical integrations beyond the first compression and expansion of the sample. Certain qualitative observations would seem to indicate that the first compression was much "harder" than those following, but that more than one clearly occurred. The noise produced by operation of the apparatus is considerable. In this series of runs, the conclusion that the oscillations of the piston were rapidly damped out was qualitatively supported by the audible effects.

In some later runs on the nitrogen-helium system, a piece of paper was taped to the outside surface of the cylinder, near the bottom. The point of a pencil supported from the concrete floor of the laboratory was lightly held against the paper. Some vertical motion of the cylinder in its supports was possible, and, when the piston was released from its initial position, the reaction was sufficient to cause a displacement of the cylinder of roughly

half an inch. Examination of the paper after the run showed traces of several oscillations. No attempt was made to determine the quantitative relation of motion of the cylinder to motion of the piston; the results indicated that the displacement of the cylinder caused by the first stroke of the piston was at least twice that caused by the second.

The galvanometer records obtained in the preliminary tests of the thermal flux meter (28) indicated that the heat loss from the sample was significant for perhaps four or five oscillations of the piston. The loss on the second compression may have been as much as one-half of the loss during the first. It is likely that the loss was proportional to a power of the sample temperature higher than the first, so that the temperature may have been high for several compressions. These records, however, were obtained from runs in which graphite was the lubricant, and in which friction was less than in the runs considered here.

Before the numerical integrations described on page 82 were carried out, some preliminary calculations had been made for a hypothetical run in which the conditions were fairly representative of the conditions of the actual runs. The sample was taken to be 50 per cent helium, 25 per cent nitrogen and 25 per cent oxygen, at an initial pressure of 2.2 psia and temperature of 77° F. The pressure of the driving air was taken as 1000 psia, and the frictional drag force F was assumed to be 50 lbs. The extreme condi-

tions achieved in successive compressions are shown in Table XXIII. In making these estimates, the usual assumptions of no heat loss and no leakage were made, and the effect of chemical reaction was neglected. It is seen that, for these assumed conditions, four or five strokes of the piston may be of sufficient intensity to cause reaction in the sample. The decline in maximum temperature between successive compressions of the sample is roughly proportional to the frictional force F, so that the effect of using a value other than 50 lbs can be estimated. In an actual run, factors such as heat transfer would tend to damp out the oscillations of the piston much more rapidly. It is also possible that in some runs, large frictional forces came into play near the bottom of the first stroke.

For the same hypothetical run, numerical integrations were carried out to predict final composition. These calculations were based on a procedure similar to that outlined on page 72 , but using a slightly different rate constant formula suggested by Daniels (10). This formula, mentioned previously, was

$$K_{cc_d} = 1.64 \times 10^{11} e^{-\frac{69500 \frac{cal}{g\,mol}}{RT}} \frac{liter}{g\,mol\ sec} \quad . \qquad (3)$$

This equation implicitly assumes concentration as a driving force. The difference between rates calculated using equation 3 and those obtained from equation 155 is not

large.

The numerical integrations were carried out for two successive strokes of the piston. The results are given in Table XXIV; the predicted mol fraction of NO after the second compression is nearly as large as after the first. This close agreement is largely fortuitous. In both strokes, the predicted maximum temperature was so large that the predicted composition followed the equilibrium path over an appreciable temperature range. If the integrations were carried out over more strokes of the piston, the predicted final composition would undoubtedly involve less NO_2, perhaps as little as one half of one mol per cent. Detailed calculations of the effects of more oscillations were not carried out, since it was felt that the assumptions were so weak that the results would be of little value.

Errors from calculation procedures

Even if the assumptions regarding the physical situation were correct, the predicted values of temperature, pressure, and composition obtained by numerical and graphical techniques are subject to some error. As mentioned previously, the sizes of the increments were chosen to keep the errors reasonably small. In most cases the error introduced in the predicted final mol fraction of NO_2 was probably less than five per cent of the indicated value. The use of smaller intervals would not be justified unless

several more important sources of error were corrected.

The disagreement between predicted and observed minimum volumes was small, except for Test 45, and for some of the predictions for Test 41. In these cases, the effect of reaction energy is large, and the use of a friction term obtained by neglecting reaction naturally leads to significant discrepancy.

For Test 41, in the cases for which the error in volume was appreciable, the predicted maximum temperature was high, and the assumed rate constants were so high that the predicted composition followed the equilibrium path over a significant range of temperature. The predicted final composition was not, therefore, greatly affected by failure to adjust the predicted minimum volume.

Similar considerations apply, although less strongly, in the case of Test 45. With the higher assumed rate constants the predicted composition followed the equilibrium composition over a large range of temperature. With the lower constant, the rate constant for decomposition varied little with temperature, and the predicted mol fraction of NO was always well above equilibrium, so that errors in the predicted maximum temperature were not very important.

The discrepancy between observed and predicted minimum volume may be more important in its effect on the results shown in Table XX, for test 45. The indicated value of A may be in error by as much as a factor of 2. Even in this case, though, the effect is smaller than the effects

of the other sources of error involved.

Chemical Analyses

In testing any given rate constant formula, predictions of final compositions based on that formula are compared with observed final compositions. Clearly it is essential to have accurate chemical analyses of the products formed in the various runs. The product samples taken for analysis passed through a collecting system in which they were in contact with the steel of the apparatus, a short length of copper tubing, stainless steel tubing, and pyrex glass tubing, stopcocks, and sample bulbs. An attempt was made to prevent gas which had passed into the manometer from flowing back through the glass system into the sample bulb, since the product gas was observed to react with the mercury in the manometer. "Halocarbon" stopcock grease was used to lubricate the stopcocks and joints of the sample bulbs and of the glass portion of the transfer system. Samples of product were usually transferred to the glass sample bulbs within fifteen or twenty minutes after a run. In some cases, these bulbs were stored for several weeks before the samples could be analyzed. Some softening of the stopcock grease was observed in this length of time. It is not known whether or not this was because of reaction with the sample.

The mass-spectrographic method of analysis has been claimed to give results accurate to within one or two per

per cent of the constituent reported or one or two tenths mol per cent of the entire sample. Comparisons of MS analyses of initial samples with compositions calculated from pressure measurements made during sample loading indicate that these limits may be somewhat optimistic, particularly with regard to the relative amounts of N_2 and O_2. Only one test of reproducibility is available. Tests 40 and 41 were run under nearly identical initial conditions. The indicated yields of NO_2 were respectively 1.92 and 2.00 mol per cent. For NO_2 this agreement seems satisfactory, but the N_2/O_2 ratio is badly in error for Test 40.

Indicated Effective Rate Constants

Particularly in view of the errors inherent in the many simplifying assumptions made, it is difficult to form definite conclusions regarding effective rate constants, from the results of a limited program of calculations. However, a few rough ideas may be obtained. The results for the various experimental runs will be discussed in order.

None of the rate constant formulas investigated gives good results for more than one or two of the runs. As is seen from Figure 34, no value of E_a (with variation allowed only above 1650° C) will give the observed result for Test 36. The closest agreement is at about 24 kcal/g mol, with an indicated absolute error in prediction of about one-half of one mol per cent. For Test 41, correct prediction is obtained using a value of about 48 to 50

kcal/g mol. For Tests 39 and 45, the indicated value is nearly zero, perhaps about 1 kcal/g mol. It is clear that use of a value of E_a which gives the best result for one test will lead to large errors for other tests.

Inspection of Figures 35 through 37 shows the "best" value of E_a depends greatly on the error parameter considered, and also indicates that there is no "good" value of E_a. For example, the function $\sum \Delta_n^2$, based on the discrepancies between observed and predicted mol fractions of NO_2,** has a minimum near an E_a of 8 kcal/g mol, and a higher, rather lat minimum near an E_a of 20 kcal/g mol. The function $\sum \Delta_n^2$, on an inert free basis, shows minima near 28 and 8 kcal/g mol. The function based on relative error, $\sum \left(\frac{\Delta_n}{obs}\right)^2$, shows a very flat minimum near 8 kcal/g mol. These minima are not at all sharp; i.e., the value of the function is not much lower at the minimum than for a wide range of E_a near the "best" value. Also, the minima are not very low, except in the case of the function based on relative error. If a "good" rate constant formula were investigated, any of these functions should reach zero at the correct value of E_a.

The fact that none of the rate constant formulas tested yields consistently good results is not surprising. The use of equation 155 (Daniels' equation) below 1650°C was

---

** The points indicated by circles in Figures 35, 36, and 37 are from Table IX. Intermediate points for the curves were estimated using values of "error in prediction" read from Figure 34.

somewhat arbitrary; it was not expected that a rate constant formula corresponding to two intersecting straight line segments on a log k vs 1/T plot would yield correct results, but it was hoped that some semi-quantitative deductions might be made regarding the magnitude of the rate constant in the high temperature region. A few such deductions may be drawn from the results of the numerical integrations, summarized in Tables IX and X, and from the results of the calculations neglecting reverse reaction, shown in Table XX.

Rate Coefficients from Numerical Integrations

Consideration of the data in Table X indicates some broad limits on the rate coefficients. For Test 36, none of the four rate constant formulas considered leads to prediction of a yield as high as that observed. Because of decomposition of NO during expansion of the sample, rate constants as high as those given by Daniels' equation indicate low yields, although the amount of NO formed at the maximum temperature is essentially the equilibrium amount. Rate constants as low as those given by equation 159 lead to prediction of inadequate formation of NO, even at the highest temperature. The predicted yields based on equations 157 and 158 are higher, although still below the observed yield. From equation 158, the value of k_{pp_d} at the maximum temperature is about 41 atm^{-1} sec^{-1}, and even at the maximum temperature, the predicted formation

is inadequate. A rate constant formula giving the same rate coefficient at the maximum temperature, but with greater activation energy, would mean lower rate constants at lower temperatures; the predicted formation of NO would be still more inadequate. The value of k_{pp_d} at the maximum temperature, given by equation 157, is about 260 atm^{-1} sec^{-1}. The corresponding value of k_{pp_f} is adequate to account for the net formation observed. In order to account for the high final yield, the value of k_{pp_d} at slightly lower temperatures should be somewhat less than given by equation 156, so that less decomposition during cooling would be predicted.

It appears, therefore, that the "best" rate constant formula should predict, at the maximum temperature of Test 36, a rate constant for decomposition of at least 50 and perhaps as high as 250 atm^{-1} sec^{-1}. The rate of decrease of k_{pp_d} with decreasing temperature should be large, corresponding to a high activation energy. The calculated maximum temperature was from 4850 to 4950° R, depending on the rate coefficients assumed. The actual value may be several per cent outside this range. Figure 38 is a plot of log k_{pp_d} vs 1/T; on this plot, a value of k_{pp_d} of 50 to 250 atm^{-1} sec^{-1} in the temperature range 4850-4950° R is indicated as being reasonable in view of the results from Test 36. It is hard to establish the value of k_{pp_d} at lower temperature, say below 4000° R, except to say that it should be somewhat below that given by equation 156.

For reference, the four Arrhenius equations used for the numerical integrations are also plotted in Figure 38.

It might be remarked that Test 36 offers some evidence in support of a fairly high activation energy. The observed yield, 3.3 mol per cent, is nearly as high as the equilibrium amount at the calculated maximum temperature, ca. 3.9 per cent. A rapid increase of k with T is indicated. Otherwise, a value of k_f at the maximum temperature, high enough to account for the formation of the equilibrium amount of NO, would correspond to high values of k_d at somewhat lower temperatures, so that the predicted composition would depart from the equilibrium composition only at much lower temperature, and the predicted final yield of NO_2 would be too low.

In the case of Test 39, the calculated maximum temperature was from 4350 to 4480° R. In order to predict the rather low observed yield, the values of k_{pp_d} in the range near and slightly below this temperature should be fairly low, comparable to the values given by equation 159. Another possibility is that the rate constant should remain well above that given by Daniels' formula, even below 3000° R, to allow appreciable decomposition on the expansion stroke, after formation of the equilibrium amount of NO at the highest temperature. This alternative seems unlikely.

The value of k_{pp_d} given by equation 159 at 4475° R

is 12.65 atm^{-1} sec^{-1}, corresponding to a zero activation energy above 1650° C (3461.7° R). For a more reasonable activation energy, such as 40 to 70 kcal/g mol, the rate constant would have to be somewhat higher at the maximum temperature to account for the observed formation. On Figure 38, a range of k_{pp_d} of 13 to 25 atm^{-1} sec^{-1} at a temperature of 4450 to 4480° R is indicated as preferred for Test 39. The large effect of errors in temperature should be remembered in evaluating this result. Again it is difficult to give the value of k_{pp_d} at temperatures well below the maximum for the run. The observed yield corresponds to equilibrium at a relatively low temperature, namely 3100° R. In this region, and below, the values of k_{pp_d} should not be much larger than those given by equation 156, but could well be much smaller.

In the case of Test 41, because of the high temperature reached, it seems reasonable to assume that considerable formation of NO occurred on compression, followed by decomposition on expansion. In order to account for the observed yield by the assumption that the amount of NO was always well below equilibrium, the maximum rate constant would have to be extremely low, even less by a factor of 2 or 3 than indicated by equation 159. Considering the results from the other tests, this seems most unlikely.

The maximum temperature in this run is high, so the rate coefficients are large over a fairly wide temperature range. It is difficult, therefore, to make precise state-

ments about the value of k_{pp_d} in any narrow temperature range. Particularly if the possibility of variation of E_a with temperature is considered, it becomes very difficult to set limits on k in the high temperature range, from about 5500 to 8000° R. If the rate is large enough to ensure close approach of the system to chemical equilibrium, further increase in the rate coefficients in this temperature range will have no effect on the predicted final yield.

Daniels' formula (equation 155 or 156) and equation 157 both give reasonable predictions for Test 41. The observed yield corresponds to the equilibrium concentration of NO at about 4860° R. The value of k_{pp_d} should therefore become fairly small at and below this temperature. It would seem reasonable to set k_{pp_d} somewhat below the value given by Daniels' formula and somewhat above the value given by equation 157 in the vicinity of 5000° R. The values at higher temperatures are hard to estimate, but, unless the activation energy decreases with temperature, the rate constants will remain higher than those given by equation 157. A region between the graphs of Daniels' formula and equation 157, in the vicinity of 5000° R, is indicated on Figure 38 as being favored by Test 41. An arrow at 7750° R indicates that the value in the high temperature region is probably above that given by equation 157.

In Test 41, more than one compression-expansion cycle may well have been significant. If such were the case, additional time at lower temperature, perhaps four or five

thousand degrees, would be available. The predicted final composition could approach the observed yield for even lower values of the rate constant. The region indicated on Figure 38 should therefore be regarded as an upper limit.

It is particularly evident in the case of Test 41 that predictions of final yield, not too far from the observed value, are given by rate constant formulas which indicate widely different values of k_{pp_d} at the maximum temperature of the run. The difficulty of setting limits on the rate coefficient from a single test of this type is therefore apparent.

In the case of Test 45, fairly strong conclusions could be drawn, were it not for the errors possibly present in calculated temperature and in the chemical analysis of the product. The observed yield of NO_2 corresponds to an equilibrium concentration of NO at a temperature of about 7360° R. This is well above the calculated maximum temperature, even allowing for correction to get calculated and observed minimum volumes into agreement. It appears almost certain, therefore, that the mol fraction of NO remained well above the equilibrium value throughout the run. The values of k_{pp_d} must therefore be well below those given by Daniels' formula.

Use of equation 159 leads to prediction of a yield only slightly too high. This equation gives a value of 12.6 atm^{-1} sec^{-1} for k_{pp_d} at the maximum temperature of 6220° R

corresponding to a zero activation energy above 1650° C. With a more reasonable activation energy, the allowable value of k_{pp_d} at the maximum temperature would be somewhat higher, since the values at slightly lower temperatures would be relatively lower. In Figure 38, a range of 15 to 25 atm^{-1} sec^{-1} in the temperature range 6200 to 6400° R is indicated as favored by the results of Test 45. This range for the rate coefficient is rather low compared to the coefficients indicated by the other tests.

For Tests 43 and 44, the numerical integrations were carried out using only Daniels' rate coefficient formula, equation 156. The results have been included in Tables IX and X.

The agreement of the predicted yield with that observed is very good for Test 43; slightly smaller values of k_{pp_d} in the range 4000-6000° R would probably lead to still better results, since less decomposition would be predicted on the expansion stroke. In this test, as in Test 41, the calculated maximum temperature is high, and the predicted yield would be insensitive to changes in the assumed rate constant in the high temperature range.

In Test 44, the calculated maximum temperature is lower. The yield predicted by the use of Daniels' formula is somewhat high. At first glance, this would seem to indicate higher values of k_{pp_d} than given by Daniels' formula, to allow more decomposition on the expansion

stroke. Considering the effect of error in temperature, however, lower values may well be possible; if the maximum temperature were slightly lower than that calculated, the amount of NO formed during compression might well be considerably less. Even if the calculated temperature is correct, prediction of the observed yield could be obtained by using rate coefficients very much lower than given by Daniels' formula, say by a factor of ten or more. For such values, the predicted mol fraction of NO would remain well below equilibrium at the maximum temperature. For Test 44, the influence of assumed rate coefficient on predicted yield should be similar to that shown for Test 39.

Rate Coefficients Based on Neglect of Reverse Reaction

From the results given in Table XX for the calculations based on an activation energy of 69,500 cal/g mol, and neglecting the reversibility of the reaction, some limits can be set on the values of the effective rate coefficients.

The value of A indicated for Test 36 is 1.45×10^{7} atm^{-1} sec^{-1}. Since there will actually be some reverse reaction, the gross formation of NO must be more than the final yield. The calculated value of A should therefore be regarded as a lower limit. The lower limit indicated for A corresponds to a value of k_{pp_d} of 44.0 atm^{-1} sec^{-1} at the calculated maximum temperature of the run, 4955° R. This point is indicated in Figure 38, with an arrow indicating that the true value may be somewhat higher. Since, in the

numerical integrations discussed earlier, the use of Daniels' equation led to prediction of too much decomposition during expansion, the best value of A should be somewhere between the lower limit of 1.45×10^7 and Daniels' value of 1×10^9 atm^{-1} sec^{-1}. The estimated maximum value of temperature was perhaps higher than the true value, because of the neglect of heat loss. This consideration also indicates that A may be higher than the calculated value of 1.45×10^7.

The value of A indicated by Test 39 was 2.62×10^7 atm^{-1} sec^{-1}. In this case, the observed yield of NO_2 corresponds to much less than the equilibrium amount of NO at the calculated maximum temperature. Significant reverse reaction, therefore, need not have occurred, and the net formation of NO may be nearly as large as the gross formation. The effect of error in temperature should be kept in mind, however. If the actual maximum was as much as ten per cent below the calculated value, the effective value of A could be higher by a factor of as much as four or five. At the calculated maximum temperature of 4475° R, the value of k_{pp_d} corresponding to an A of 2.62×10^7 atm^{-1} sec^{-1} is 20.3 atm^{-1} sec^{-1}. This point is plotted in Figure 38. The arrow again indicates that the correct value may be somewhat higher.

The value of A obtained for Test 45 was considerably lower, namely 3.44×10^5 atm^{-1} sec^{-1}. At the calculated

maximum temperature of 6220° R, the value of k_{pp_d} computed from this value of A is 19.3 atm^{-1} sec^{-1}. This value is shown on the plot, Figure 38. Since the observed yield of NO_2 is well above the amount corresponding to the equilibrium amount of NO at the maximum calculated temperature, the rate of the formation reaction is probably never as large as the net rate of reaction. The gross decomposition is therefore not much greater than the observed net decomposition, and the best value of A should not be much larger than the value calculated.

From another viewpoint, however, it is possible that the best value of A for Test 45 is higher. Because of the large amount of NO present in the sample throughout the run, and because of the relatively long time near maximum temperature, it is quite likely that the energy lost as heat was considerable. The calculated maximum temperature may be ten or even twenty per cent too high. If this were the case, the calculated maximum value of k_{pp_d} should apply at a lower temperature than indicated in Figure 38. This shift corresponds to a higher value of A, retaining the same activation energy.

Data from the other decomposition runs, Tests 48 and 49, also seem to indicate relatively low rate coefficients. In Test 48, the reported yield of NO, 3.5 mol per cent, would be in equilibrium at a temperature of 5870° R, while the maximum temperature of the run, calculated neglecting reaction, was only 4540° R. Even allowing for the endo-

thermic decomposition of NO, the highest temperature of the run was undoubtedly below that at which the observed yield would be in equilibrium. In Test 49, the yield of 1.0 per cent NO corresponds to equilibrium at 4620° R, whereas the maximum temperature (neglecting reaction) was 9060° R.

It appears, therefore, that equilibrium is not achieved at the maximum temperature of a run unless the maximum is quite high; this situation indicates effective rate coefficients lower than those of equation 155, at least in the range above 3000° R.

The reported yields from the final tests of the series, Tests 50 and 51, in which graphite was used as the lubricant, are very low, and subject to much uncertainty. These low yields would require rate coefficients either enormously larger or enormously smaller than those of equation 155. More experimental data will be required to clarify the effect of the lubricant.

All of the calculations discussed above seem to indicate lower effective rate coefficients than given by equation 155.** At the lower limit of applicability, equation 156 gives an effective rate coefficient higher by a factor

---

** The rate coefficients have been applied in a range of temperature well above that covered by Daniels' investigations, and at vastly higher pressure. The suggestion of values lower than those obtained by extrapolation of Daniels' equation is in no way to be construed as a criticism of his work, which was chosen merely as a convenient point of departure.

of about ten than indicated by the works of Vetter (19) or Jellinek (13), or by an extrapolation of the data of Kaufman and Kelso (23) (cf. Figure 1). At the upper end of its range (1850° C), equation 156 is in fair agreement with other reported values, although most of those were obtained by indirect methods.

The results from the present work are subject to much uncertainty because of the many simplifying assumptions made in treating the data. All of the calculations, however, are consistent with effective rate coefficients at least ten times less than those of equation 155. The empirical Arrhenius equation of Kaufman and Kelso, equation 19, would probably give better results for the "formation" runs than did equation 156, but would still give rate coefficients much too high for the "decomposition" run.

Only a limited number of combinations of A and E_a were covered by the calculations. Interpretation of the results in terms of acceptance or rejection of the simple bimolecular mechanism, equation 104, and the simple temperature dependence, equation 154, is difficult. If the yield of NO is below the equilibrium mol fraction for the highest temperature of a run, or if the initial charge contained NO, there is <u>some</u> combination, and probably several, of A and E_a which will predict the observed yield. Without trying all possible combinations, or at least a wide range, it is hard to state categorically that no combination of A and E_a would apply to two or three given different runs.

It appears clear, however, that the results from Test 45 cannot be reconciled with the results from the "formation" runs, on the basis of the simple mechanism. Even if the lowest limits from Tests 36 and 39 are chosen, reference to Figure 38 shows that, with any reasonable activation energy, extrapolation from the region favored by either of these tests, to the maximum calculated temperature of Test 45, will give an effective rate coefficient for decomposition which is much too high. Rate coefficients consistent with the results of Test 41 are even farther above the values indicated by Test 45.

Even if the temperature dependence of the coefficient k_{pp_d} were modified, it does not seem that any but the most strangely contrived curve of k_{pp_d} vs. $1/T$ could satisfy both Test 45 and the "formation" runs. On the basis of the calculated conditions, therefore, it is necessary to reject the simple bimolecular mechanism.

In the "decomposition" runs, any oxygen must come from the NO decomposed. The ratio O_2/NO is, therefore, much higher in the "formation" runs. Mechanisms such as those proposed by Vetter (19) or by Wise and Frech (20), in which the effective second order rate coefficients appear higher for high O_2/NO ratios, might explain the present results.

Unfortunately, the possible errors in the calculated conditions are so large that the simple mechanism cannot be unequivocally rejected on the basis of these preliminary

studies. The need for better experimental data and more refined calculation of temperature is clear.

Relative Weight of Various Runs

Different ranges of experimental conditions, as typified by the several exploratory runs, each have peculiar advantages for the calculation of effective rate coefficients. Ironically, there are corresponding disadvantages in each of the four runs considered in detail which vitiate the conclusions reached.

For example, the yield for Test 36 is high, and nearly as large as the equilibrium mol fraction of NO at the calculated maximum temperature of the run. This high yield rules out very low rate coefficients near the maximum temperature, since obviously significant reaction occurred. At least for temperatures somewhat below the maximum, very high coefficients are also impossible, since little net decomposition occurred on the expansion stroke. The combination argues for a high activation energy. Unfortunately, in order to calculate conditions from the limited experimental data, many simplifying assumptions were made. For this run, the assumption of ideal gas behavior is particularly weak, since the maximum pressure was so high. The compressibility factor was probably significantly above unity at the extreme conditions, so that the true maximum temperature may be higher than that calculated. In that event, the equilibrium mol fraction of NO at the true maxi-

mum temperature could be well above the observed yield. For example, at 5500° R, corresponding to an error of about ten per cent in the calculated temperature, the equilibrium mol fraction is 6.05 per cent; at 6000° R, it is 7.96 per cent. Thus, if the real maximum temperature was as much as ten or twenty per cent higher than that calculated, the allowable rate coefficients would be much higher than those indicated by the calculated conditions. In order to have any confidence in the calculated rate coefficients, it is essential that more reliable estimates of temperature be obtained.

In the case of Test 39, on the basis of the calculated conditions, it appears plausible that little reaction occurred, and that the system did not reach equilibrium at the maximum temperature. Thus the test is evidence for low rate coefficients. The conclusions are again weakened by uncertainty in calculated temperature. The maximum temperature is rather low, so that the predicted yield is markedly dependent on the calculated maximum temperature. The "decreased temperature" calculations described on page 97 and summarized in Table XXI show that an uncertainty of as little as ten per cent in the temperature can result in error by a factor of four or five in the predicted yield. Again it is clear that more reliable estimates of temperature are essential if effective rate coefficients are to be obtained.

Conditions such as those of Test 41 offer the advantage that the predicted yield does not depend too strongly on the calculated maximum temperature; this corresponds to a "high

maximum" run such as is illustrated in Figure 32. The final composition is determined, not by the maximum temperature, but by the behavior in the region in which the predicted composition departs from the equilibrium curve. For a given temperature in this region, the pressure is known with an error comparable to the error in maximum temperature. Since the piston is fairly far from its point of zero velocity, the velocity is known with an uncertainty comparable to the square root of the relative uncertainty in the maximum temperature. The uncertainty in the predicted yield is therefore comparable to the relative error in the maximum temperature. Uncertainties of twenty or thirty per cent in the predicted yield are undesirable, but certainly less severe than uncertainties by factors of four or five.

The drawback to tests such as Test 41 is that the predicted yield is relatively insensitive to changes in the assumed rate coefficients. Reference to Table X shows that, allowing for errors due to uncertainty in the calculated temperature, it would be impossible to choose between equations 156 and 157, although these give significantly different rate coefficients at moderately high temperatures. In spite of this drawback, I am inclined to give greater weight to Test 41 than to Tests 36 and 39, in which the effect of error in calculated maximum temperature is so much greater.

Test 45 has the great advantage inherent in "decomposition" runs. In the "formation" runs, the yield is always

less than the maximum possible, which corresponds to the equilibrium amount of NO at the maximum temperature of the run. It is not obvious, from the results of a single run, whether there was close approach to equilibrium at the maximum temperature, followed by net decomposition of NO during expansion of the sample, or whether the amount of NO at the maximum temperature remained well below equilibrium. These possibilities correspond, respectively, to "high" and "low" rate coefficients. In a "decomposition" run, if the initial mol fraction of NO is well above the amount corresponding to equilibrium at the maximum temperature, the results will clearly indicate whether the rate constants were large enough to allow approach to equilibrium at the maximum temperature. If the yield of NO_2 is above the amount corresponding to NO in equilibrium at the maximum temperature, it is obvious that the rate constant for decomposition remained fairly low, and reasonable upper limits may be set. Calculations neglecting the effect of reversibility may be made with some confidence. If the yield is below the maximum equilibrium quantity, it is clear that the rate coefficient was high enough to allow approach to equilibrium at the maximum temperature, and rough lower limits can be established.

The weakness on Test 45 again arises from the uncertainty in the calculated temperature. The maximum temperature of this run was undoubtedly below that at which the observed yield would be at equilibrium; rough

upper limits may therefore be set for the effective rate coefficient by neglecting the reversibility of the reaction. The limit thus set is indicated on Figure 38 for a temperature of 6220° R, and is well below the effective rate coefficients indicated by the "formation" runs. Unfortunately, this temperature may be badly in error. The sample contained a relatively large fraction of NO, and was at high temperature for a relatively long time (cf. Figure 18); heat loss may have been large. If the real maximum temperature were as much as twenty per cent less than that calculated, the maximum value of the rate constant indicated on Figure 38 should be much further to the right, corresponding to a higher rate coefficient at a given temperature. It would no longer be possible to say that the results from Test 45, and the results from the "formation" runs, cannot be reconciled on the basis of the simple bimolecular mechanism.

VI. CONCLUSIONS AND RECOMMENDATIONS

Conclusions

1) The ballistic piston offers a mechanically simple method of producing extremely high temperature and pressure in a sample under study. It has been shown in these preliminary studies that mixtures of nitrogen, oxygen, nitric oxide, and helium can be subjected to high temperature and pressure without great net leakage, and with little damage to the equipment. Maximum calculated temperatures from 4400° R to 13800° R, and calculated maximum pressures from 4900 to 33,000 psia were achieved.

2) It has been shown that appreciable net reaction can be obtained using this equipment. Up to 3.3 per cent NO_2 was obtained starting with nitrogen and oxygen; with NO as the starting material, almost all can be decomposed.

3) Qualitatively, the effects of increased maximum temperature and pressure are as expected, as shown in Figures 12, 13, and 14. For the "formation" runs, increase in either maximum temperature or maximum pressure promotes an increase in the yield of NO_2.

4) For the "formation" runs, the yields were always below those corresponding to equilibrium at the calculated maximum temperatures, despite the rather crude assumptions used to calculate these temperatures.

5) Results of calculations of limited scope indicate

that the effective rate coefficients are lower than given by equation 155, which had been chosen as a point of reference. The rate coefficients for decomposition which appear reasonable for each of the runs, are shown in Figure 38. There is some evidence for an activation energy as high as that of equation 155; the pre-exponential factor of equation 155 is at least ten and perhaps as much as fifty times too large, on the basis of the "formation" runs. The single "decomposition" run considered indicates that the pre-exponential factor of equation 155 is as much as two thousand times too large.

6) On the basis of the calculated conditions, the results from the "decomposition" run, Test 45, are incompatible with the results from the "formation" runs; that is, there are no values of A and E_a for an Arrhenius equation which can apply to both sets. Even if E_a is a function of temperature, no value of A can satisfy both sets.

If real, this discrepancy would be grounds for rejecting the simple mechanism assumed in the calculations; but, the apparent discrepancy can be explained on the basis of large errors in the calculated conditions and in the observed mass spectrographic analyses. Further work is essential before the simple mechanism can be firmly accepted or rejected.

7) The attempt to investigate catalytic effects of the lubricants was inconclusive. If the reported analyses and calculated conditions are all correct, the effect is very important; however, the results can be explained on the basis of errors in the analyses, which were from different sources,

or merely on the basis of differences in the lubricating efficiency of graphite and "molylube."

Future Work

In view of the labor involved in making numerical integrations to predict final product compositions, further such calculations should be deferred until better experimental data have been obtained, and until high-speed digital computing equipment is available. A discussion of the programming of a computer to handle the numerical integrations is beyond the scope of this thesis, but the difficulties do not seem insurmountable. A procedure for trial and error solution of finite difference equations, such as described on page 72, could probably be adapted to machine computation.

With regard to the experimental program, it is clearly essential that accurate chemical analyses of products be obtained. The importance of these data is sufficient to justify the expenditure of considerable effort in selecting the best method of analysis. It may be necessary to employ several chemical and physical methods, including the mass spectograph, in order to obtain adequate and highly reliable information regarding product composition.

As has been pointed out before, the labor of making numerical integrations would be substantially reduced if more variables were measured. The measurement of pressure would be a significant step forward, and, at the time of the writing of this thesis, installation of instrumentation for the

measurement of pressure as a function of time is being carried out. Although position-time data have been obtained for the downstroke of the piston, it will probably remain necessary to use sample pressure to determine the volume-time relation on the expansion stroke. The pressure measurements, when they become available, and the piston-position-time measurements for the downstroke of the piston, will make possible the straightforward calculation of the pressure-volume and volume-time relations in advance of any numerical integrations involving chemical kinetics. These relations would then be available for each run before chemical rate calculations were started, and would not need to be calculated for each assumed rate constant formula.

Comparison of piston velocity predicted from pressure data with that obtained from the position vs. time measurements would afford a check on the consistency of these measurements, and would serve to detect the existence of unexpectedly large frictional forces, should such forces arise near the bottom of the piston stroke.

In order to calculate temperature with a satisfactory degree of accuracy, the effects of side reactions, including ionization and dissociation of N_2 and O_2, must be taken into account. This calculation would require a knowledge of the rates of these reactions, and is liable to be a formidable obstacle. If temperature could be measured, the errors due to neglecting side reactions would be much less serious, since they do not markedly affect the mol fractions of the

compounds of primary interest. If temperature as well as pressure can be measured as a function of time or piston position, the only variable remaining to be determined by numerical integration of assumed rate equations is composition. Experimental determination of composition, with acceptable accuracy, will probably not be possible, except for the final products.

Measurement of temperature, perhaps by optical means, may eventually be possible, but, at least for some time to come, it will be necessary to calculate temperature. If the calculation is based on information regarding the energy added by compression, it will be necessary to consider the heat loss, as well as the energy effects of all of the chemical reactions which take place. The early results obtained with the "thermal flux meter" (28) indicate that it may be possible to determine heat loss to the bottom of the cylinder, but the total heat loss and heat as a function of time will have to be estimated on the basis of some assumed behavior. This operation will undoubtedly involve a trial and error solution of the assumed equations.

Another approach to the estimation of temperature, probably more straightforward, would be to calculate it from the observed volume and pressure of the sample. This would require fairly good data on the thermodynamic properties of the mixture. Longwell (5) has pointed out advantages in the use of "co-volume" equations of state for estimation of the behavior of samples in the ballistic piston. It will be

desirable to compute temperature both from PVT data and from the energy of the sample.

One fairly simple step which would remove a major source of uncertainty would be the addition of equipment to prevent the piston from again compressing the sample, after the first compression-expansion cycle. At the time of this writing, equipment which will retain the piston at the top of the first upstroke has been designed (41). It should be completed and installed before any more detailed calculations regarding chemical kinetics are attempted.

Another fairly simple variation in the experimental procedure would be the use of pistons of different weights. If two runs were made, with other initial conditions identical but with pistons of different weights, the results will in many cases yield semi-quantitative conclusions regarding the magnitude of the chemical rate constants. In the two runs, volume-pressure and volume-temperature relations would be nearly the same, but the time scale would be changed, roughly with the one-half power of the piston weight (7).

If, with the heavier piston, the yield of NO_2 is well below that corresponding to the equilibrium amount of NO at the maximum temperature of the run, it is not clear whether the mol fraction of NO approached equilibrium closely at the high temperature and then declined, or whether it remained well below equilibrium throughout the high temperature region. The first possibility corresponds to fairly high rate constants, the second to relatively low rate constants. The re-

sults of the run with the lighter piston should clarify the situation somewhat. If the yield is higher, the high rate constants are favored, since shorter time for cooling would mean faster "freezing" of the reaction. If the yield is lower, the smaller rate constants are favored, since shorter time near the maximum temperature would mean less formation of NO. (The foregoing comments apply to runs in which the initial sample contains nitrogen and oxygen.)

At the time of this writing, pistons of 32.09 lbs., nearly the same as used in the preliminary studies, and of 3.29 lbs. are in use. Several runs on the nitrogen-oxygen system have been made with each of these pistons, but detailed analysis of the results is not yet available. Three or four pistons should be available, so that rate calculations could be made for runs in which a range of piston weights had been used. These calculations, however, should not be attempted until more fundamental problems of the program have been solved.

Utility of Apparatus

The attractive feature of the ballistic piston as a research tool is the range of conditions which it makes available for study. The combinations of temperature and pressure obtained cannot be duplicated in a static apparatus. Even at low pressure, the more extreme temperatures could not be held for more than a very short time.

The obvious disadvantage of the ballistic piston, as a

tool for study of reaction rates, is that the analysis of the data to obtain the information desired is so complicated. No straightforward calculation of rates is possible; it is only possible to check the applicability of an assumed mechanism and the concommitant rate constants. The assumptions must include the temperature dependence of each of the rate coefficients involved. Particularly if more than one reaction is of interest, or if a complicated mechanism is hypothesized, numerous rate coefficients are involved. For each, several constants in a rate coefficient formula must be assumed. The number of combinations of such constants which must be investigated becomes astronomical for a mechanism of any complexity, or if several reactions are considered.

It would seem reasonable to suggest, therefore, that the ballistic piston apparatus would be most useful in conjunction with other types of equipment, for the investigation of a system over a wide range of conditions. The kinetics of a system might be investigated at high temperature and low pressure by the use of devices such as the shock tube, and if the effects of pressure at moderate temperature could be investigated using high pressure cells, it may be possible to use the ballistic piston to extend the investigation into the region of high temperature and pressure. The use of other types of equipment would offer the advantage that some idea of the form of rate constant formulas and reaction schemes to be tested could be obtained before starting the laborious treatment of data from the ballistic piston.

Observations made in this laboratory by G. N. Richter in the course of an investigation of the thermal conductivity of nitric oxide at high pressures (42) suggest that the rate of decomposition of NO is markedly influenced by pressure. Even at temperatures as low as 40° F, appreciable decomposition was observed for pressures above 1000 psi. The rate of decomposition appeared to increase rapidly with increasing pressure. The need for further experimental work to clarify the effect of pressure is indicated, since Richter's observations might be explained by catalytic effects. The relatively low rate coefficients obtained in the present study, for Test 45, suggest that the effect of pressure is not so large.

As a result of the preliminary studies discussed in this thesis, the writer is convinced that, if the ballistic piston is to be used to study chemical kinetics in the nitrogen-oxygen system, two problems must be solved before substantial progress can be made.

First, a dependable system of chemical analysis must be developed; this work should receive top priority. Second, better estimates of temperature must be obtained. If calculated temperatures are uncertain by as much as ten per cent, it is not possible to accept or reject the simple bimolecular mechanism with any confidence, and the effective rate coefficients from different runs may differ by factors of over one hundred. As mentioned previously, calculation of temperature both from energy considerations and from PVT data is highly desirable; if the two approaches agree, the calculated tempera-

ture can be accepted with increased confidence as the average temperature. These approaches could give the same average temperature even if the temperature of the sample were not uniform. If future work shows that the samples do not remain uniform in temperature during compression, the "average" temperatures could not be used in calculation of chemical rates. An attempt to extend the numerical integrations discussed in this thesis to take non-uniform temperature into account would be so complicated as to be fruitless, unless the temperature distributions were established from experimental measurements.

While the utility of the ballistic piston as a tool for study of chemical reactions is by no means firmly established, the range of conditions that may be obtained is so great that more exploratory work is believed to be justified.

REFERENCES

1. Carrington, T., and Davidson, N. R., J. Phys. Chem., 57, 418-27 (1953).

2. Britton, D., Davidson, N., and Schott, G., Disc. Farad. Soc., No. 17, 58-68 (1954).

3. Britton, D., and Davidson, N., J. Chem. Phys., 23, 2461L (1955).

4. Glick, H. S., Squire, W., and Hertzberg, A., Project Squid Technical Report CAL-63-P, Cornell Aero. Lab. (1955).

5. Longwell, P. A., Ph.D. Thesis, California Institute of Technology (1957).

6. Ryabinin, Yu. N., Markevich, A. M., and Tamm, I. I., Doklady Akad. Nauk. (USSR), 95, No. 1, 111-13 (1954).

7. Longwell, P. A., and Sage, B. H., Manuscript 2745, Department of Chemical Engineering, California Institute of Technology (1955).

8. Shreve, R. N., The Chemical Process Industries, Ch. XX, McGraw-Hill Book Co., New York (1945).

9. Gilbert, N., and Daniels, F., Ind. Eng. Chem., 40, 1719-23 (1948).

10. Daniels, F., C. & E. News, 33, 2370 (1955).

11. Ermenc, E. D., Chem. Eng. Prog., 52, No. 4, 149-53 (1956).

12. Nernst, W., Z. Anorg. Chem., 49, 213-28 (1906).

13. Jellinek, K., Z. Anorg. Chem., 49, 229-76 (1906).

14. Rossini, F. D., Pitzer, K. S., et al., Selected Values of Physical and Thermodynamic Properties of Hydrocarbons and Related Compounds, pg. 748, API Research Project 44, Published for the American Petroleum Institute by Carnegie Press, Carnegie Institute of Technology, Pittsburgh, Penn. (1953).

15. Wise, H., and Frech, M., J. Chem. Phys., 20, 22-4 (1952).

16. Daniels, F., C. & E. News, 31, 3872 (1953).

17. Daniels, F., Private Communication (1955).

18. Zeldovich, J., Acta Physicochem. URSS, 21, 577-620 (1946).

19. Vetter, K., Z. Electrochem., 53, 369-76 (1949).

20. Wise, H., and Frech, M., J. Chem. Phys., 20, 1724-7 (1952).

21. Kaufman, F., and Kelso, J. R., J. Chem. Phys., 21, 751L (1953).

22. Wise, H., and Frech, M., J. Chem. Phys., 21, 752L (1953).

23. Kaufman, F., and Kelso, J. R., BRL Report No. 923, Ballistic Research Laboratories, Aberdeen Proving Ground, Md. (1954); also, J. Chem. Phys., 23, 1702-7 (1955).

24. Friedel, R. A., Sharkey, A. G., Jr., Shultz, J. L., and Humbert, C. R., Anal. Chem., 25, 1314-20 (1953).

25. Rossini, F. D., Pitzer, K. S., et al., op. cit., pg. 631.

26. Kobe, K. A., and Pennington, R. E., Pet. Ref., 29, No. 7, 129-33 (1950).

27. Goff, J. A., Gratch, S., and Van Voorhis, S. W., Trans. ASME, 72, 725-39 (1950).

28. Wilburn, N. P., Unpublished data.

29. Benitez, L. E., and Penner, S. S., J. App. Phys., 21, 907-8 (1950).

30. Penner, S. S., J. App. Phys., 21, 685-95 (1950).

31. Hottel, H. C., in W. H. McAdams' Heat Transmission, 3rd ed., Ch. 4, McGraw-Hill Book Co., New York (1954).

32. Hougen, O. A., and Watson, K. M., Chemical Process Principles, Part Two: Thermodynamics, pp. 489, 622, John Wiley & Sons, Inc., New York (1947).

33. Hall, N. A., and Ibele, W. E., Trans. ASME, 76, 1039-56 (1954).

34. Gaydon, A. G., and Wolfhard, H. G., Flames, pg. 282, Chapman & Hall, Ltd., London (1953).

35. Rossini, F. D., Pitzer, K. S., et al., op. cit., pg. 703.

36. Bodenstein, M., et al., Z. Phys. Chem., 100, 68-123 (1922).

37. Yost, D. M., and Russell, H. R., Jr., Systematic Inorganic Chemistry of the Fifth and Sixth Group Non-metallic Elements, pp. 29-30, Prentice-Hall, Inc., New York (1946).

38. Frost, A. A., and Pearson, R. G., Kinetics and Mechanism, pg. 180, John Wiley & Sons, New York (1953).

39. Treacy, J. C., and Daniels, F., J. Am. Chem. Soc., 77, 2033-6 (1955).

40. Gilliland, E. R., Mason, E. A., and Oliver, R. C., Ind. Eng. Chem., 45, 1177-85 (1953).

41. Wilburn, N. P., and Sage, B. H., Unpublished.

42. Richter, G. N., Ph.D. Thesis, California Institute of Technology (1957).

LIST OF TABLES

TABLE I

Conditions of Runs

Test Number	Initial Sample Pressure, psia.	Initial Sample Temp., °F.	Driving Air Pressure, psia.	Driving Air Temp., °F.	Composition of Charge mol per cent			Final Height of Lead Gauge,	Yield of NO_2
					N_2	O_2 or NO	He + A	inches	mol per cent
36	2.9630	72.68	999.1	82.4	46.26	53.03	0.44	0.1104	3.32
38	2.2972	73.22	1004.1	81.05	12.50	12.48	75.03	?	1.03
39	2.2612	71.24	580.8	85.10	43.49	43.73	12.78	0.2577	0.37
40	1.8919	68.54	688.0	84.74	24.35	24.38	51.26	≥0.1592	2.00
41	1.8770	72.77	688.0	84.56	24.25	24.37	51.38	0.1803	1.92
42	2.2002	71.33	1004.2	84.11	12.51	12.48	75.01	0.1735	1.39
43	2.1527	71.64	718.4	79.38	18.49	18.39	63.12	0.2913	1.30
44	3.2055	73.31	917.6	82.94	44.44	45.13	10.43	0.1942	1.21
45	2.0193	78.17	524.6	81.63	47.60	12.72 NO	39.68	0.3441	4.68
48	2.0209	75.78	481.7	82.72	65.30	16.44 NO	18.26	0.3495	3.5 NO
49	1.9417	79.70	638.9	85.91	17.94	18.18 NO	63.88	0.2875	1.0 NO
50	2.1397	77.00	718.6	82.04	18.39	18.45	63.16	0.2121	0.4 NO
51	2.1742	78.17	609.3	82.22	18.46	18.43	63.12	0.2768	0.2 NO

TABLE II

Results of Mass Spectrographic Analysis
Mol Per Cent

Test		N_2	O_2	He	A	NO_2	NO	N_2O	H_2O	CO_2	SO_2
36	Charge	45.73	52.69	-	0.43	-	-	-	1.15	-	-
	Product	41.95	52.08	-	0.47	3.32	-	-	0.58	1.60	-
38	P	11.80	9.08	77.34	0.08	1.03	-	-	0.19	0.42	0.06
39	P	45.44	42.16	11.20	0.25	0.37	-	-	0.13	0.32	0.13
40	P	16.11	39.89	40.75	0.27	2.00	-	-	0.20	0.58	0.20
41	C	24.50	23.35	51.71	0.18	-	-	-	0.26	-	-
	P	23.18	18.83	55.06	0.16	1.92	-	-	0.17	0.40	0.28
42	C	12.74	11.70	75.15	0.10	-	-	-	0.31	-	-
	P	15.15	10.80	71.88	0.11	1.39	-	-	0.06	0.47	0.14
43	C	19.53	17.27	62.71	0.14	-	-	-	0.35	-	-
	P	18.05	14.88	65.28	0.12	1.30	-	-	0.12	0.17	0.08
44	C	46.22	43.26	9.98	0.33	-	-	-	0.21	-	-
	P	45.98	40.82	10.79	0.33	1.21	-	-	0.18	0.62	0.07
45	C	46.29	-	38.98	0.11	-	14.33	-	0.29	-	-
	P	49.73	3.44	41.70	0.12	4.68	-	-	0.20	0.07	0.06
48	P	71.5	4.9	19.5	0.4	-	3.5	0.2	Trace	-	-
49	P	25.6	6.0	67.1	0.1	-	1.0	0.2	Trace	-	0.03
50	P	19.8	12.1	63.6	0.2	-	0.4	0.1	Trace	3.8	-
51	P	18.1	14.4	66.2	0.2	-	0.2	0.9	Trace	-	-

TABLE III

Extreme Conditions of Runs,
Neglecting Reaction

Test Number	10^3 x Minimum V*	T*	Temp., °R	P*	Pressure, psia	F, lb
36	1.131	9.521	5069	8421	24951	33.3
39	2.600	8.451	4487	3251	7351	24.5
40*	≥1.610	≤16.321	≤8621	≤10134	≤19173	
41	1.814	15.628	8321	8614	16169	-35.5
42	1.741	26.115	13867	15001	33006	
43	2.907	16.022	8513	5512	11865	-51.6
44	1.964	8.978	4785	4572	14655	18.8
45[1]	3.445	10.806	5812	3137	6334	- 7.88
48[1]	3.484	8.478	4540	2433	4918	
49[1]	2.889	16.803	9063	5817	11295	
50[2]	2.134	18.199	9767	8528	18248	
51[2]	2.783	16.260	8746	5842	12702	-128.4

* Lead gauge hit in sampling.

[1] Initial sample contains NO.

[2] Graphite lubricant.

TABLE IV

Composition Parameters

Test	NO_2[1] Mol Per Cent	NO Mol Per Cent	He + A[3] Mol Per Cent	NO_2 Mol Per Cent Inert Free	NO Mol Per Cent Inert Free	$\frac{\tilde{n}_{NO}^2}{\tilde{n}_{N_2}\tilde{n}_{O_2}}$	$\frac{\tilde{n}_{NO}}{(\tilde{n}_{N_2}\tilde{n}_{O_2})^{1/2}}$	$\tilde{n}_{N_{2_o}}\tilde{n}_{O_{2_o}}$	$(\tilde{n}_{N_{2_o}}\tilde{n}_{O_{2_o}})^{1/2}$	$\tilde{n}_{N_{2_o}}\tilde{n}_{O_{2_o}}$	$(\tilde{n}_{N_{2_o}}\tilde{n}_{O_{2_o}})^{1/2}$	$P_{max}\tilde{n}_{O_{2_o}}$ psia	$P_{max}(\tilde{n}_{N_{2_o}}\tilde{n}_{O_{2_o}})^{1/2}$	
36	3.32	3.266[2]	0.44	3.335	3.280	0.004626	0.06801	0.24659	0.49658			13300	12390	
39	0.37	0.369	12.78	0.424	0.423	0.0000722	0.008497	0.190186	0.43610			3214	3205	
40	2.00	1.980	51.26	4.147	4.063	0.007173	0.08469	0.059379	0.24368			4675	4672	
41	1.92	1.902	51.38	3.990	3.912	0.006630	0.08142	0.059094	0.24309			3941	3931	
42	1.39	1.380	75.01	5.681	5.583	0.01367	0.1169	0.015610	0.12494			4120	4124	
43	1.30	1.292	63.12	3.565	3.504	0.005273	0.07262	0.033998	0.18439			2182	2188	
44	1.21	1.203	10.43	1.352	1.343	0.00741	0.08722	0.200566	0.44705			6613	6563	
45	4.68	4.573[1]	39.68	7.380	7.582	0.00937	0.3152	0.0161764	0.12719	0.0343145	0.18528	402.8[6]	805.6[7]	1173[5]
48		3.5	16.26		4.28	0.03637	0.1624	0.0270424	0.16445	0.0604495	0.24586	404.4[6]	808.7[7]	1209[5]
49		1.0	63.88		2.77	0.00408	0.0639	0.0330524	0.18180	0.0245695	0.15675	1027[6]	2054[7]	1771[5]
50		0.4	63.16		1.09	0.000432	0.0220	0.033925	0.18419			3366	3361	
51		0.2	63.12		0.54	0.000119	0.0109	0.034012	0.18442			2341	2343	

[1] Reported Mass Spectrographic Analysis of Product
[2] Corresponding to Reported NO_2
[3] Initial Sample, Calculated from Pressure Measurements
[4] $\tilde{n}_{NO_o}^2$
[5] Pseudo $\tilde{n}_{N_{2_o}}$ and $\tilde{n}_{O_{2_o}}$
[6] 1/2 $\tilde{n}_{NO_o}$ used for $\tilde{n}_{O_{2_o}}$
[7] $\tilde{n}_{NO}$ used for $(\tilde{n}_{N_{2_o}}\tilde{n}_{O_{2_o}})^{1/2}$

TABLE V

Equilibrium Temperatures for Yields of NO

Test	T_{eq}, ^{o}R
36	4654
39	3116
40	4910
41	4862
42	5344
43	4727
44	3823
45	7357
48	5871
49	4619
50	3667
51	3243

TABLE VI.

Example of Trial and Error Calculations for Typical Numerical Integration
Test 41, Equation 157

V^*	T	T^*	$\frac{10^4}{T}$	log k_{pp_f}	log k_{pp_d}	k_{pp_f}	k_{pp_d}	P^*	$P^*_{av}\Delta V^*$	u^{*2}	Δu^{*2}	u^*	u^*_{av}	$10^5\Delta\theta$	$\tilde{n}_{eq}$	$\tilde{n}_{NO}$	$\tilde{n}_{N_2}\tilde{n}_{O_2}k_{pp_f}$	$\tilde{n}_{NO}{}^2k_{pp_d}$	r^*	r^*_{av}	$10^3\Delta\tilde{n}_{NO}$	T_{av}	$\frac{\tilde{C}_v}{R}$	ΔT^*	T^*	θ reaction
5.00×10^{-3}	5481.14	10.2940	1.82444	0.99218	2.77681	9.8215	598.15	2058.80	0.498916	43.3444	(1.6586)	6.584	6.646	(3.762)		0.017476	0.530418	0.182661	93.81	(88.62)	(3.334)	5441	2.5393	(0.1482)	10.2940	116.310
4.8×10^{-3}	5546	10.4158	1.80310	1.06185	2.81039	11.5305	646.23	2169.96	0.422876	41.9386	1.4058	6.476	6.530	3.063		.020500										
	5547.06	10.4178	1.80276	1.06296	2.81092	11.5601	647.03	2170.38	0.422918	41.9384	1.4060	"		"		.020413		0.271578	97.89	95.88	2.937	5514	2.5425	0.1238		
	5546.96	10.4176	1.80279	1.06286	2,81087	11.5574	646.95	2170.33	0.422913	"	"	"		"		.020429		0.269611	99.06	96.40	2.953			0.1236		
	5547.01	10.4177	1.80277	1.06293	2.81091	11.5593	647.01	2170.35	0.422915	"	"	"		"		.020427		0.270001	98.90	96.32	2.950			0.1237		
	"	"	"	"	"	"	"	"	"	"	"	"		"		.020427	.626895	0.269946	98.95	96.35	2.951			"		
												"		"		.020427	.626892	.269943	98.94	96.34	"			"	10.4177	121.373
4.6×10^{-3}	5616	10.5473	1.78063	1.13521	2.84574	13.653	701.03	2292.89	.446324	40.4546	1.4838	6.360	6.418	3.116		.023500										
	5616.44	10.5481	1.78049	1.13567	2.84596	13.667	701.39	2293.07	.446342	40.4546	"	"		"		.023536		.387144	100.61	99.77	3.109	5502	2.5452	0.1304		
	5616.49	10.5482	1.78047	1.13574	2.84600	13.669	701.45	2293.09	.446344	40.4545	1.4839	"		"		.023533		.388530	100.40	99.67	3.106			0.1305		
																.023533	.731453	.388464	100.45	99.69	"			"	10.5482	124.489

Equations for Test 41:

$$\frac{\tilde{C}_v}{R}\Delta T^* + 36.7826\,\Delta\tilde{n}_{NO} = -P^*_{av}\Delta V^*$$

$$P^*_{av}\Delta V^* = 0.300801\,\Delta(u^{*2})$$

$$r^* = 0.127722\,P^*\left\{k_{pp_f}\left(0.242470 - \frac{\tilde{n}_{NO}}{2}\right)\left(0.243717 - \frac{\tilde{n}_{NO}}{2}\right) - k_{pp_d}\tilde{n}_{NO}{}^2\right\}$$

$$T_o = 532.46\ {}^oR$$

TABLE VII

Equilibrium Constant,[1] Rate Coefficients,[2] and Standard Enthalpy of Formation[3] of NO.

T,°K	T,°R	K	$\Delta H_{f\phi}$	Equation 156 (Daniels)		Equation 157		Equation 158		Equation 159	
			kcal/g mol	k_{pp_d} (atm^{-1} sec^{-1})	k_{pp_f}	k_{pp_d} (atm^{-1} sec^{-1})	k_{pp_f}	k_{pp_d} (atm^{-1} sec^{-1})	k_{pp_f}	k_{pp_d} (atm^{-1} sec^{-1})	k_{pp_f}
1200	2160	2.7659×10^{-7}	21.642	2.2003×10^{-4}	6.086×10^{-11}						
1300	2340	1.1137×10^{-6}	21.646	2.0708×10^{-3}	2.306×10^{-9}						
1400	2520	3.6779×10^{-6}	21.651	1.4148×10^{-2}	5.204×10^{-8}						
1500	2700	1.0402×10^{-5}	21.656	7.4815×10^{-2}	7.782×10^{-7}						
1750	3150	8.2848×10^{-5}	21.657	2.092	1.733×10^{-4}	4.490	3.720×10^{-4}	8.578	7.107×10^{-4}	12.65	1.048×10^{-3}
2000	3600	3.9259×10^{-4}	21.651	2.5438×10^{1}	9.987×10^{-3}	1.891×10^{1}	7.424×10^{-3}	1.471×10^{1}	5.774×10^{-3}	12.65	4.966×10^{-3}
2250	4050	1.3178×10^{-3}	21.634	1.7755×10^{2}	2.340×10^{-1}	5.786×10^{1}	7.624×10^{-2}	2.237×10^{1}	2.948×10^{-2}	12.65	1.667×10^{-2}
2500	4500	3.4666×10^{-3}	21.607	8.4022×10^{2}	2.913	1.415×10^{2}	4.907×10^{-1}	3.129×10^{1}	1.085×10^{-1}	12.65	4.385×10^{-2}
2750	4950	7.6503×10^{-3}	21.571	2.9972×10^{3}	2.293×10^{1}	2.943×10^{2}	2.251	4.117×10^{1}	3.150×10^{-1}	12.65	9.677×10^{-2}
3000	5400	1.4758×10^{-2}	21.521	8.649×10^{3}	1.276×10^{2}	5.416×10^{2}	7.993	5.175×10^{1}	7.637×10^{-1}	12.65	1.867×10^{-1}
3500	6300	4.1348×10^{-2}	21.386	4.574×10^{4}	1.891×10^{3}	1.412×10^{3}	5.840×10^{1}	7.413×10^{1}	3.065	12.65	5.230×10^{-1}
4000	7200	8.8760×10^{-2}	21.229	1.595×10^{5}	1.416×10^{4}	2.898×10^{3}	2.573×10^{2}	9.707×10^{1}	8.616	12.65	1.123
4500	8100	1.5994×10^{-1}	21.050	4.214×10^{5}	6.739×10^{4}	5.070×10^{3}	8.109×10^{2}	1.197×10^{2}	1.915×10^{1}	12.65	2.023
5000	9000	2.5407×10^{-1}	20.887	9.166×10^{5}	2.329×10^{5}	7.930×10^{3}	2.015×10^{3}	1.416×10^{2}	3.597×10^{1}	12.65	3.214

[1] For reaction $N_2 + O_2 \rightarrow 2\ NO$

[2] As defined by Equation 121

[3] For one mol of NO

TABLE VIII

Predicted "Yields" of NO and Corresponding
Predicted Yields of NO_2, Mol Per Cent

Test Number	Observed NO_2	Equation 156 (Daniels) NO	Equation 156 (Daniels) NO_2	Equation 157 NO	Equation 157 NO_2	Equation 158 NO	Equation 158 NO_2	Equation 159 NO	Equation 159 NO_2
36	3.32	2.026	2.047	2.555	2.588	2.630	2.665	1.434	1.444
39	0.37	1.698	1.713	1.562	1.574	0.6870	0.6894	0.3440	0.3446
41	1.92	1.462	1.473	2.176	2.200	3.882	3.959	4.463	4.565
43	1.30	1.174	1.181						
44	1.21	1.794	1.810						
45	4.68	1.080	1.086	1.580	1.593	2.560	2.593	4.818	4.937

TABLE IX

Error Parameters

A. Errors in Predictions

Test	Equation	156	157	158	159
	E_a, cal/g mol	69,500	50,000	15,000	0
36	Error,[1,2]	-1.273	-0.732	-0.655	-1.876
	Error, inert free[1]	-1.279	-0.735	-0.658	-1.884
	Error, fraction of observed value	-0.3834	-0.2205	-0.1973	-0.5651
39	Error	1.343	1.204	0.319	-0.025
	Error, inert free	1.540	1.381	0.366	-0.029
	Error, fraction	3.630	3.254	0.862	-0.068
41	Error	-0.447	0.280	2.039	2.645
	Error, inert free	-0.929	0.582	4.237	5.496
	Error, fraction	-0.2328	0.146	1.062	1.378
45	Error	-3.594	-3.087	-2.087	0.257
	Error, inert free	-6.052	-5.198	-3.514	0.433
	Error, fraction	-0.7679	-0.6596	-0.4459	0.0549

[1] mol per cent.

[2] Predicted mol percentage of NO_2 minus observed.

TABLE IX - continued

Error Parameters

B. Various Parameters

Parameter	Equation E_a, cal/g mol	156 69,500	157 40,000	158 15,000	159 0
$\sum \Delta_n$	, mol per cent	-3.971	-2.335	-0.384	1.001
$\sum \Delta_n$	, mol per cent inert free	-6.720	-3.970	0.431	4.016
$\sum \frac{\Delta_n}{obs}$		2.246	2.520	1.281	0.800
$\sum \Delta_n^2$	, (mol per cent)^2	16.54	11.59	9.044	10.58
$\sum \Delta_n^2$	, (mol per cent)^2 inert free	41.50	29.81	30.87	33.94
$\sum (\frac{\Delta_n}{obs})^2$		13.97	11.09	2.109	2.226
$\sum \lvert \Delta_n \rvert$	, mol per cent	6.657	5.303	5.100	4.803
$\sum \lvert \Delta_n \rvert$	, mol per cent inert free	9.800	7.896	8.775	7.842
$\sum \lvert \frac{\Delta_n}{obs} \rvert$		.5.014	4.280	2.567	2.066

TABLE X

Selected Information from Numerical Integrations

Test Number / Equation		36: 156 Daniels	36: 157	36: 158	36: 159
Initial conditions Observed minimum volume ratio Observed yield, Mol per cent NO_2	T_o, °R P_o, psia v^* NO_2	532.37 2.9630 1.1306×10^{-3} 0.32			
Extreme conditions, calculated neglecting reaction	T^* T, °R P^* P, psia F, lb.	9.5211 5060.8 2421.5 24950 33.27			
Reaction negligible until	v^* T, °R k_{pp_d}, atm^{-1} sec^{-1} k_{pp_f}, atm^{-1} sec^{-1}	3.4×10^{-3} 3708 2.297×10^{-2}	3.2×10^{-3} 3774 1.956×10^{-2}	3.05×10^{-3} 3627 1.379×10^{-2}	3.05×10^{-3} 3627 9.405×10^{-3}
Predicted concentration of NO within one per cent of equilibrium concentration	v^* T, °R k_{pp_d}, atm^{-1} sec^{-1} k_{pp_f}, atm^{-1} sec^{-1} $\bar{n}_{NO}$	1.25×10^{-3} 4723 1629 8.490 0.03422	not reached on downstroke		
Predicted minimum volume	$10^3 v^*$ T^* T, °R P^* P, psia k_{pp_d}, atm^{-1} sec^{-1} k_{pp_f}, atm^{-1} sec^{-1} $\bar{n}_{NO}$	1.1106 9.1229 4857 8214.3 24340 2342 15.43 0.03865	1.1192 9.1224 4360 8256.1 24170 256.9 1.696 0.03803	1.1277 9.3080 4955 8253.8 24460 41.29 0.3186 0.02056	1.1302 9.4355 5004 8348.5 24740 12.65 0.1085 0.00810
Predicted concentration of NO reaches equilibrium concentration	v^* T, °R k_{pp_d}, atm^{-1} sec^{-1} k_{pp_f}, atm^{-1} sec^{-1} $\bar{n}_{NO}$	close at min. volume	1.13×10^{-3} 4645 251.1 1.615 0.03840	1.54×10^{-3} 4500 31.28 0.1084 0.02866	2.7×10^{-3} 3898 12.65 0.01142 0.01449
Predicted concentration of NO reaches 1.1 times equilibrium concentration	v^* T, °R k_{pp_d}, atm^{-1} sec^{-1} k_{pp_f}, atm^{-1} sec^{-1} $\bar{n}_{NO}$	1.60×10^{-3} 4305 446.1 1.043 0.02577	1.40×10^{-3} 4586 144.5 0.6709 0.03407	1.65×10^{-3} 4413 29.49 0.08617 0.02859	2.9×10^{-3} 3519 12.65 9.265×10^{-3} 0.01449
Predicted concentration of NO reaches twice equilibrium concentration	v^* T, °R k_{pp_d}, atm^{-1} sec^{-1} k_{pp_f}, atm^{-1} sec^{-1} $\bar{n}_{NO}$	3.55×10^{-3} 3567 21.63 7.674×10^{-3} 0.02052	2.75×10^{-3} 3619 33.71 2.475×10^{-2} 0.02607	2.7×10^{-3} 3641 18.64 1.456×10^{-2} 0.02728	4.2×10^{-3} 3429 10.63 [illegible]$\times10^{-3}$ 0.01439
Primary reaction small after	v^* T, °R k_{pp_d}, atm^{-1} sec^{-1}	3.85×10^{-3} 3404 14.20	3.8×10^{-3} 3481 13.42	3.65×10^{-3} 3469 12.75	3.0×10^{-3} 3781 12.65
Predicted yield	Mol per cent NO_2	2.047	2.588	2.665	1.444

Test Number / Equation	39: 156 Daniels	39: 157	39: 158	39: 159
Initial conditions / Observed	530.93 2.2612 2.5997×10^{-3} 0.37			
Extreme conditions	8.4512 4427.0 3250.9 7351 24.48			
Reaction negligible until	4.8×10^{-3} 3713 2.29×10^{-2}	4.6×10^{-3} 3763 1.[illegible]$\times10^{-2}$	4.4×10^{-3} 3815 1.322×10^{-2}	4.2×10^{-3} 3871 1.065×10^{-2}
Within one per cent of equilibrium	not reached on downstroke			
Predicted minimum volume	2.593 8.2116 4360 3166.8 7161 535.8 1.404 0.02094	2.5996 8.3183 4416 3199.6 7235 121.5 0.3574 0.01148	2.6023 8.4057 4463 3230.1 7304 30.51 0.09837 0.00371	2.6030 8.4279 4475 3237.8 7321 12.65 0.04174 0.00176
Reaches equilibrium concentration	2.63×10^{-3} 4338 499.0 12.51 0.02137	3.3×10^{-3} 4078 61.52 0.08665 0.01620	5.8×10^{-3} 3466 12.70 3.269×10^{-3} 0.00688	
Reaches 1.1 times equilibrium	3.0×10^{-3} 4176 283.5 0.4997 0.01984	3.5×10^{-3} 4005 52.30 0.06178 0.01616	6.3×10^{-3} 3376 7.983 1.523×10^{-3} 0.00686	not covered
Reaches twice equilibrium	4.8×10^{-3} 3623 20.45 1.198×10^{-2} 0.01724	5.3×10^{-3} 3521 15.09 4.640×10^{-3} 0.01574	not covered in calc'ns.	
Primary reaction small after	5.3×10^{-3} 3513 16.49	5.0×10^{-3} 3586 18.17	4.0×10^{-3} 3893 19.54	5.0×10^{-3} 3649 12.65
Predicted yield	1.713	1.574	0.689	0.345

Test Number / Equation	41: 156 Daniels	41: 157	41: 158	41: 159
Initial conditions / Observed	532.46 1.8770 1.2142×10^{-3} 1.92			
Extreme conditions	15.6279 8321.0 8614.2 16170 -35.53			
Reaction negligible until	1.16×10^{-2} 4021 0.1946	1.06×10^{-2} 4170 0.1303	9.4×10^{-3} 4377 0.0780	8.1×10^{-3} 4646 0.0577
Within one per cent of equilibrium	4.75×10^{-3} 5464 10335 170.3 0.02905	2.6×10^{-3} 6757 2084 130.2 0.05352	not reached on downstroke	
Predicted minimum volume	1.7077 14.5421 7743 8515.5 15980 2.945×10^{5} 3.791×10^{4} 0.07295	1.7266 14.5417 7743 8422.3 15810 4125 530.9 0.07395	1.7759 14.5551 7750 8196.2 15300 111.0 14.35 0.07300	1.8165 15.0930 8036 8309.0 15600 12.65 1.949 0.03474
Reaches equilibrium concentration	very close at min. volume		1.80×10^{-3} 7706 109.9 13.82 0.07350	2.9×10^{-3} 6612 12.65 0.6976 0.05042
Reaches 1.1 times equilibrium	7.2×10^{-3} 4723 1626 8.503 0.01805	4.6×10^{-3} 5546 646.3 11.53 0.03342	2.4×10^{-3} 6967 91.12 6.761 0.06413	3.25×10^{-3} 6326 12.65 0.5365 0.05032
Reaches twice equilibrium	1.15×10^{-2} 3938 114.3 0.1145 0.02495	9.0×10^{-3} 4314 99.92 0.2377 0.02322	5.75×10^{-3} 5074 44.02 0.4080 0.04460	5.50×10^{-3} 5160 12.65 0.1335 0.04835
Primary reaction small after	1.30×10^{-2} 3748 50.75	1.30×10^{-2} 3724 26.41	1.40×10^{-2} 3578 14.37	1.40×10^{-2} 3563 12.65
Predicted yield	1.473	2.200	3.959	4.565

Test Number / Equation	45: 156 Daniels	45: 157	45: 158	45: 159	42: 156 Daniels	44: 156 Daniels
Initial conditions / Observed	537.26 2.0193 3.4451×10^{-3} 4.68				531.33 2.1527 2.9069×10^{-3} 1.30	533.00 3.2059 1.9639×10^{-3} 1.21
Extreme conditions	10.3063 5812.3 2136.7 6334 -7.88				16.0216 8512.7 5511.6 11360 -31.56	8.9752 4785.4 4571.7 14650 18.82
Reaction negligible until	1.9×10^{-2} 3046 1.060	1.95×10^{-2} 3016 2.691	1.9×10^{-2} 3046 1.060	1.9×10^{-2} 3046 1.060	1.50×10^{-2} 4077 0.2773	4.6×10^{-3} 3697 0.0204
Within one per cent of equilibrium	8.2×10^{-3} 5086 4208.6 39.74 0.01602	6.7×10^{-3} 5702 773.0 16.72 0.02465	not reached on downstroke		7.1×10^{-3} 5576 12498 231.6 0.02328	2.0×10^{-3} 4586 1091 4.449 0.02734
Predicted minimum volume	4.0143 12.0528 6483 3002.5 6063 6.062×10^{4} 2.978×10^{3} 0.03449	3.9041 12.0529 6483 3027.3 6234 1661 91.59 0.03448	3.725 12.0064 6458 3123.1 6508 78.15 3.751 0.03792	3.6236 11.5660 6221 3101.9 6445 12.65 0.4835 0.07973	3.7015 15.0167 7979 5398.5 11620 .05964	1.9446 8.6635 4618 4455 14280 1200 5.293 0.02847
Reaches equilibrium concentration	very close at min. volume		always more than equilibrium		close at min. volume	close at min. volume
Reaches 1.1 times equilibrium	1.02×10^{-2} 4702 1561 7.955 0.01382	6.4×10^{-3} 5473 592.5 9.631 0.02325	4.6×10^{-3} 6904.8 74.35 3.102 0.03533	always more	1.0×10^{-2} 4050 2359 15.55 0.01508	2.6×10^{-3} 4266 390.0 0.8384 0.02293
Reaches twice equilibrium	1.70×10^{-2} 3901 98.00 8.915×10^{-2} 0.01103	1.25×10^{-2} 4301 97.49 0.2258 0.01673	3.4×10^{-3} 4834 38.53 0.2436 0.02812	always more	1.50×10^{-2} 3992 141.8 0.1624 0.01292	4.6×10^{-3} 3605 26.0 0.01012 0.01022
Primary reaction small after	1.5×10^{-2} 3740 48.91	1.9×10^{-2} 3674 33.15	1.8×10^{-2} 3697 15.29	1.9×10^{-2} 3441 11.34	1.82×10^{-2} 3742 50.74	4.8×10^{-3} 3550 20.88
Predicted yield	1.086	1.593	2.593	4.937	1.181	1.010

TABLE XI

Finite Difference Calculations for Test 36
Daniels' Equation

10^3 V*	T*	T °R	r* sec^{-1}	$\tilde{n}_{NO}$	$\tilde{n}_{eq}$	10^5 θ sec.	10^5 θ sec.
4.1508	6.574	3500	0.350				64.330
4.0	6.646	3538	0.502	.000009		2.057	62.273
3.6	6.853	3648	1.374	.000057		7.643	56.687
3.2	7.089	3774	4.07	.000200		13.462	50.868
2.90	7.290	3881	9.75	.000494		18.025	46.305
2.60	7.515	4001	24.55	.001255		22.814	41.516
2.4	7.677	4087	45.74	.002394		26.170	38.170
2.2	7.846	4177	84.16	.004618		29.698	34.632
2.0	8.018	4268	141.8	.008803		33.453	30.877
1.84	8.154	4341	182.5	.014079		36.679	27.651
1.68	8.299	4418	178.3	.020533		40.182	24.148
1.55	8.438	4492	135.2	.025477		43.325	21.005
1.45	8.565	4560	101.7	.028623	.03004	46.011	18.319
1.35	8.710	4637	82.96	.031408	.032185	49.065	15.265
1.25	8.871	4723	69.20	.034224	.03465	52.771	11.559
1.15	9.048	4817	43.48	.037299	.03747	58.223	6.107
1.11061	9.1229	4857	11.13	.038648	.03870	64.330	0
1.13	9.084	4836	-11.32	.038163		68.592	4.262
1.15	9.046	4816	-33.73	.037533	.03743	70.410	6.080
1.25	8.864	4719	-57.54	.034882	.03454	75.864	11.534
1.35	8.698	4631	-64.60	.032586	.03200	79.572	15.242
1.45	8.545	4549	-64.05	.030613	.02974	82.627	18.297
1.55	8.403	4474	-60.76	.028932	.02771	85.315	20.985
1.65	8.271	4403	-55.85	.027505	.02587	87.761	23.431
1.75	8.146	4337	-50.22	.026298	.02423	90.034	25.704
1.88	7.995	4256	-42.77	.025014	.02230	92.797	28.467
2.04	7.824	4165	-34.13	.023795	.02020	95.974	31.644
2.20	7.666	4081	-26.69	.022889	.01837	98.966	34.636
2.40	7.486	3985	-19.27	.022081	.01640	102.508	38.178
2.60	7.322	3898	-13.76	.021529	.01470	105.881	41.551
2.80	7.171	3817	-9.776	.021151	.01325	109.120	44.790
3.0	7.032	3743	-6.974	.020892	.01200	112.250	47.920
3.25	6.873	3659	-4.554	.020677	.01064	116.037	51.707
3.55	6.700	3567	-2.774	.020520	.00928	120.430	56.100
4.0	6.472	3445	-1.358	.020394	.00766	126.777	62.447
4.4	6.294	3351	-0.743	.020339	.00653	132.224	67.894
4.8	6.135	3266	-0.418	.020309	.00562	137.525	73.195
5.8	5.800	3088	-0.112	.020281		150.288	85.958

TABLE XII

Finite Difference Calculations for Test 39
Daniels' Equation

10^3 V*	T*	T °R	r* sec^{-1}	$\tilde{n}_{NO}$	$\tilde{n}_{eq}$	10^5 θ sec.	10^5 θ sec.
5.798793	6.592	3500	0.148	taken as 0		taken as 0	111.342
5.4	6.741	3579	0.300	.000018		8.304	103.038
5.0	6.906	3666	0.655	.000057		17.021	94.321
4.6	7.087	3763	1.492	.000150		26.237	85.105
4.2	7.288	3869	3.587	.000384		36.128	75.214
4.0	7.396	3927	5.592	.000620		41.413	69.929
3.8	7.510	3987	9.076	.001024		46.994	64.348
3.6	7.629	4050	14.30	.001708		52.956	58.386
3.4	7.751	4115	22.44	.002879		59.427	51.915
3.2	7.874	4180	33.93	.004891		66.627	44.715
3.0	7.993	4244	46.43	.008265		74.985	36.357
2.8	8.104	4303	48.85	.013457		85.603	25.739
2.7	8.158	4331	39.25	.016698		82.904	18.438
2.62	8.202	4355	22.78	.019526		102.107	9.235
2.605	8.209	4358	17.68	.020144	.02175	105.187	6.155
2.593	8.212	4360	9.45	.020940	.02177	111.342	0
2.6	8.201	4354	4.28	.021263	.02166	116.045	4.703
2.63	8.171	4338	-0.68	.021366		122.164	10.822
2.67	8.135	4319	-3.57	.021262		126.979	15.637
2.7	8.108	4305	-4.91	.021144	.02059	129.798	18.456
2.8	8.024	4260	-7.31	.020692		137.120	25.778
3.0	7.865	4176	-8.39	.019839	.01795	147.780	36.438
3.2	7.718	4098	-7.79	.019154		156.185	44.843
3.4	7.581	4025	-6.69	.018628		163.434	52.092
3.6	7.452	3957	-5.53	.018229		169.953	58.611
3.8	7.332	3893	-4.47	.017929		175.962	64.620
4.0	7.218	3833	-3.56	.017703		181.590	70.248
4.2	7.112	3776	-2.82	.017534		186.921	75.579
4.6	6.915	3671	-1.74	.017311	.00951	196.904	85.562
5.0	6.738	3577	-1.08	.017182	.00828	206.210	94.868
5.6	6.503	3453	-0.532	.017081		219.265	107.923
6.2	6.298	3344	-0.269	.017034		231.530	120.188
7.0	6.060	3217	-0.114	.017007		247.000	135.658
7.5	5.928	3147	-0.068	.016999		256.275	144.933

TABLE XIII

Finite Difference Calculations for Test 41
Daniels' Equation

10^3 V*	T*	T °R	r* sec^{-1}	$\tilde{n}_{NO}$	$\tilde{n}_{eq}$	10^5 θ sec.	10^5 θ sec.
14.23454	6.949	3700	0.0793	taken as 0		taken as 0	198.256
13	7.211	3839	0.2453	.000020		14.530	183.726
12	7.448	3966	0.6421	.000069		26.469	171.787
11.2	7.658	4078	1.432	.000164		36.148	162.108
10.4	7.888	4200	3.286	.000381		45.959	152.297
9.6	8.139	4334	7.728	.000895		55.924	142.332
8.8	8.410	4478	18.199	.002128		66.067	132.189
8.0	8.695	4629	39.84	.005000		76.426	121.830
7.4	8.910	4744	60.65	.008980		84.363	113.893
6.8	9.136	4864	68.10	.014321		92.472	105.784
6.2	9.402	5006	52.75	.019406		100.789	97.467
5.6	9.731	5181	42.42	.023370		109.360	88.896
5.0	10.118	5388	45.73	.027263	.027625	118.253	80.003
4.5	10.492	5587	50.66	.030976		125.983	72.273
4.0	10.924	5816		.035365	.035447	134.101	64.155
3.4	11.545	6147		→	.041835	144.576	53.680
2.9	12.182	6487			.048579	154.268	43.988
2.5	12.805	6818			.055263	163.130	35.126
2.1	13.573	7227			.063585	174.079	24.177
1.9	14.034	7473			.068532	181.520	16.736
1.8	14.289	7609			.071260	186.721	11.535
1.75	14.424	7680			.072695	190.462	7.794
1.70771	14.542	7743			.073950	198.256	0
	Returns Along Same Path to						
3.8	11.116	5918		→	.037396	259.024	60.768
4.2	10.742	5720			.033627	265.712	67.456
4.6	10.408	5542	-39.59	.030549	.030372	272.101	73.845
5.0	10.110	5383	-39.61	.027862	.027551	278.257	80.001
5.5	9.777	5206	-34.94	.025035	.024509	285.692	87.436
6.0	9.479	5047	-29.34	.022719	.02191	292.895	94.639
6.6	9.158	4876	-23.24	.020518	.01924	301.292	103.036
7.2	8.870	4723	-17.83	.018846	.01697	309.469	111.213
7.8	8.609	4584	-13.30	.017609		317.465	119.209
8.4	8.370	4456	-9.692	.016714		325.309	127.053

TABLE XIII - Continued

Finite Difference Calculations for Test 41
Daniels' Equation

10^3 V*	T*	T °R	r^* sec^{-1}	$\tilde{n}_{NO}$	$\tilde{n}_{eq}$	10^5 θ sec.	10^5 θ sec.
9.0	8.150	4339	-6.935	.016079		333.023	134.767
9.8	7.883	4197	-4.355	.015519		343.135	144.879
10.6	7.642	4069	-2.703	.015175		353.078	154.822
11.5	7.397	3938	-1.575	.014945	.00758	364.092	165.836
12.5	7.152	3808	-0.868	.014803		376.148	177.892
13.5	6.932	3691	-0.483	.014725		388.040	189.784
15	6.640	3535	-0.206	.014668		405.619	207.363
17	6.307	3358	-0.070	.014640		428.660	230.404

TABLE XIV

Finite Difference Calculations for Test 45
Daniels' Equation

10^3 V*	T*	T °R	r* sec^{-1}	$\tilde{n}_{NO}$	$\tilde{n}_{eq}$	10^5 θ sec.	10^5 θ sec.
19.75498	5.578	3000	-0.483	taken as .127191		taken as 0	319.904
18	5.786	3112	-1.168	.126997		25.174	294.730
16.5	5.990	3222	-2.611	.126605		47.116	272.788
15	6.228	3350	-6.203	.125681		69.532	250.372
13.5	6.520	3507	-16.10	.123261		92.531	227.373
12	6.917	3720	-48.10	.116434		116.269	203.635
11	7.323	3939	-113.53	.104146		132.622	187.282
10.3	7.769	4179	-216.10	.085427		144.387	175.517
9.8	8.226	4424	-299.92	.063077		152.987	166.917
9.4	8.644	4649	-279.39	.042202		160.007	159.897
9.0	9.004	4843	-162.63	.026328		167.174	152.730
8.6	9.263	4982	-57.59	.018735		174.512	145.392
8.4	9.364	5037	-25.21	.017310		178.253	141.651
8.2	9.456	5086	-4.20	.016823	.016650	182.047	137.857
8.0	9.542	5132	+7.89	.016915		185.900	134.004
7.7	9.669	5201	14.66	.017605	.018001	191.797	128.107
7.2	9.893	5321	15.80	.019178	.019450	202.032	117.872
6.6	10.189	5480	16.27	.021263		215.032	104.872
6.0	10.523	5660		→	.023693	229.188	90.716
5.4	10.906	5866			.026352	245.134	74.770
4.8	11.348	6104			.029481	264.366	55.538
4.4	11.686	6285			.031891	281.313	38.591
4.2	11.871	6384			.033197	293.200	26.704
4.014267	12.053	6483			.034485	319.904	0
	Return Along Equilibrium Path to						
6.0						410.620	90.716
6.6	10.187	5479		→	.021410	424.776	104.872
7.2	9.889	5319			.019430	437.776	117.872
7.8	9.619	5174	-7.73	.017909		449.956	130.052
8.4	9.373	5042	-11.06	.016680		461.519	141.615
9.0	9.150	4921	-9.55	.015540	.01479	472.598	152.694
9.8	8.879	4776	-7.70	.014319	.01320	486.775	166.871
11	8.520	4583	-5.28	.013012		507.050	187.146
12	8.256	4440	-3.72	.012289		523.245	203.341
13.5	7.906	4252	-2.12	.011623		546.630	226.726
15	7.602	4089	-1.18	.011261	.00683	569.165	249.261
17	7.253	3901	-0.536	.011025	.00545	598.206	278.302
20	6.819	3667	-0.171	.010892	.00399	640.146	320.242

TABLE XV

Finite Difference Calculations for Test 36
Equation 159

10^3 V*	T*	T °R	r* sec^{-1}	$\tilde{n}_{NO}$	$\tilde{n}_{eq}$	10^5 θ sec.	10^5 θ sec.
4.150836	6.574	3500	0.287	"0"		"0"	63.654
4.0	6.646	3538	0.339	.000006	.00888	2.057	61.597
3.6	6.853	3648	0.543	.000031	.01048	7.643	56.011
3.2	7.090	3775	0.906	.000072	.01251	13.462	50.192
2.9	7.294	3883	1.374	.000124	.01444	18.025	45.629
2.6	7.526	4007	2.159	.000207	.01682	22.814	40.840
2.4	7.700	4099	2.983	.000293	.01874	26.170	37.484
2.2	7.892	4201	4.208	.000418	.02100	29.699	33.955
2.0	8.107	4316	6.085	.000609	.02371	33.457	30.197
1.84	8.298	4418	8.344	.000840	.02625	36.688	26.966
1.68	8.510	4531	11.68	.001189	.02924	40.205	23.449
1.55	8.701	4632	15.64	.001618	.03205	43.370	20.284
1.45	8.860	4717	19.80	.002098	.03448	46.091	17.563
1.35	9.032	4808	25.22	.002797	.03721	49.213	14.441
1.25	9.217	4907	32.53	.003912	.04024	53.081	10.573
1.17	9.371	4989	39.89	.005554	.04285	57.601	6.053
1.14	9.426	5018	42.69	.006816	.04380	60.659	2.995
1.130209	9.436	5023	42.92	.008098	.04397	63.654	0
1.14	9.400	5004	40.57	.009349	.04335	66.651	2.997
1.18	9.296	4949	34.68	.010777	.04158	70.435	6.781
1.23	9.180	4887	29.06	.011689	.03963	73.298	9.644
1.29	9.052	4819	23.79	.012381	.03753	75.923	12.269
1.36	8.913	4745	19.03	.012922	.03532	78.458	14.804
1.44	8.767	4667	14.89	.013345	.03305	80.962	17.308
1.52	8.632	4595	11.73	.013642	.03100	83.200	19.546
1.60	8.506	4528	9.294	.013857	.02917	85.253	21.599
1.8	8.224	4378	5.253	.014184	.02526	89.853	26.199
2.0	7.980	4248	2.950	.014348	.02211	93.955	30.301
2.21	7.755	4129	1.532	.014434	.01940	97.918	34.264
2.44	7.538	4013	0.623	.014476	.01696	101.975	38.321
2.7	7.322	3898	0.044	.014489	.01470	106.302	42.648
3.0	7.103	3781	-0.309	.014482	.01263	111.041	47.387
3.4	6.850	3647	-0.518	.014457	.01046	117.046	53.392
3.85	6.607	3517	-0.592	.014421		123.483	59.829
4.4	6.354	3382	-0.385	.014382	.00689	131.012	67.358
5.0	6.119	3258	-0.176	.014361		138.909	75.255

TABLE XVI

Finite Difference Calculations for Test 39
Equation 159

10^3 V*	T*	T °R	r* sec^{-1}	$\tilde{n}_{NO}$	$\tilde{n}_{eq}$	10^5 θ sec.	10^5 θ sec.
5.798793	6.5922	3500	0.121	"0"		"0"	110.586
5.4	6.741	3579	0.170	.000012		8.304	102.282
5.0	6.906	3667	0.245	.000030		17.021	93.565
4.6	7.088	3763	0.359	.000057		26.238	84.348
4.2	7.291	3871	0.541	.000101		36.130	74.456
3.8	7.520	3992	0.839	.000174		46.996	63.590
3.4	7.781	4131	1.349	.000308		59.432	51.154
3.0	8.083	4291	2.261	.000586		75.023	35.563
2.8	8.252	4381	2.977	.000866		85.731	24.855
2.7	8.342	4429	3.431	.001106		93.213	17.373
2.64	8.396	4458	3.736	.001345		99.878	10.708
2.61	8.423	4472	3.892	.001576		105.929	4.657
2.602979	8.428	4475	3.919	.001758	.02436	110.586	0
2.61	8.419	4470	3.862	.001939		115.245	4.659
2.64	8.387	4453	3.671	.002167		121.295	10.709
2.7	8.327	4421	3.335	.002401		127.965	17.379
2.8	8.233	4371	2.860	.002633		135.452	24.866
3.0	8.057	4278	2.135	.002901		146.168	35.582
3.4	7.751	4115	1.242	.003159		161.779	51.193
3.8	7.487	3975	0.754	.003281		174.235	63.649
4.2	7.258	3853	0.472	.003346		185.120	74.534
4.6	7.055	3745	0.303	.003383		195.030	84.444
5.0	6.873	3649	0.198	.003406	.00921	204.263	93.677
5.5	6.670	3541	0.118	.003423		215.117	104.531
6.0	6.490	3446	0.0651	.003432	.00673	225.395	114.809

TABLE XVII

Finite Difference Calculations for Test 41
Equation 159

10^3 v^*	T^*	T °R	r^* sec^{-1}	$\tilde{n}_{NO}$	$\tilde{n}_{eq}$	10^5 θ sec.	10^5 θ sec.
14.23454	6.949	3700	.0246	"0"		"0"	196.809
13	7.211	3839	.0369	.000005		14.530	182.279
12	7.449	3966	.0637	.000011		26.469	170.340
11	7.717	4109	.1013	.000020		38.588	158.221
10.2	7.955	4236	.1500	.000032		48.435	148.374
9.4	8.221	4377	.227	.000050		58.442	138.367
8.7	8.480	4515	.332	.000075		67.351	129.458
8.1	8.726	4646	.469	.000106		75.120	121.689
7.5	8.998	4791	.673	.000150		83.033	113.776
6.9	9.300	4952	.987	.000216		91.116	105.693
6.3	9.641	5133	1.479	.000317	.02331	99.405	97.404
6.0	9.828	5233	1.829	.000387	.02497	103.641	93.168
5.5	10.169	5414	2.649	.000547	.02810	110.863	85.946
5.0	10.554	5620	3.927	.000789	.03178	118.329	78.480
4.6	10.901	5804	5.488	.001078	.03521	124.523	72.286
4.2	11.289	6011	7.825	.001502	.03918	130.966	65.843
3.85	11.671	6214	10.88	.002048	.04317	136.865	59.944
3.4	12.233	6513	17.07	.003157	.04912	144.937	51.872
3.0	12.816	6824	26.26	.004831	.05538	152.783	44.026
2.7	13.318	7091	37.04	.006882	.06082	159.318	37.491
2.4	13.887	7394	53.03	.010224	.06695	166.797	30.012
2.2	14.307	7618	67.58	.013791	.07145	172.729	24.080
2.0	14.756	7857	85.11	.019598	.07622	180.323	16.486
1.9	14.979	7976	93.28	.024445	.07857	185.739	11.070
1.85	15.078	8029	95.35	.028281	.07961	189.807	7.002
1.816461	15.093	8036	89.19	.034738	.07977	196.809	0
1.85	14.909	7938	72.74	.040394	.07783	203.831	7.022
1.9	14.720	7838	60.65	.043109	.07583	207.918	11.109
2.0	14.394	7664	44.36	.045959	.07237	213.370	16.561
2.2	13.841	7370	24.82	.048566	.06646	221.037	24.228
2.4	13.370	7119	13.57	.049693	.06137	227.042	30.233
2.7	12.767	6798	4.121	.050325	.05485	234.629	37.820
3.0	12.255	6525	-0.779	.050419	.04936	241.268	44.459
3.4	11.676	6217	-3.956	.050220	.04322	249.250	52.441
3.85	11.129	5926	-5.376	.049829	.03753	257.469	60.660
4.2	10.761	5730	-5.730	.049494	.03382	263.480	66.671

TABLE XVII - Continued

Finite Difference Calculations for Test 41
Equation 159

10^3 V*	T*	T °R	r* sec^{-1}	$\tilde{n}_{NO}$	$\tilde{n}_{eq}$	10^5 θ sec.	10^5 θ sec.
4.6	10.388	5531	-5.750	.049116	.03018	270.048	73.239
5.0	10.058	5355	-5.566	.048758	.02706	276.364	79.555
5.5	9.692	5160	-5.215	.048347	.02376	283.981	87.172
6.0	9.368	4988	-4.822	.047977		291.350	94.541
6.3	9.191	4894	-4.588	.047774		295.673	98.864
6.9	8.869	4722	-4.144	.047404		304.134	107.325
7.5	8.583	4570	-3.745	.047078		312.387	115.578
8.1	8.326	4433	-3.392	.046790		320.466	123.657
8.7	8.094	4309	-3.083	.046533		328.398	131.589
9.4	7.849	4179	-2.772	.046267		337.495	140.686
10.2	7.598	4046	-2.470	.046000		347.713	150.904
11	7.372	3925	-2.217	.045765		357.770	160.961
12	7.119	3791	-1.953	.045508		370.148	173.339
13.5	6.790	3615	-1.642	.045181		388.379	191.570
15	6.506	3464	-1.405	.044910		406.282	209.473
17	6.182	3292	-0.457	.044714		429.739	232.930

TABLE XVIII

Finite Difference Calculations for Test 45
Equation 159

10^3 V*	T*	T °R	r* sec^{-1}	$\tilde{n}_{NO}$	$\tilde{n}_{eq}$	10^5 θ sec.	10^5 θ sec.
19.75498	5.5777	3000	-0.483	.127191		"0"	325.069
18	5.786	3112	-1.168	.126997		25.174	299.895
16.5	5.990	3222	-2.611	.126605		47.116	277.953
15	6.228	3350	-6.203	.125681		69.532	255.537
13.5	6.517	3506	-12.78	.123435		92.530	232.539
12	6.864	3692	-14.37	.120218		116.265	208.804
10.6	7.246	3897	-16.18	.116707		139.293	185.776
9.8	7.497	4032	-17.40	.114416		152.944	172.125
9.0	7.778	4184	-18.79	.111864		167.054	158.015
8.4	8.013	4310	-19.95	.109743		178.008	147.061
7.8	8.273	4450	-21.24	.107406		189.358	135.711
7.2	8.562	4605	-22.29	.104807		201.203	123.866
6.6	8.886	4780	-24.21	.101882		213.688	111.381
6.0	9.255	4978	-25.88	.098538		227.040	98.029
5.5	9.605	5166	-27.33	.095327	.01760	239.107	85.962
5.0	10.004	5381	-28.73	.091582	.02019	252.462	72.607
4.5	10.466	5629	-29.82	.087033	.02330	267.975	57.094
4.2	10.783	5800	-30.07	.083669	.02550	279.190	45.879
4.0	11.017	5926	-29.83	.080960	.02713	288.228	36.841
3.8	11.275	6064	-28.88	.077496	.02896	300.010	25.059
3.7	11.419	6142	-27.74	.075055	.02999	308.626	16.443
3.65	11.502	6186	-26.61	.073210	.03058	315.415	9.654
3.623597	11.566	6221	-24.74	.070733	.03103	325.069	0
3.65	11.566	6221	-22.68	.068451	.03103	334.705	9.636
3.7	11.528	6200	-21.19	.066966	.03076	341.477	16.408
3.8	11.438	6152	-19.33	.065227	.03012	350.062	24.993
4.0	11.252	6052	-16.92	.063107	.02879	361.778	36.709
4.2	11.070	5954	-15.22	.061668	.02751	370.745	45.676
4.5	10.812	5815	-13.31	.060086	.02569	381.854	56.785
5.0	10.422	5606	-11.06	.058224	.02300	397.186	72.117
5.5	10.077	4520	-9.435	.056878	.02067	410.357	85.288
6.0	9.770	5255	-8.198	.055833	.01865	422.236	97.167
6.6	9.442	5078	-7.046	.054835	.01657	435.358	110.289
7.2	9.151	4922	-6.145	.054029		447.606	122.537
7.8	8.890	4781	-5.423	.053359		459.210	134.141
8.4	8.654	4654	-4.832	.052791		470.314	145.245
9.0	8.439	4539	-4.341	.052301		481.019	155.950

TABLE XVIII - Continued

Finite Difference Calculations for Test 45
Equation 159

10^3 V*	T*	T °R	r^* sec^{-1}	$\tilde{n}_{NO}$	$\tilde{n}_{eq}$	10^5 θ sec.	10^5 θ sec.
9.8	8.180	4400	-3.804	.051741		494.792	169.723
10.6	7.948	4275	-3.369	.051265		508.100	183.031
12	7.593	4084	-2.782	.050579		530.517	205.448
13.5	7.269	3910	-2.322	.049992		553.582	228.513
15	6.990	3760	-1.975	.049514		575.892	250.823
16.4	6.761	3636	-1.724	.049139		596.177	271.108
18	6.529	3512	-1.496	.048775		618.841	293.772
20	6.274	3375	-0.800	.048449		646.535	321.466
23	5.947	3199	-0.235	.048265		687.020	361.951

TABLE XIX

Calculations Neglecting Reverse Reaction:
Test 36

$10^3 v^*$	P^*	Temp ^oR	$10^5\ \theta$ sec.	k_{ppf} $atm^{-1}\ sec^{-1}$	$P^*\ k_{ppf}$ $atm^{-1}\ sec^{-1}$
4.1508	1584	3500	taken 0	0.00444	7.031
3.6	1904	3648	7.643	0.01452	27.64
3.05	2357	3827	15.719	0.05384	126.9
2.6	2894	4006	22.814	0.1774	513.4
2.3	3387	4148	27.910	0.4236	1435
2.0	4051	4313	33.457	1.089	4411
1.84	4505	4413	36.688	1.865	8403
1.68	5058	4523	40.204	3.277	16570
1.55	5600	4621	43.368	5.283	29590
1.45	6091	4702	46.087	7.707	46940
1.35	6659	4786	49.204	11.31	75320
1.3	6978	4830	51.000	13.71	95670
1.25	7323	4873	53.058	16.57	121300
1.2	7695	4916	55.572	19.89	153100
1.17	7931	4940	57.519	21.98	174300
1.14	8171	4959	60.419	23.80	194500
1.1277	8254	4955	63.792	23.44	193500
1.14	8114	4924	67.172	20.61	167200
1.16	7922	4892	69.280	17.99	142500
1.18	7743	4864	70.788	15.95	123500
1.2	7573	4838	72.033	14.23	107800
1.24	7255	4789	74.101	11.48	84020
1.28	6962	4744	75.842	9.376	65280
1.33	6626	4692	77.743	7.357	48750
1.39	6260	4632	79.763	5.572	34880
1.45	5929	4577	81.588	4.268	25310
1.57	5355	4475	84.850	2.572	13770
1.65	5024	4413	86.825	1.866	9375
1.8	4495	4307	90.232	1.053	4733
2.1	3689	4124	96.297	0.3685	1359
2.4	3108	3972	101.742	0.1422	442.0
2.7	2672	3841	106.792	0.05928	158.4
3.0	2334	3727	111.563	0.02631	61.40
3.4	1986	3596	117.608	0.00964	19.15
3.7	1781	3509	121.960	0.00477	8.504

TABLE XX

Results of Graphical Integrations, Neglecting Reversibility

Test Number	36	39	45
$\int P^* k_{pp}\, d\theta$, atm^{-1}	46.868	4.838	122800
$P_{B_o} \int P^* k_{pp}\, d\theta$	9.449	0.7444	16870
$(\tilde{n}_{N_2}\ \tilde{n}_{O_2})_{av.}$	0.2306	0.1894	
$(\tilde{n}^2_{NO})_{av}$			0.006368
Calculated $\Delta\tilde{n}_{NO}$ for $A = 10^9$ atm^{-1} sec^{-1}	2.254	0.1410	-107.5
Observed $\Delta\tilde{n}_{NO}$	0.03266	0.00369	-0.08146
Factor	69.01	38.18	2093
Indicated A, atm^{-1} sec^{-1}	1.45×10^7	2.62×10^7	3.44×10^5

TABLE XXI

Results of "Decreased Temperature" Calculations

	Test 36		Test 39		Test 41		Test 45	
	Original	Decreased T	Original	Decreased T	Original	Decreased T	Original	Decreased T
Maximum Temperature °R	4860	4374	4420	3978	7743	6970	6483	5835
Equilibrium NO at Max. Temp., mol per cent	3.8787	2.5148	2.303	1.421	7.3946	5.8321	3.4486	2.5945
Predicted NO at Max. Temp., mol per cent	3.8080	1.4369	1.1476	0.1645	"	nearly "	3.4476	2.5823
Highest mol per cent NO	3.84	1.927	1.6196	0.2828	"	"	12.7191	12.7191
Predicted Final NO, mol per cent	2.555	1.830	1.562	0.2828	2.172	2.163	1.58	1.528
Observed Final NO, mol per cent	3.266		0.369		1.902		4.573	

TABLE XXII

Leakage

Test Number	Net Loss, per cent: Assuming No Composition Change	Net Loss, per cent: Corrected for Change in Composition
40	3.3	2.3
41	5.7	4.8
42	0.5	-0.2
43	4.1	3.5
44	3.7	3.2
45	4.2	1.9
49	4.7	4.1
50	4.0	3.8
51	7.0	6.5

TABLE XXIII

Successive Strokes in Hypothetical Case, Neglecting Reaction

Stroke	V^* at Bottom	Temperature at Bottom, ^oR	V^* at Beginning of Stroke
1	1.7163×10^{-3}	8351	1.0
2	2.6654×10^{-3}	7070	0.98255
3	4.4528×10^{-3}	5806	0.95533
4	8.1669×10^{-3}	4579	0.91100
5	1.6849×10^{-2}	3424	0.83644
6	3.9329×10^{-2}	2409	0.71213
7	9.8641×10^{-2}	1618	0.52634

TABLE XXIV

Predicted Yields in Hypothetical Case*

	Bottom of Stroke			
	V*	Temp. °R	Mol Fraction NO	Final Mol Fraction NO
First Stroke	1.5865×10^{-3}	7785	0.0769	.0152
Second Stroke	2.579×10^{-3}	6683	0.0538	.0146

*Assumed Conditions:

Charge: 50 mol per cent Helium
25 per cent nitrogen
25 per cent oxygen

Initial pressure 2.2 psia.
Initial Temperature 77° F.

Driving air pressure 1000 psia.
Frictional drag 50 lb.

LIST OF FIGURES

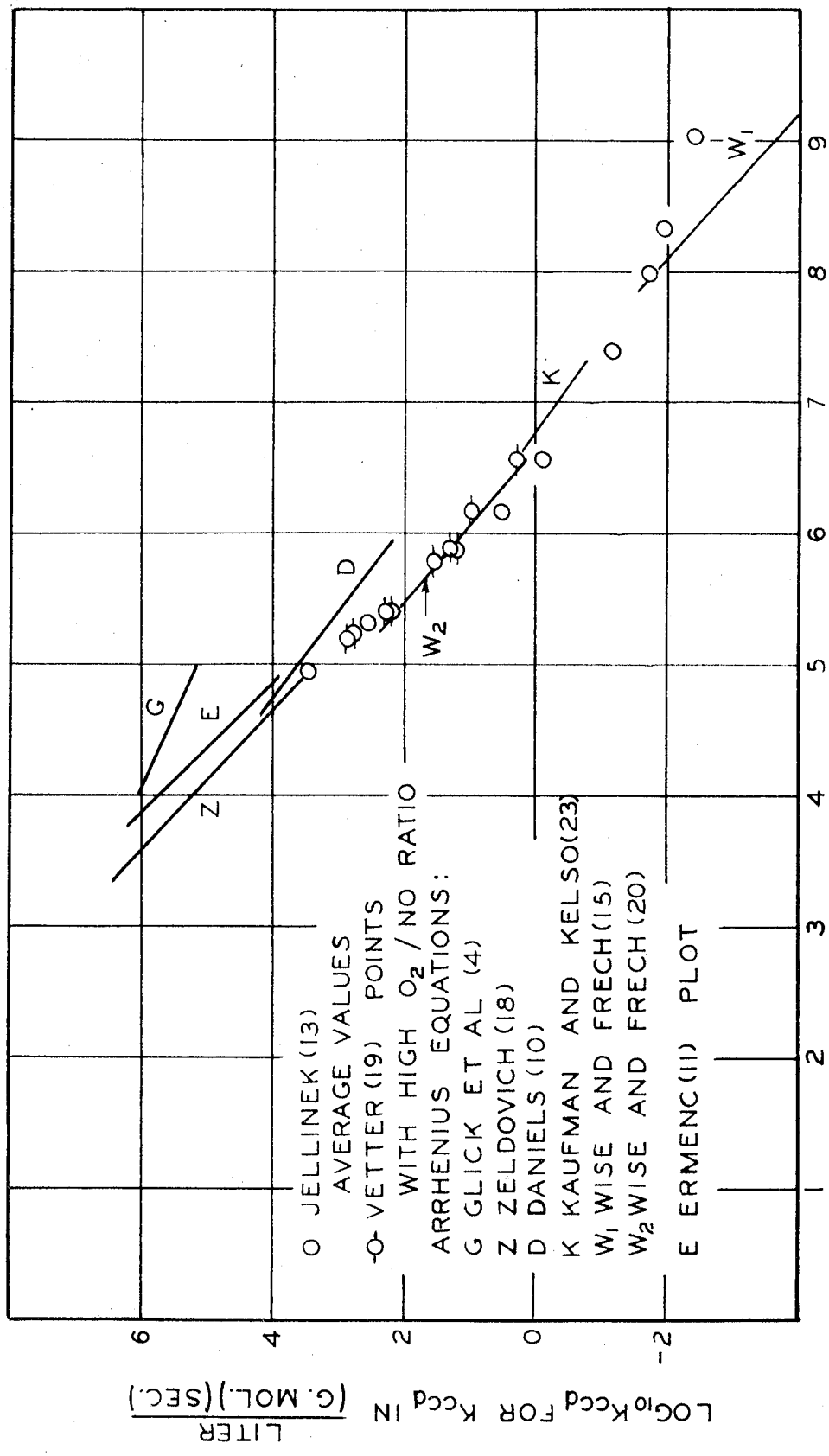

Figure 1. Rate Coefficients for Decomposition of Nitric Oxide

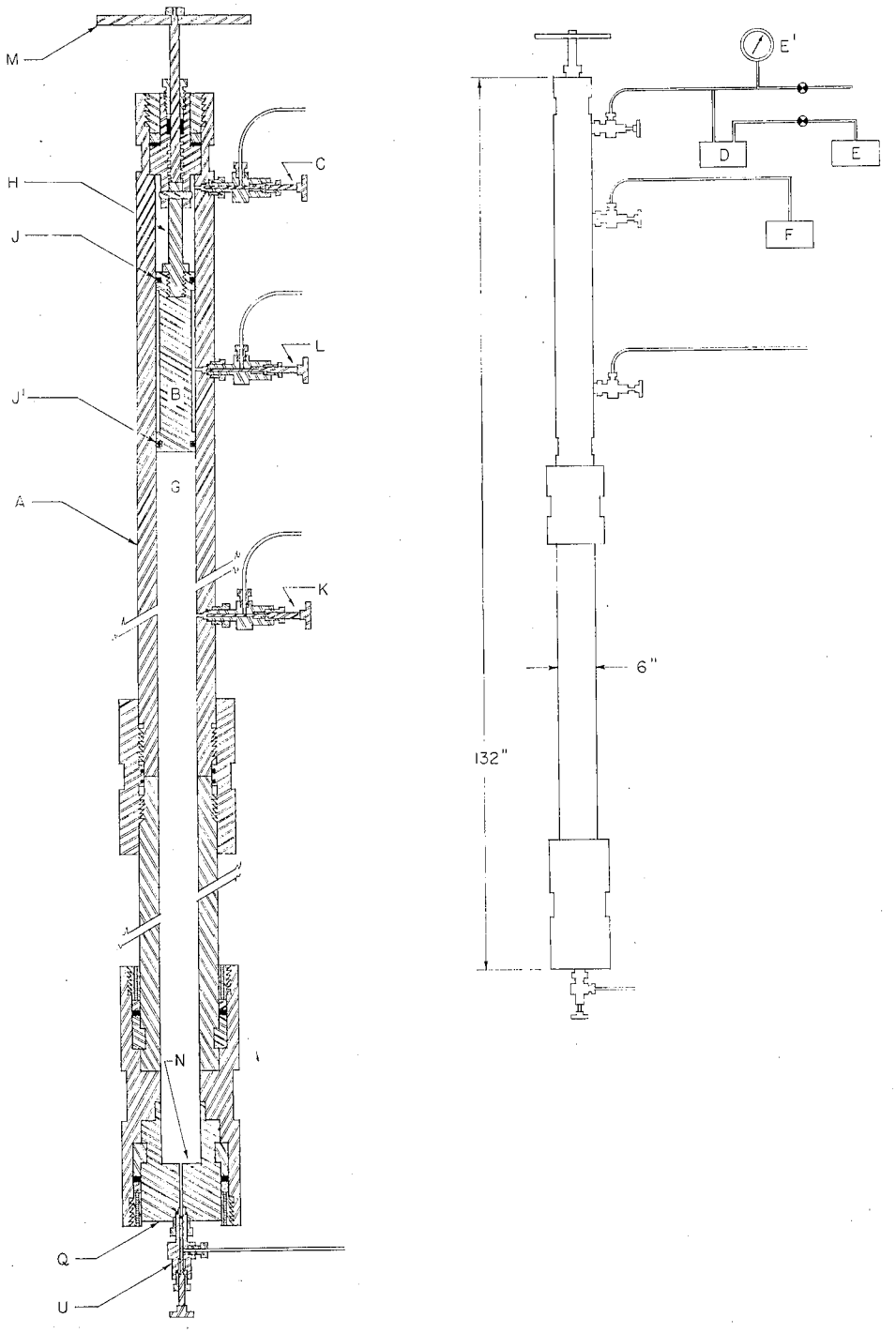

Figure 2. Schematic Diagram of Apparatus

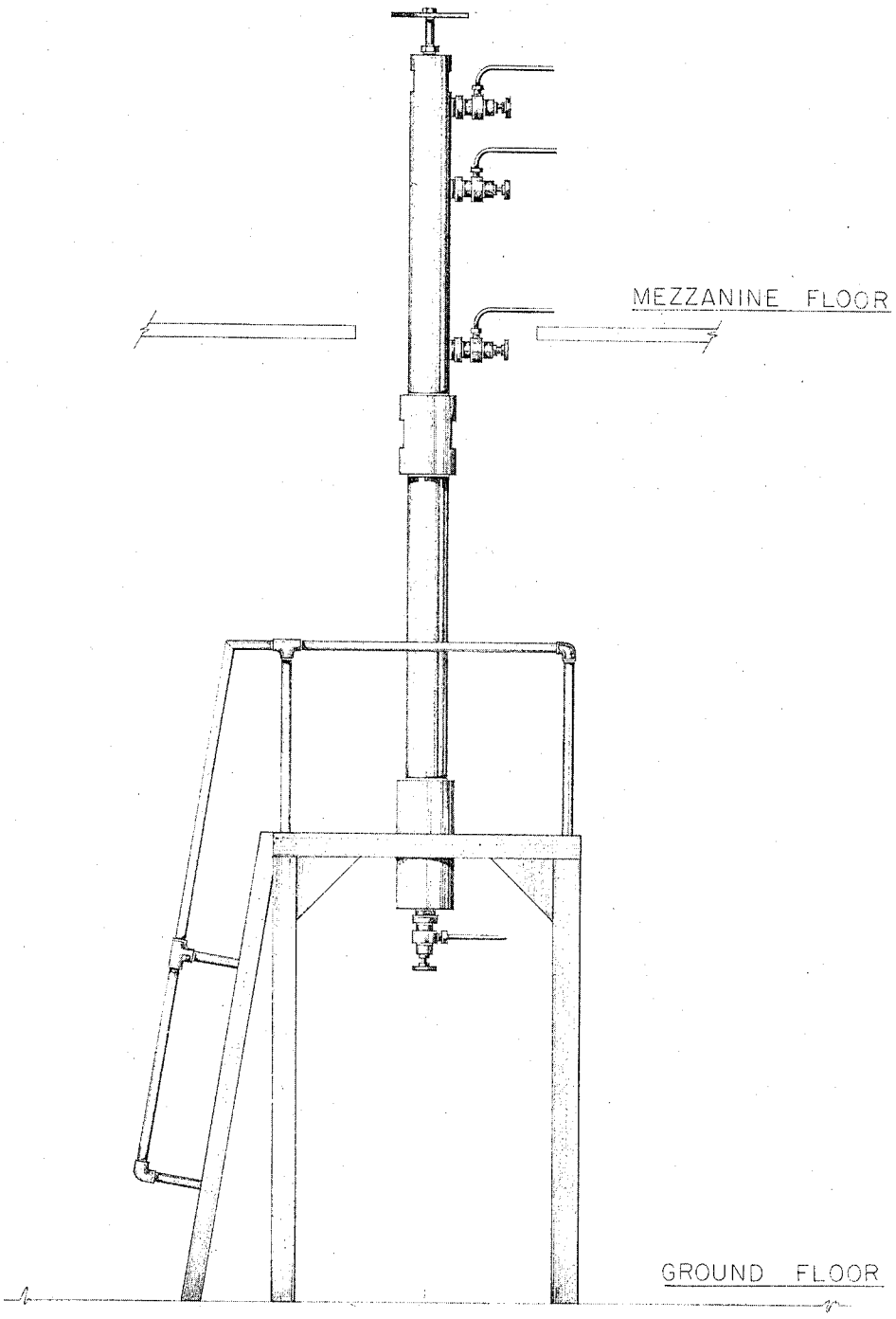

Figure 3. Installation of Apparatus

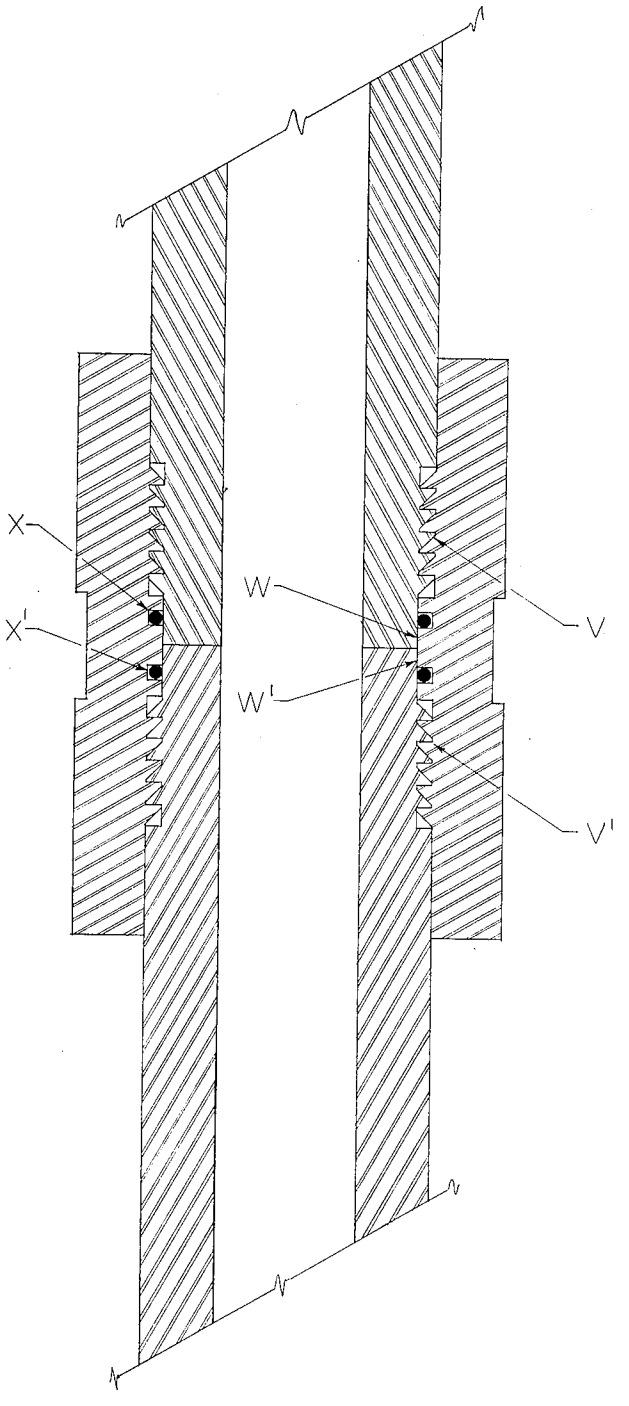

Figure 4. Juncture of Sections of Cylinder

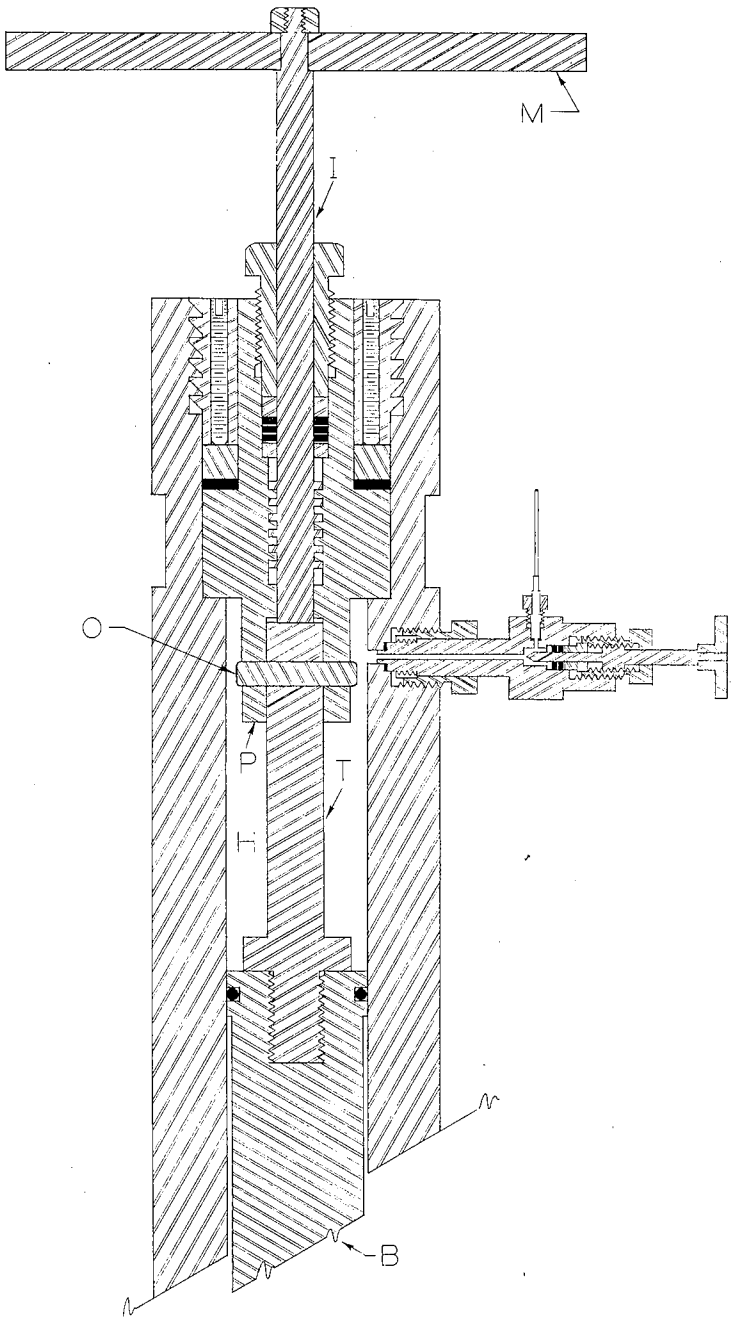

Figure 5. Details of Upper Closure and Release Mechanism

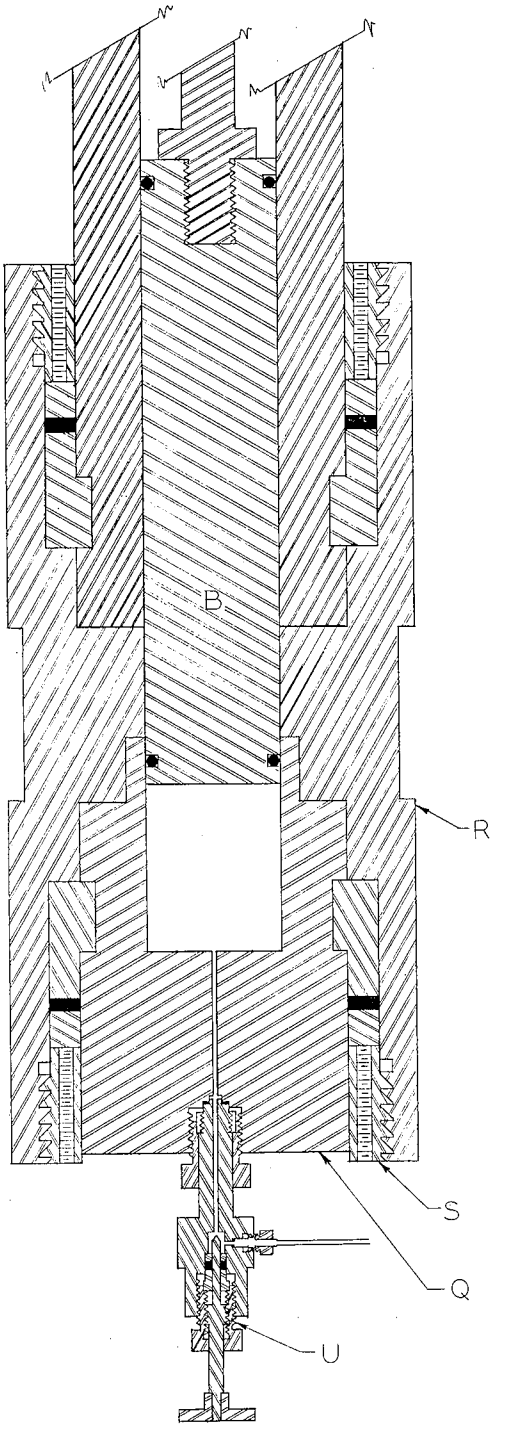

Figure 6. Details of Bottom Closure

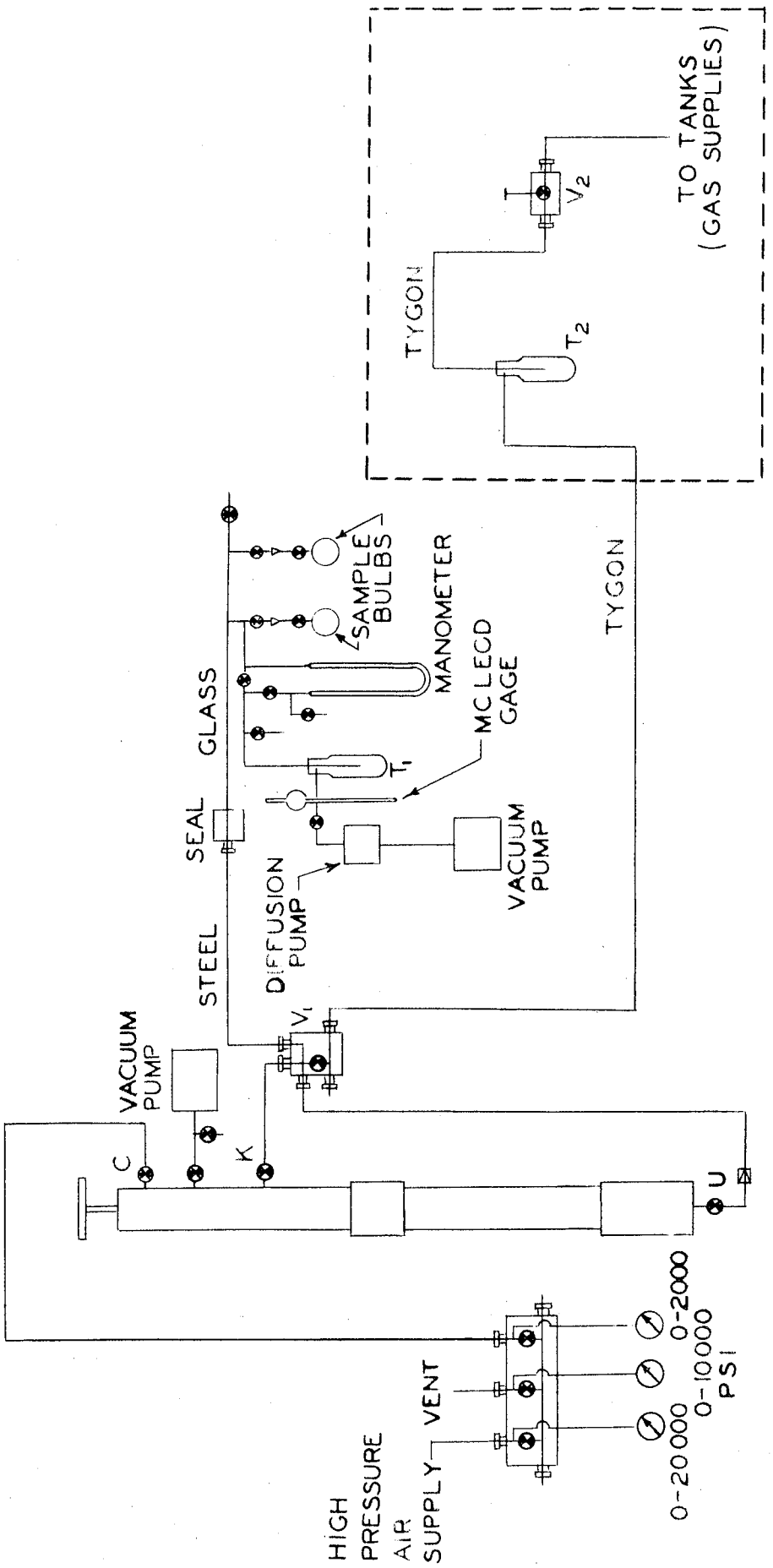

Figure 7. Schematic Diagram of Sample Transfer System

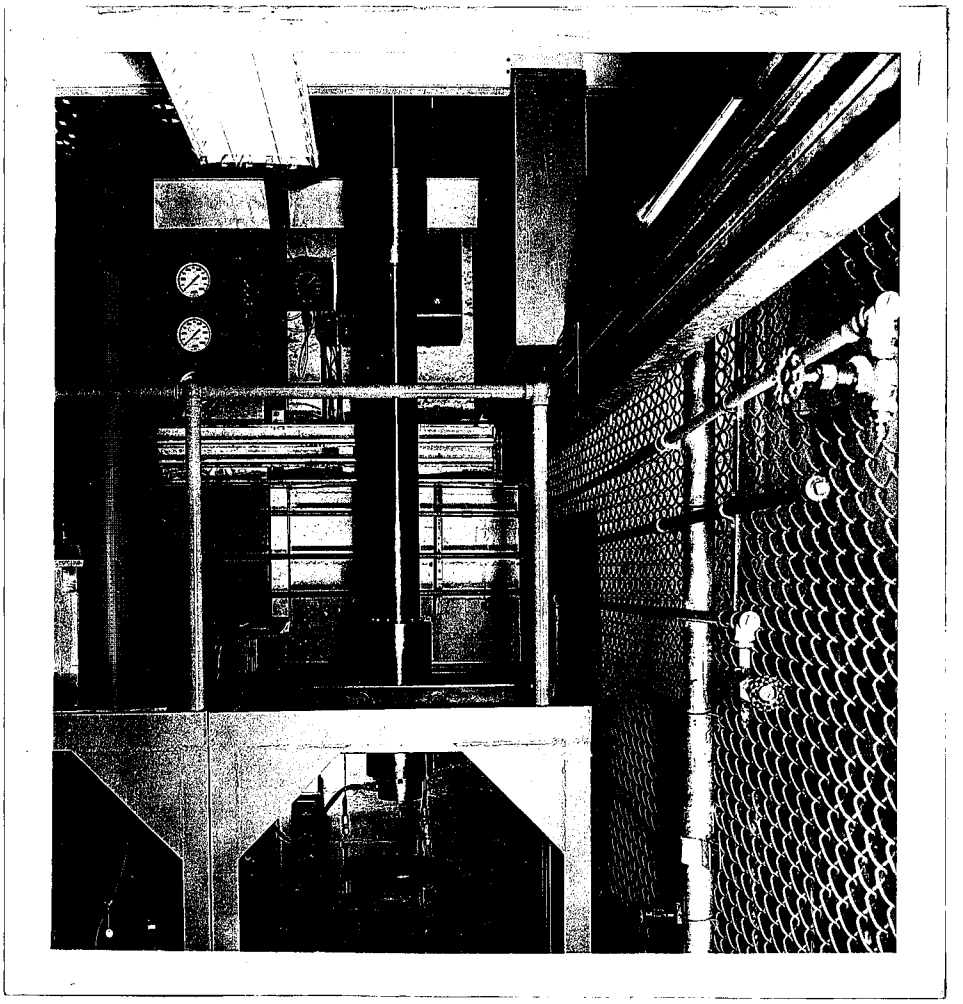

Figure 8. Photograph of Lower Portion of Apparatus

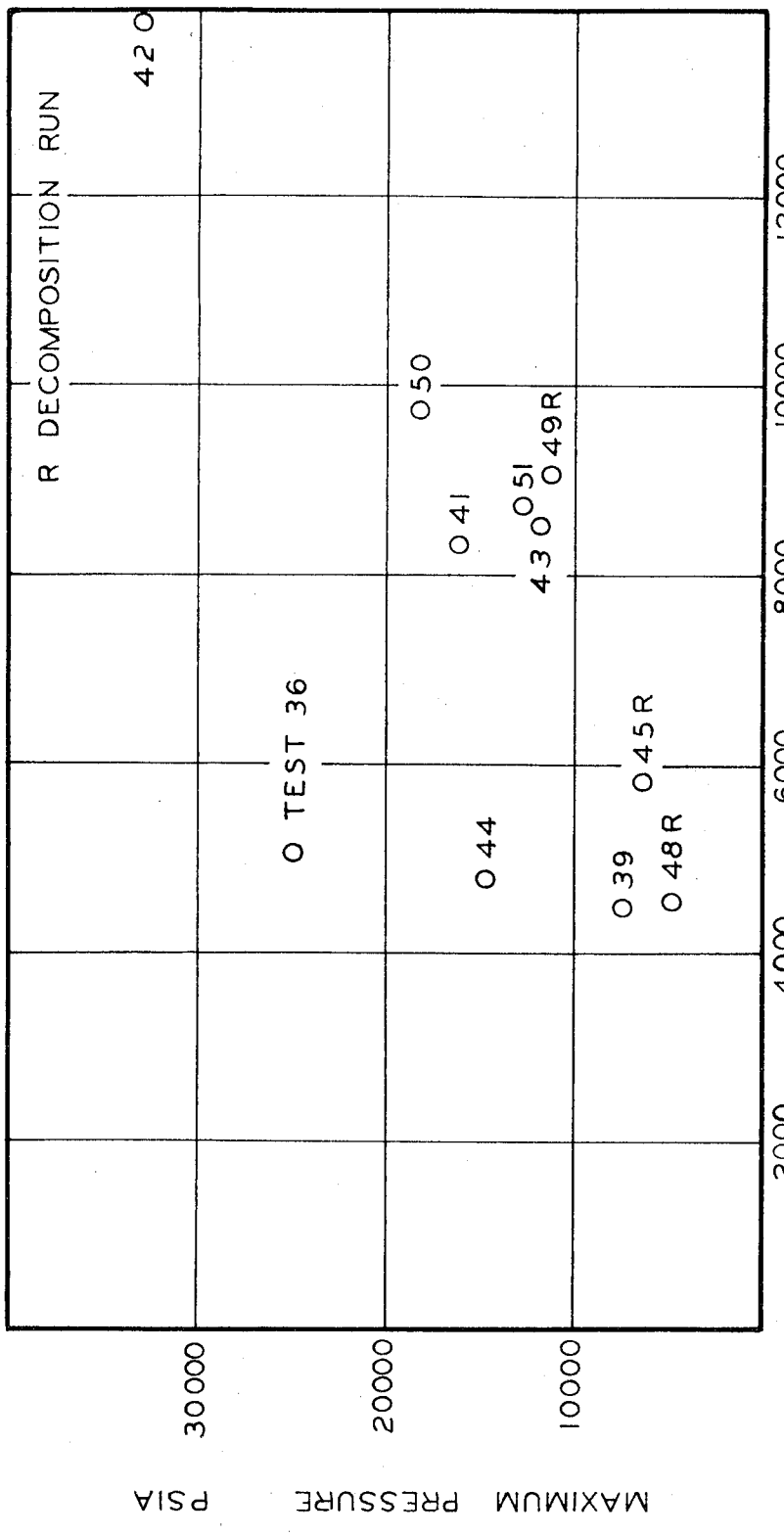

Figure 9. Extreme Conditions in Runs, Neglecting Reaction

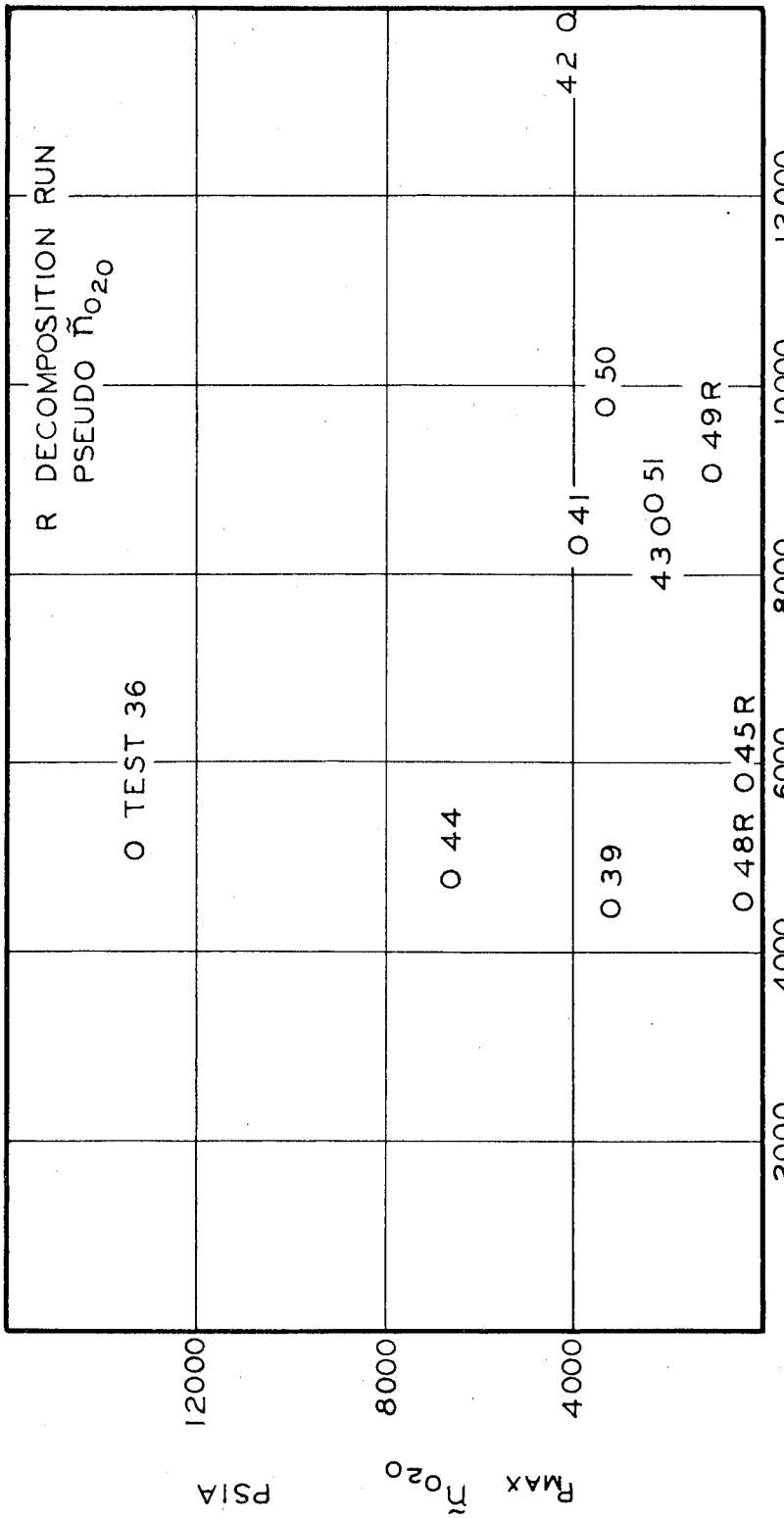

Figure 10. Extreme Conditions in Runs, Neglecting Reaction Maximum Possible Partial Pressure of Oxygen vs. Maximum Temperature

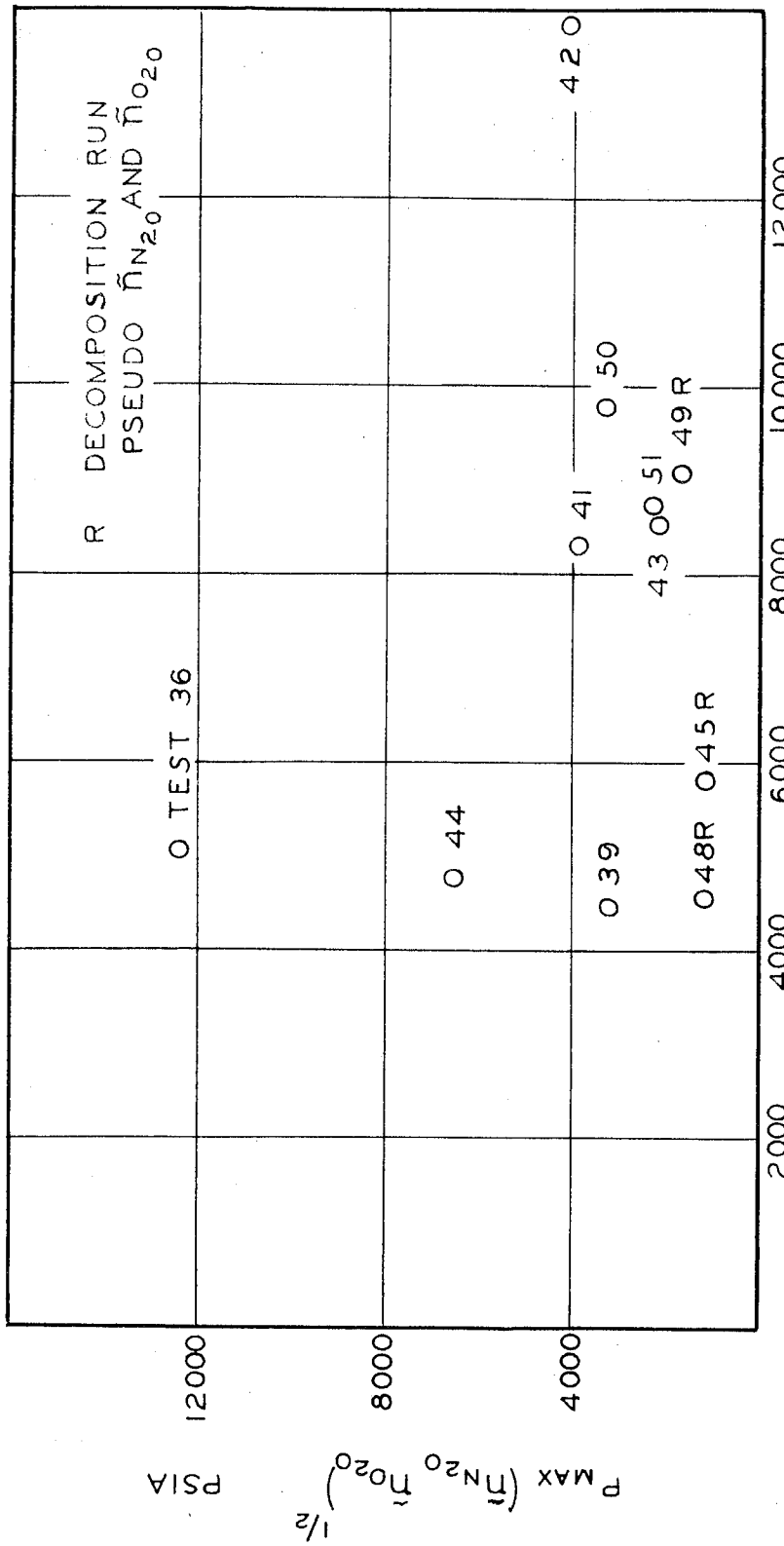

Figure 11. Extreme Conditions in Runs, Neglecting Reaction Partial Pressure Function vs. Maximum Temperature

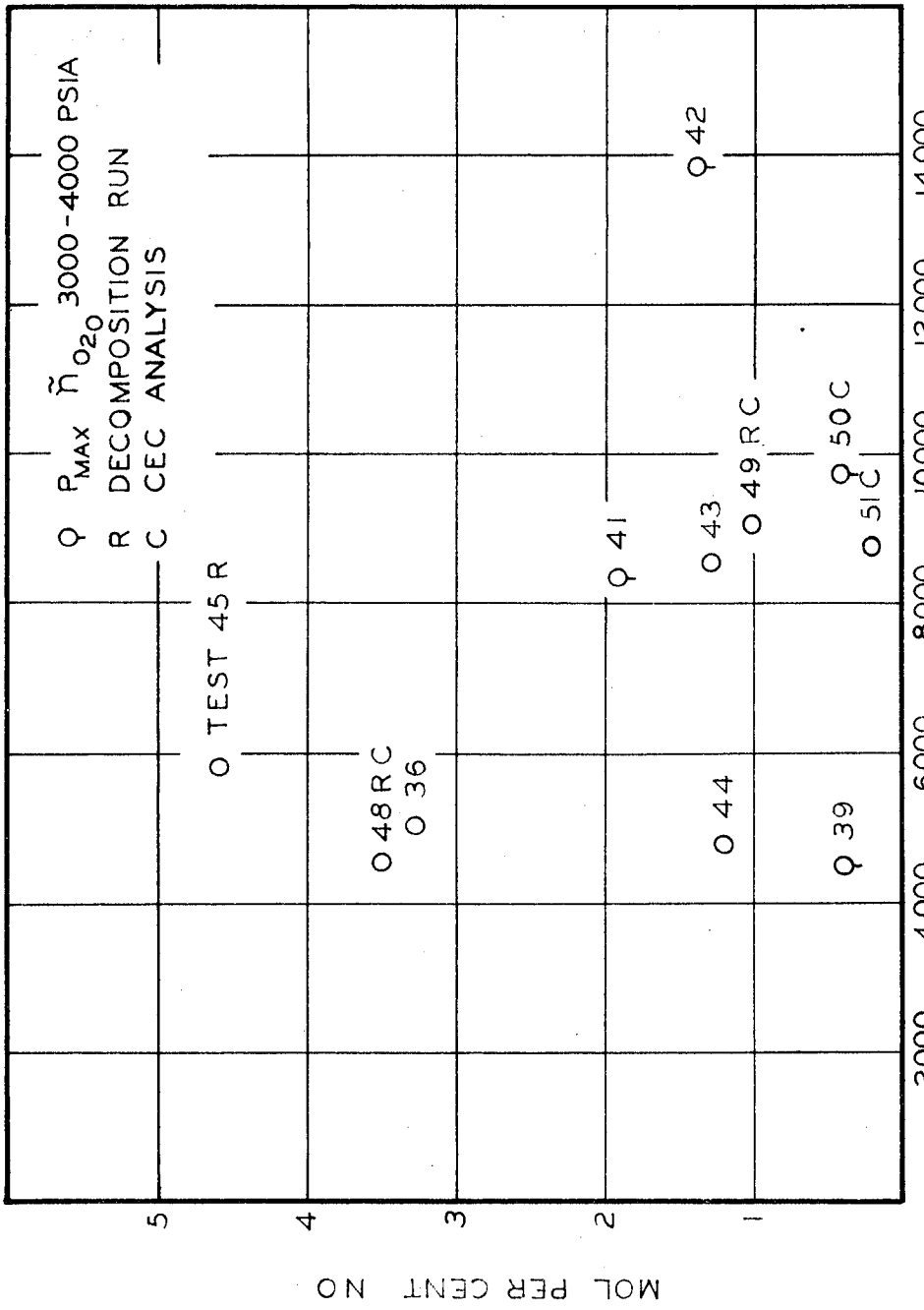

Figure 12. Yield of Nitric Oxide vs. Maximum Temperature

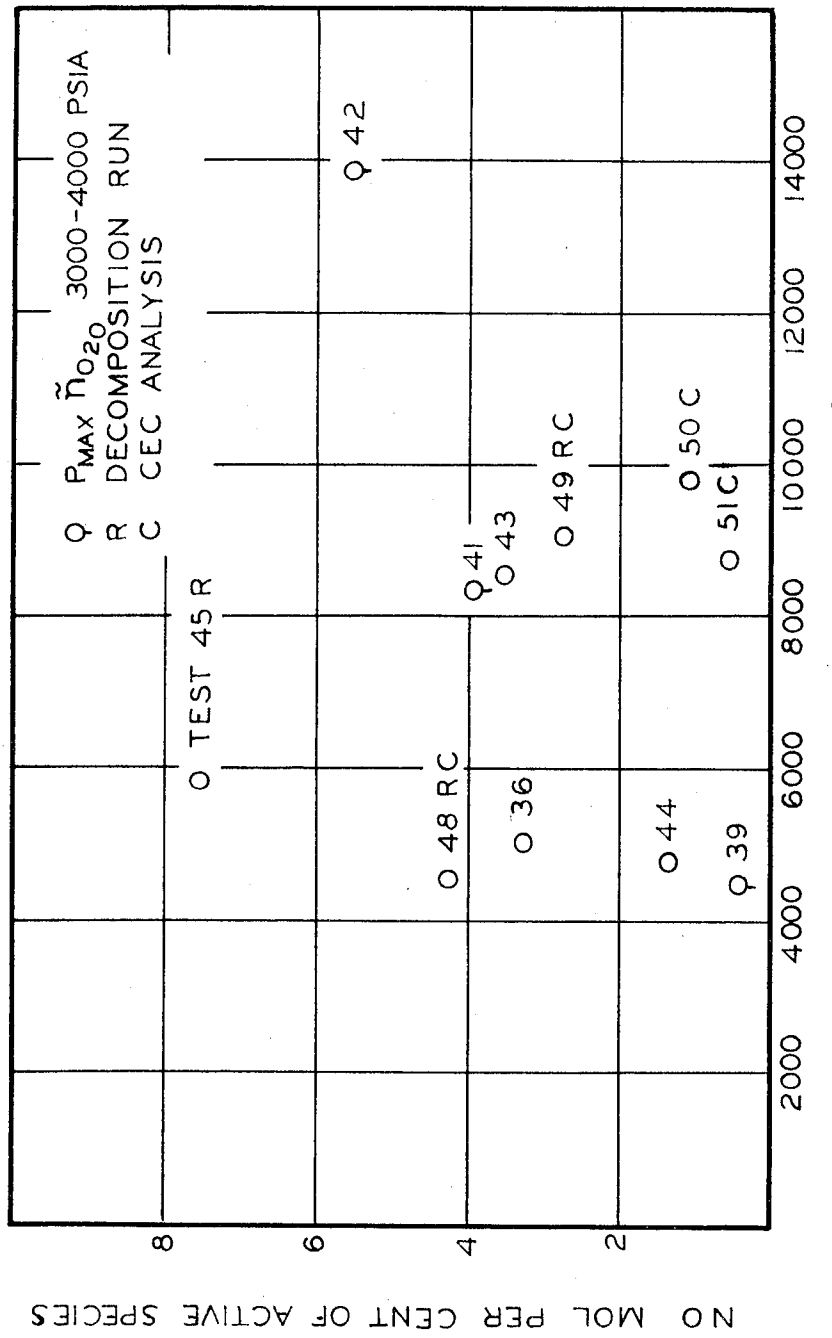

Figure 13. Inert Free Yield of Nitric Oxide vs. Maximum Temperature

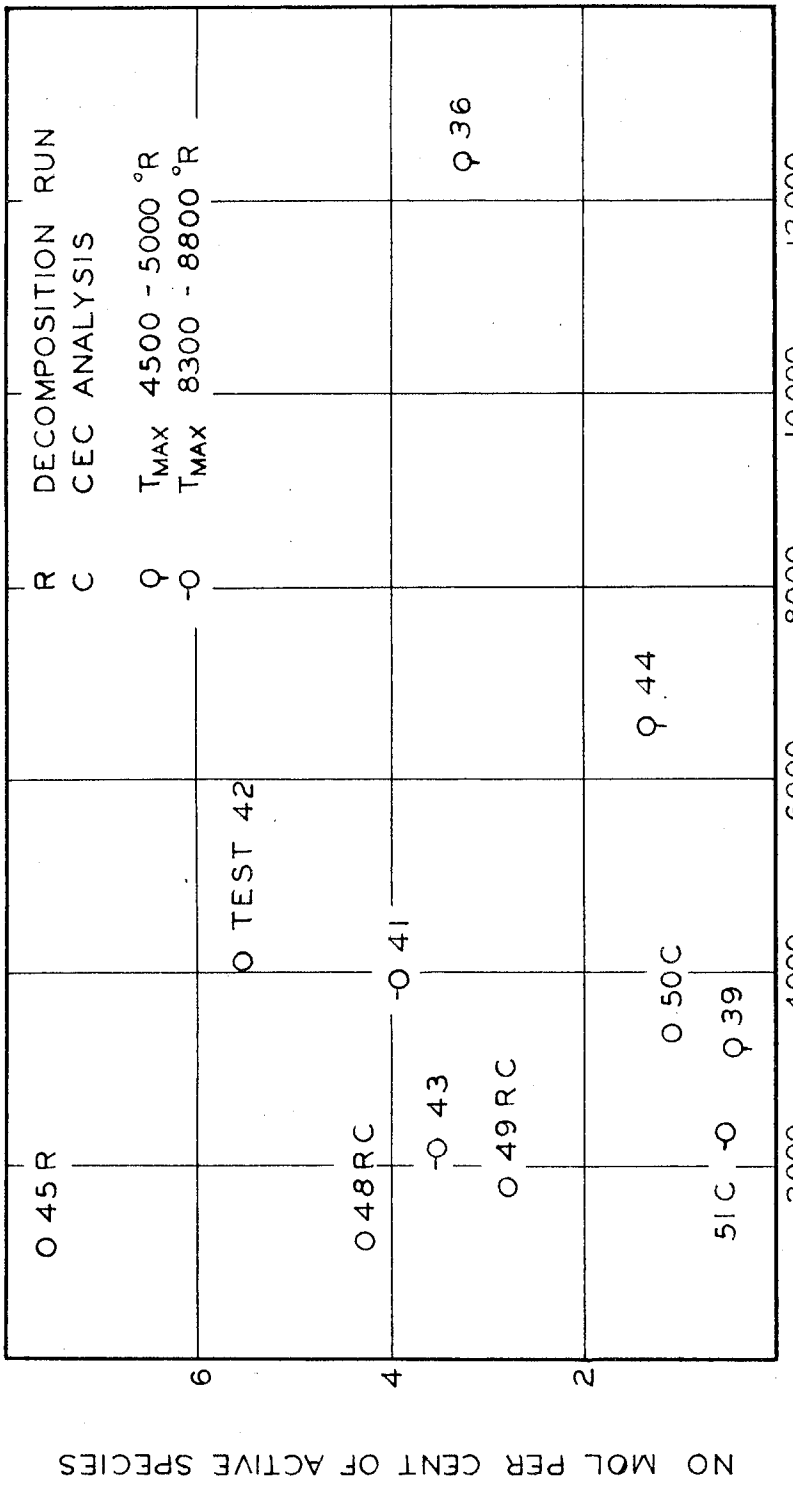

Figure 14. Inert Free Yield of Nitric Oxide vs. $P_{max}\ (\tilde{n}_{N_2O}\ \tilde{n}_{O_2O})^{\frac{1}{2}}$

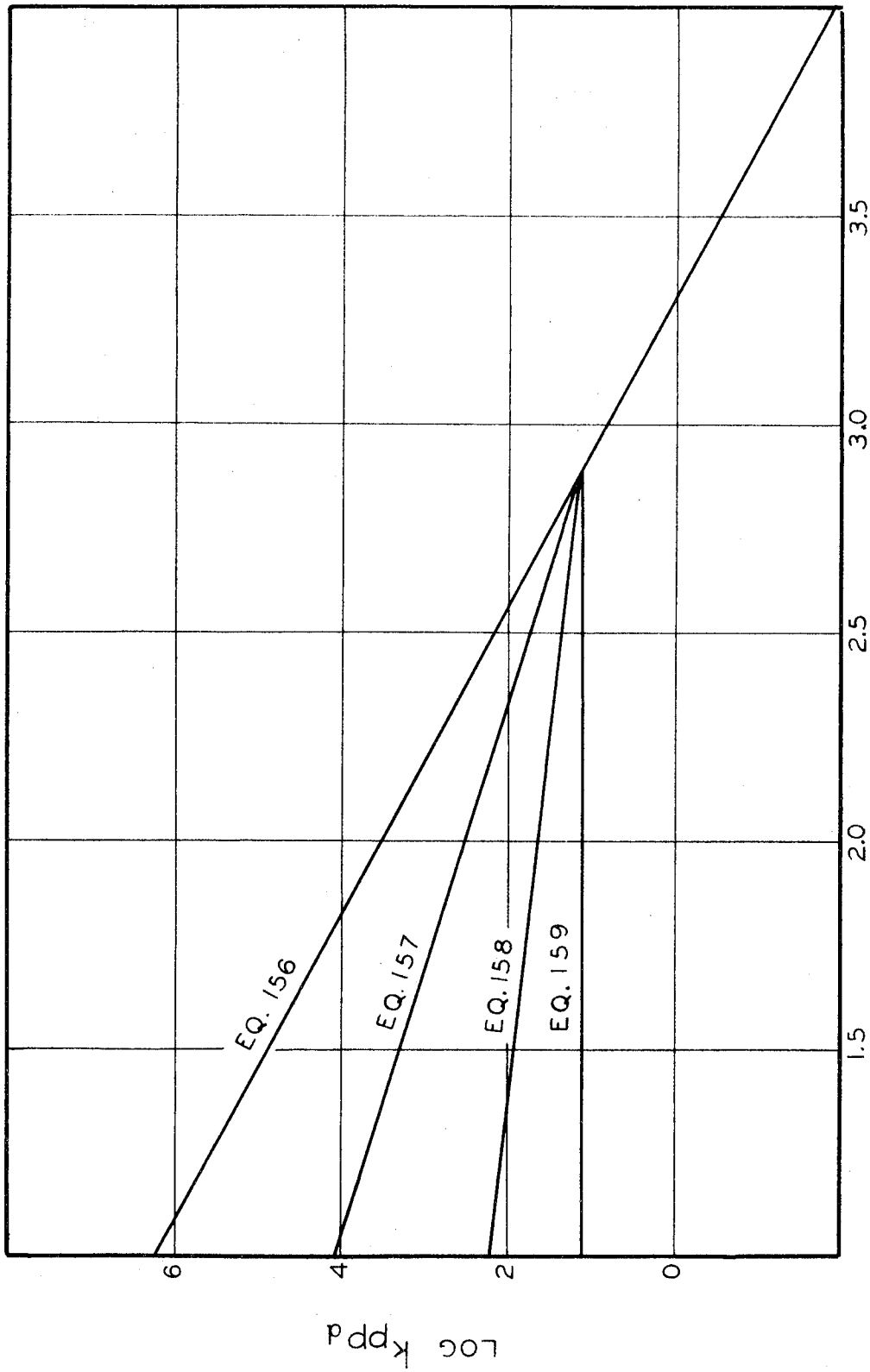

Figure 15. Arrhenius Equations Used in Rate Calculations

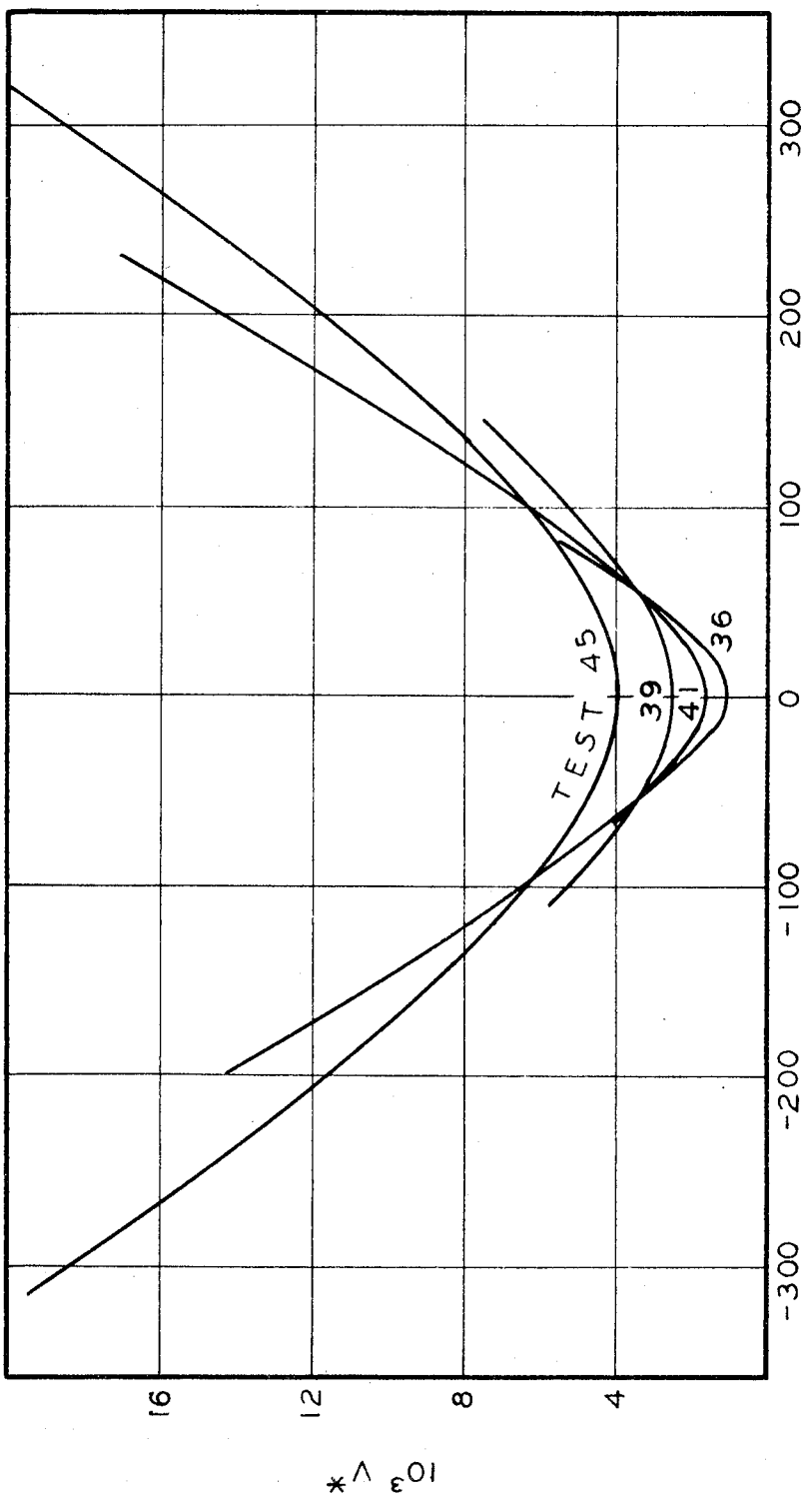

Figure 16. Volume-Time Relations in Regions of Interest

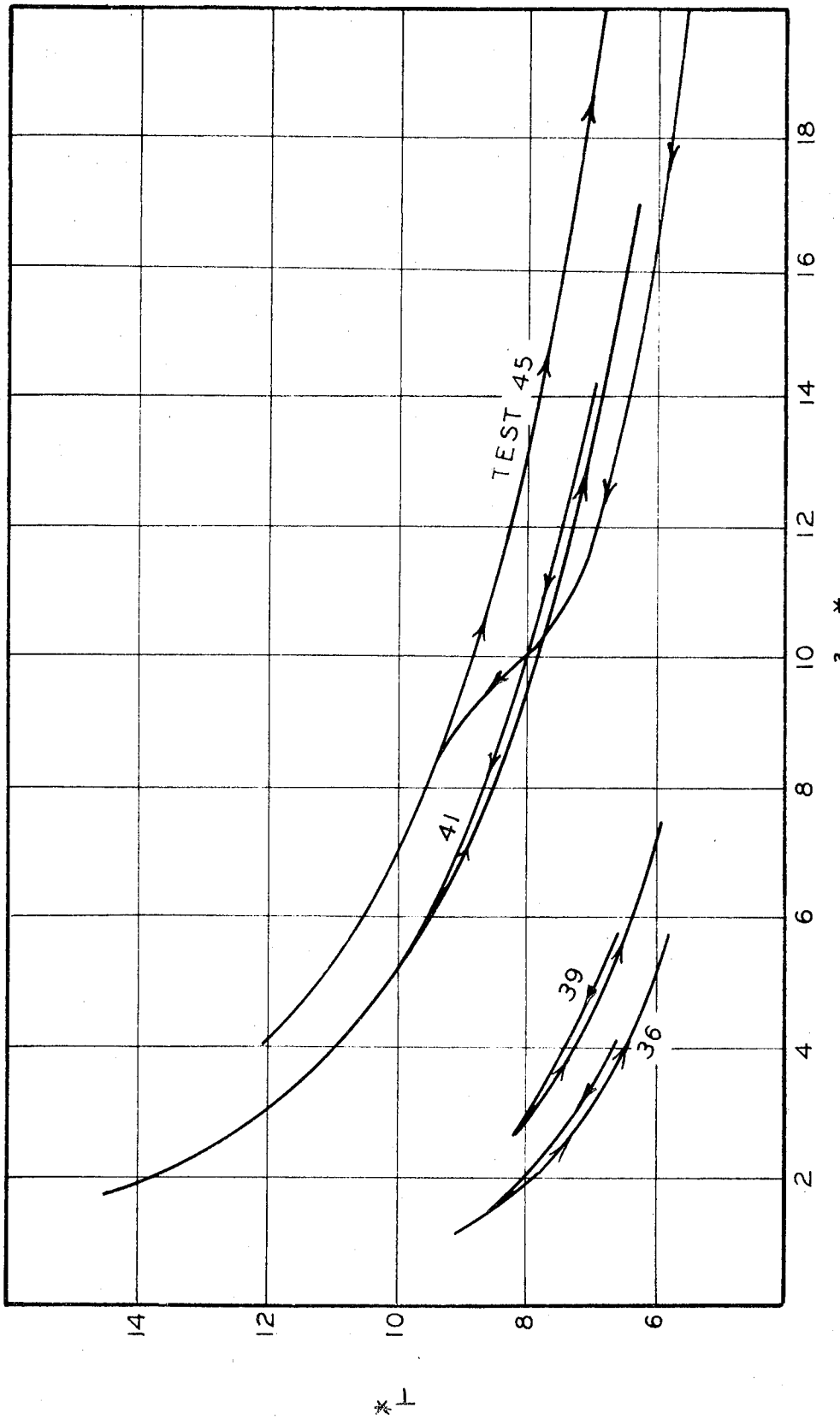

Figure 17. Volume-Temperature Relations in Regions of Interest

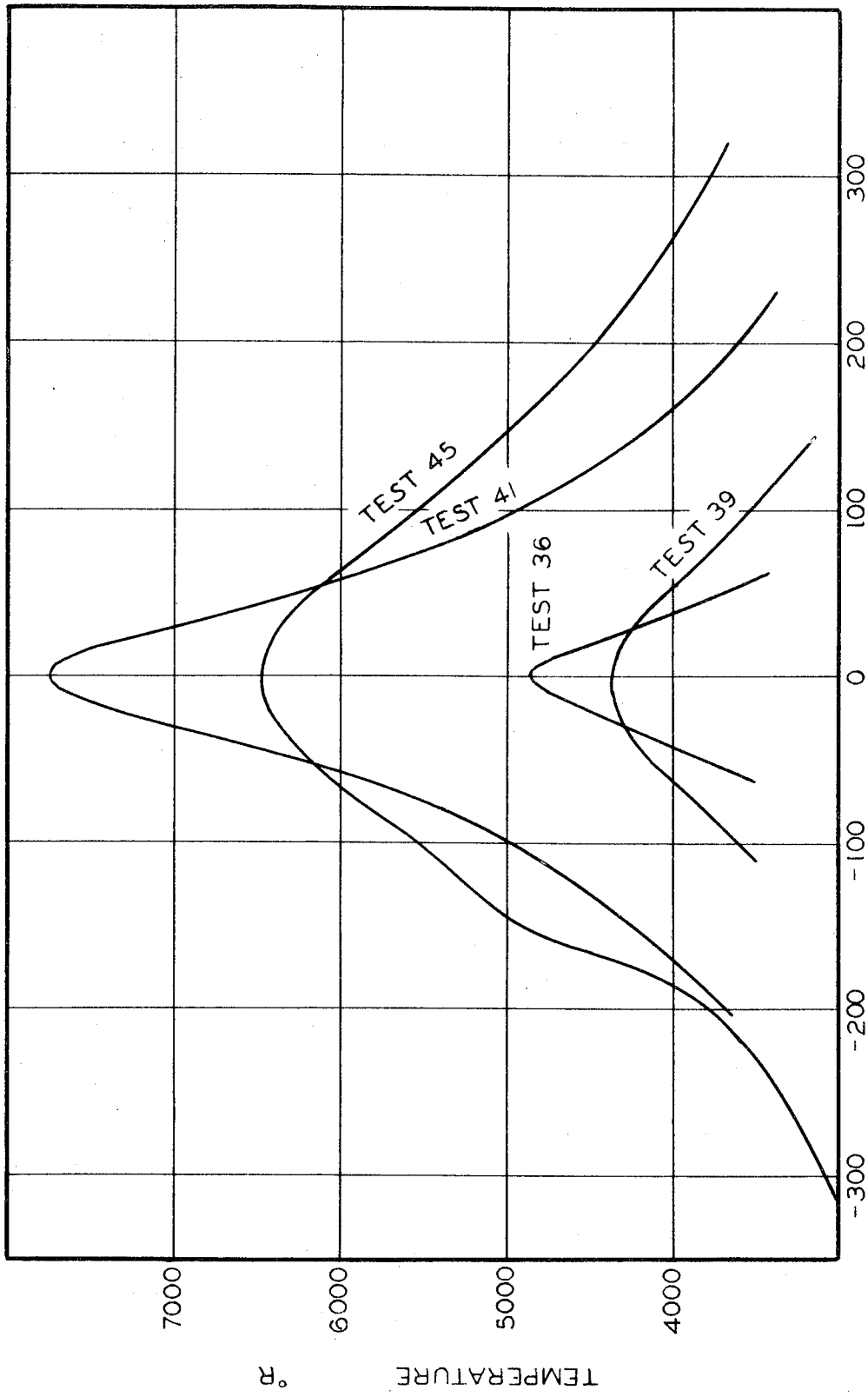

Figure 18. Temperature-Time Relations in Regions of Interest

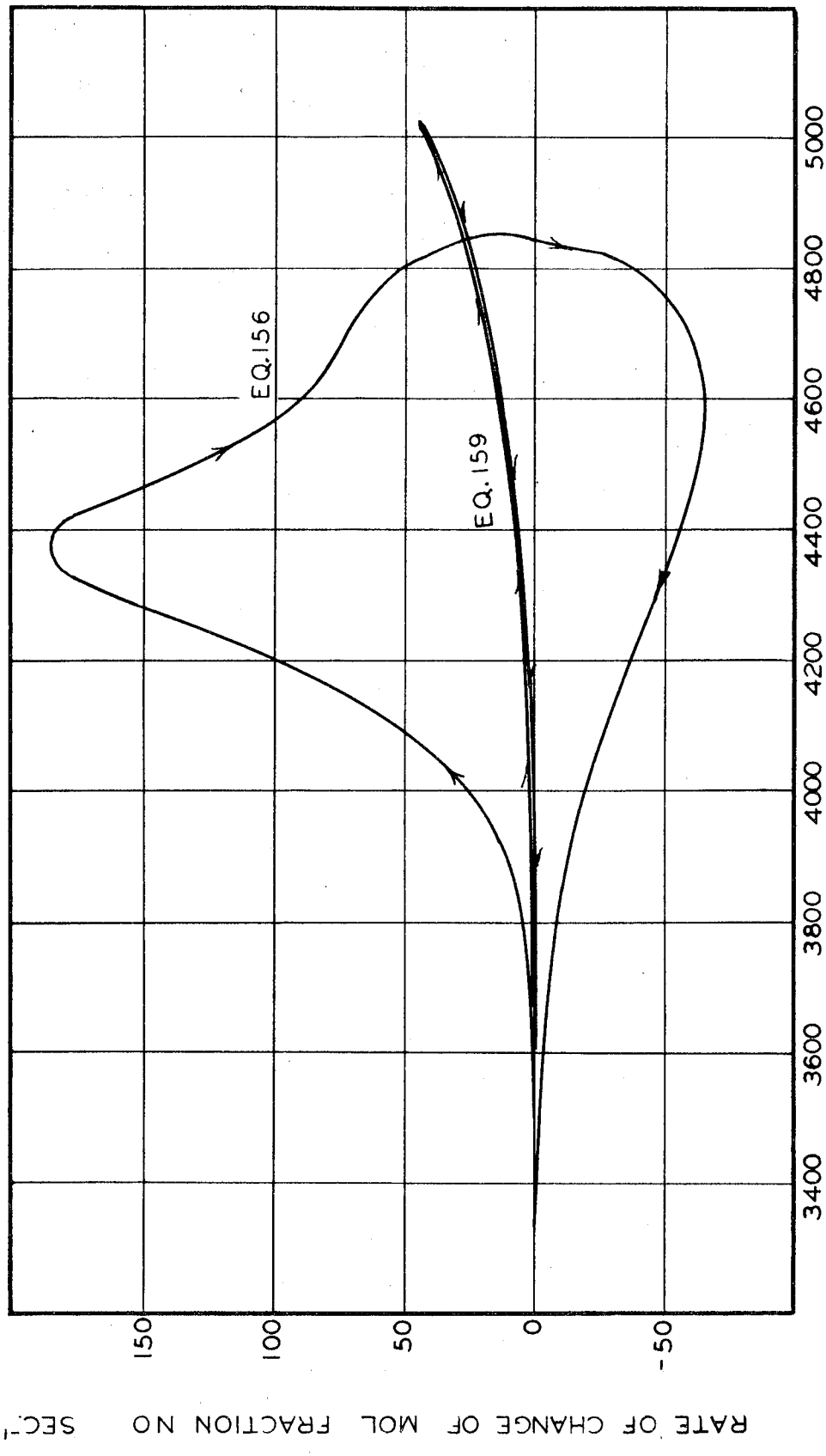

Figure 19. Predicted Rate vs. Temperature, Test 36

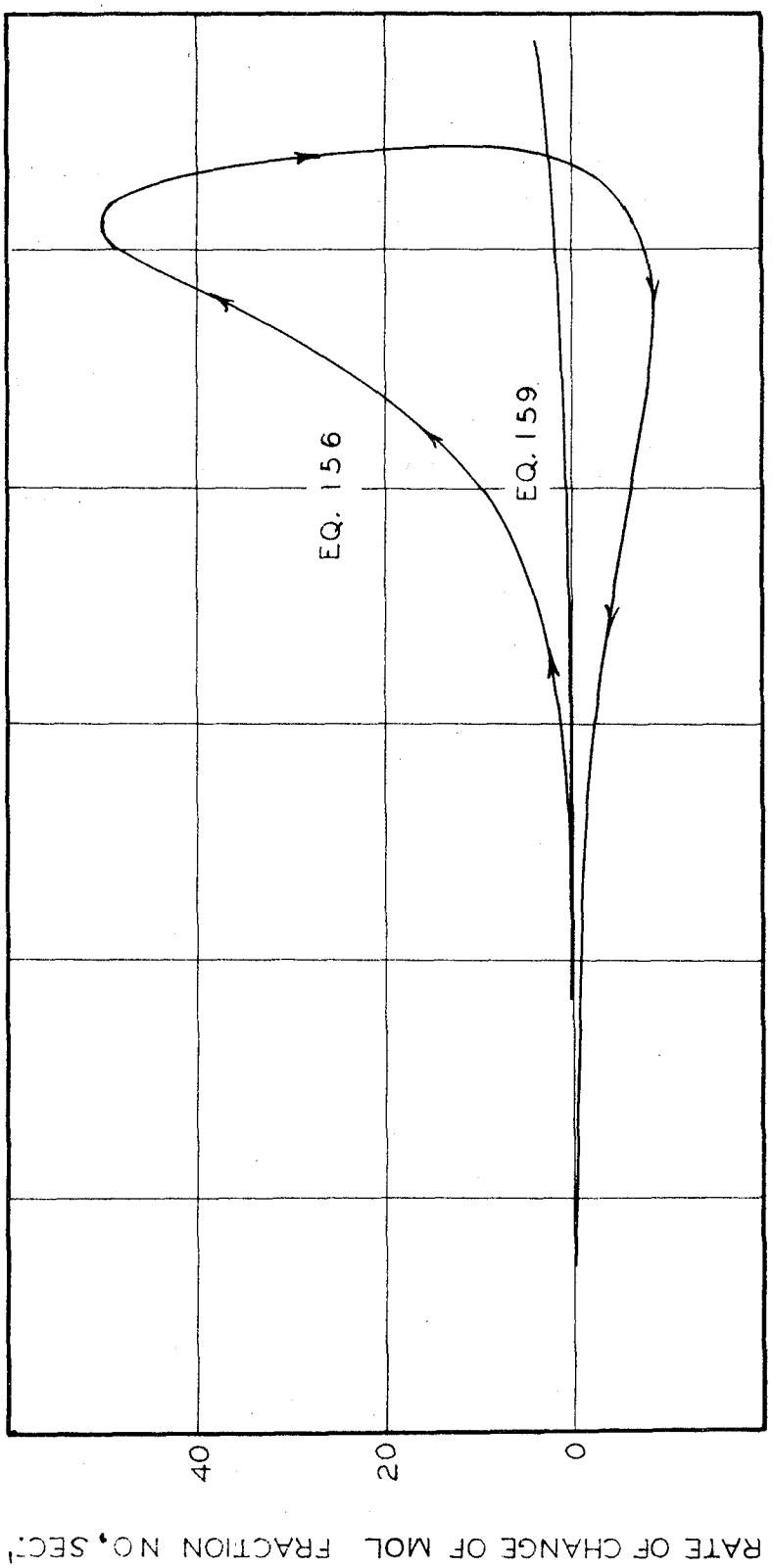

Figure 20. Predicted Rate vs. Temperature, Test 39

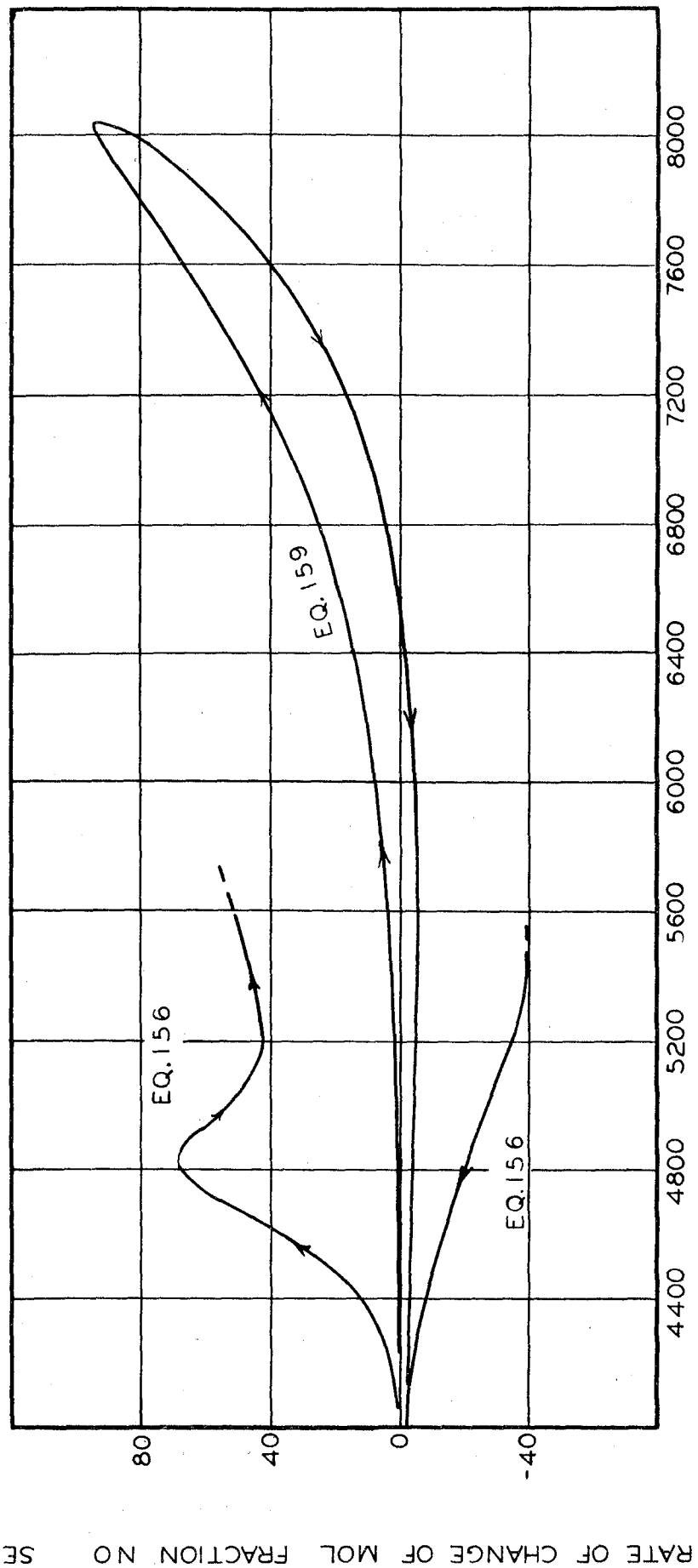

Figure 21. Predicted Rate vs. Temperature, Test 41

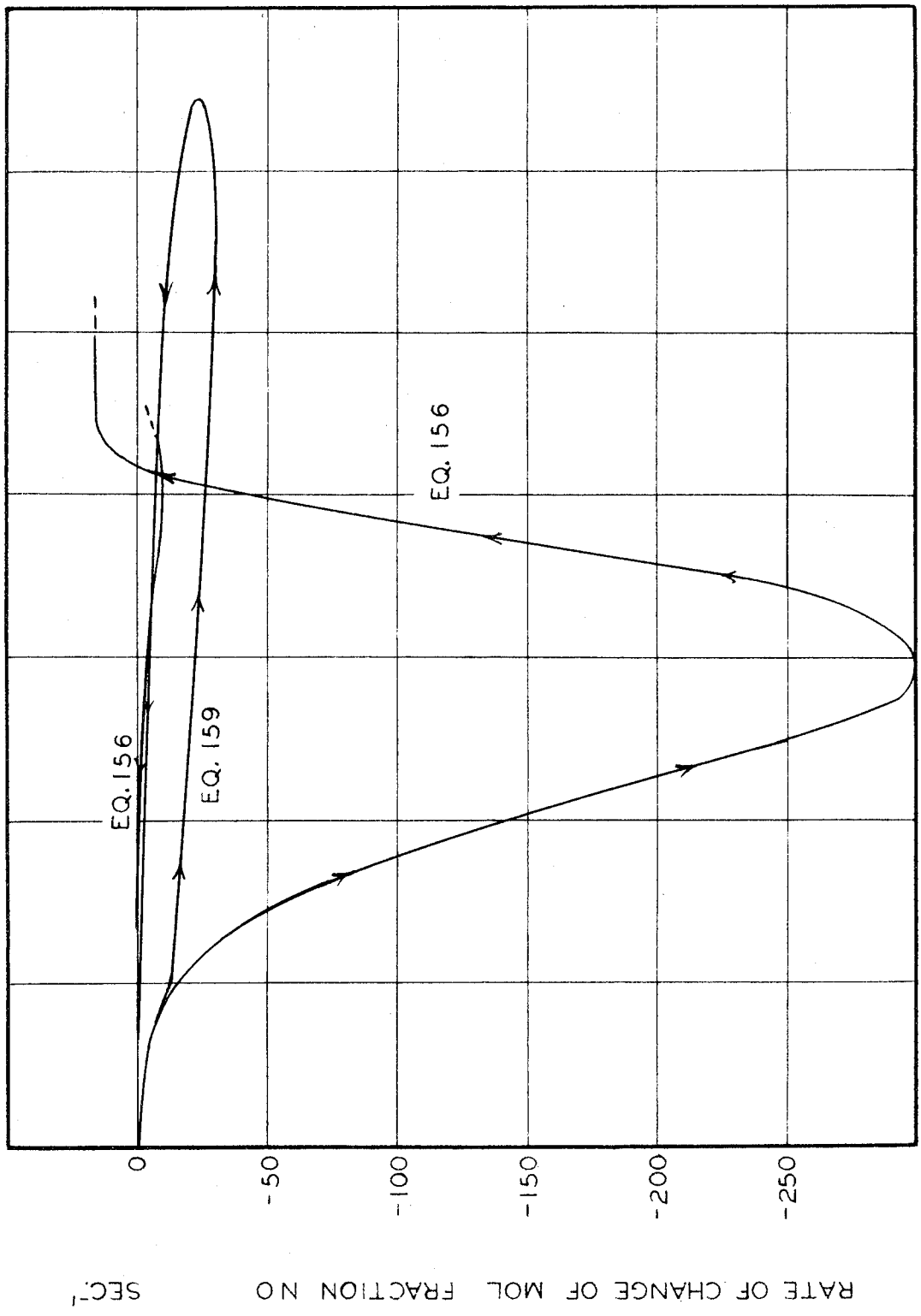

Figure 22. Predicted Rate vs. Temperature, Test 45

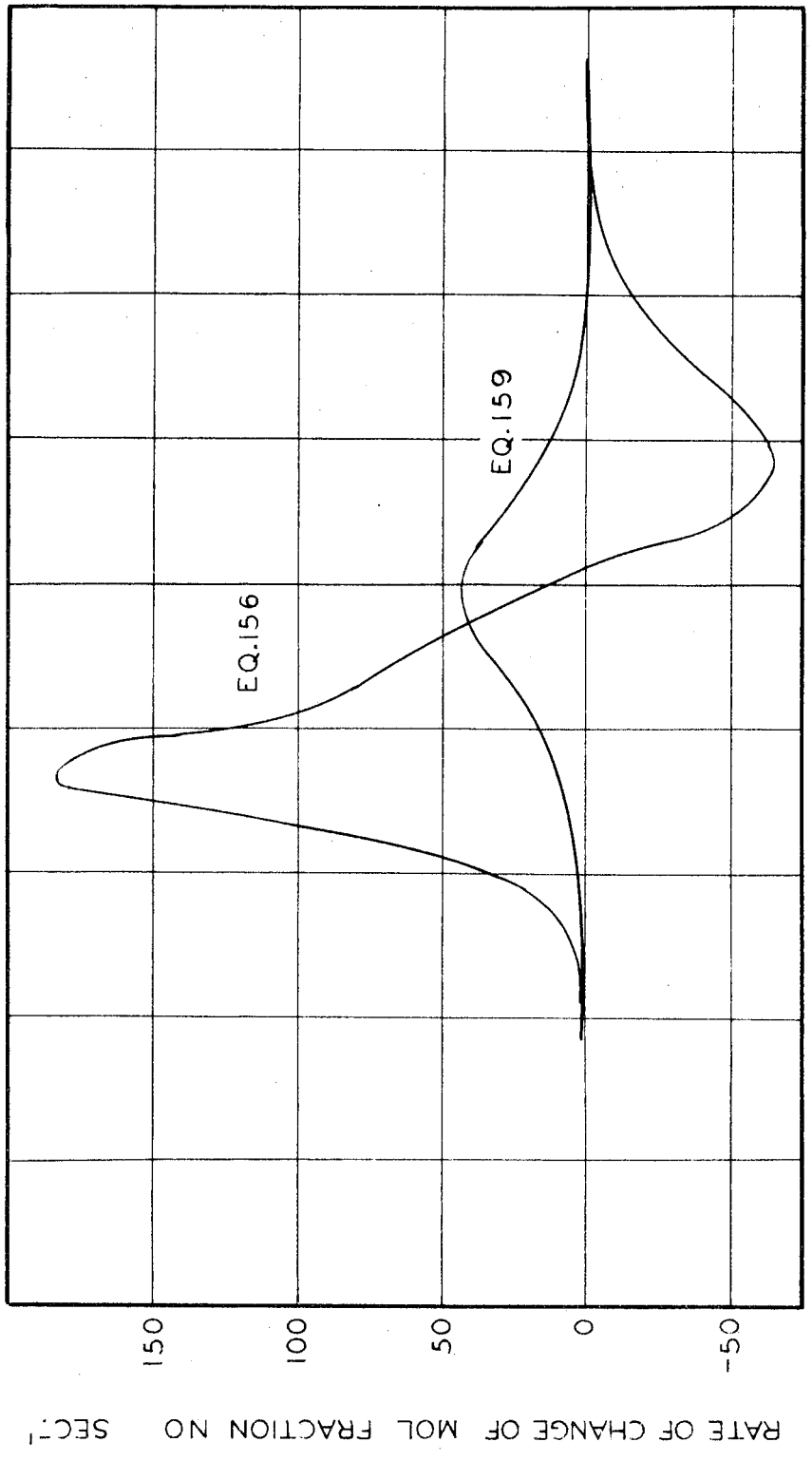

Figure 23. Predicted Rate vs. Time, Test 36

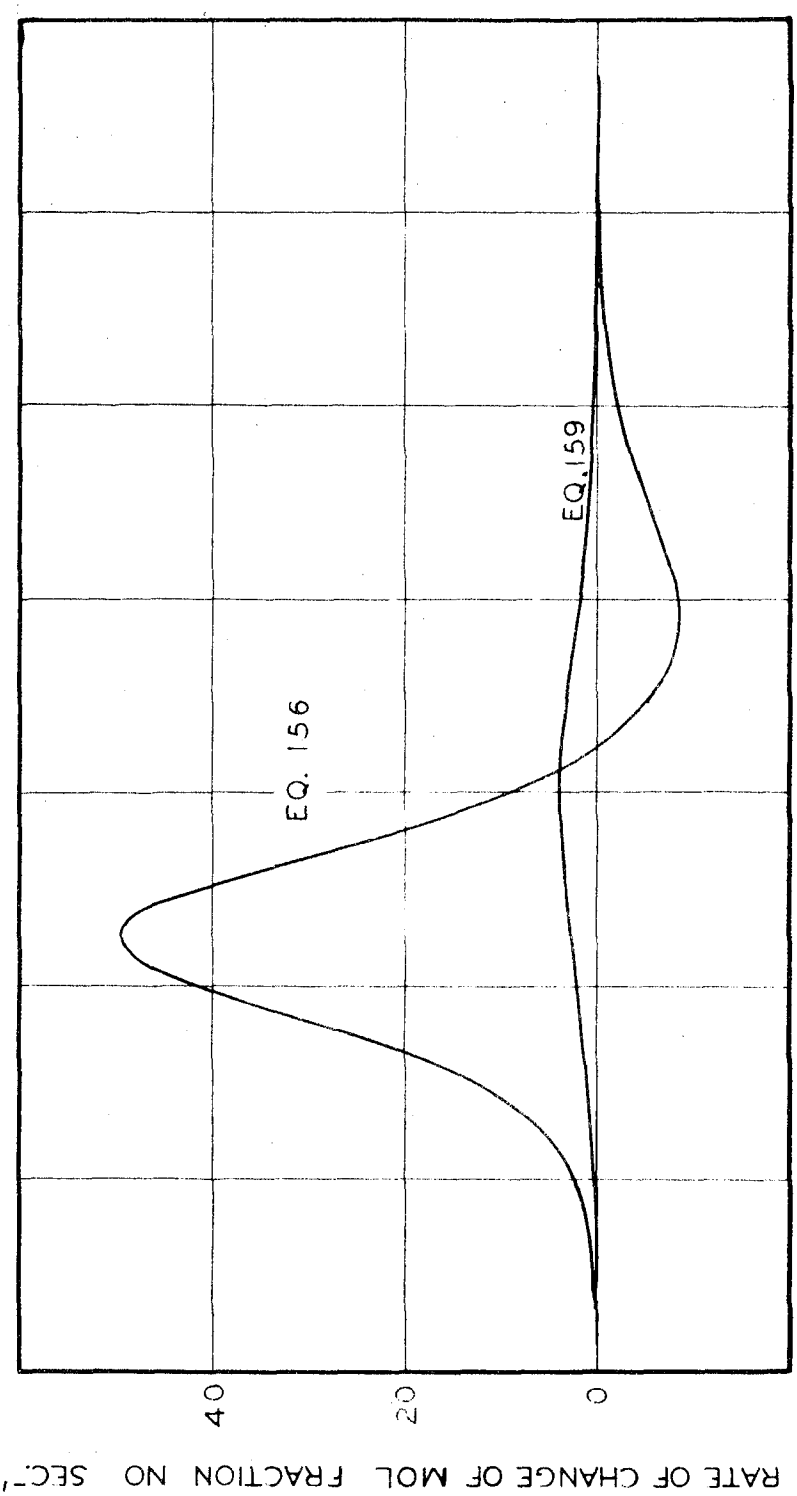

Figure 24. Predicted Rate vs. Time, Test 39

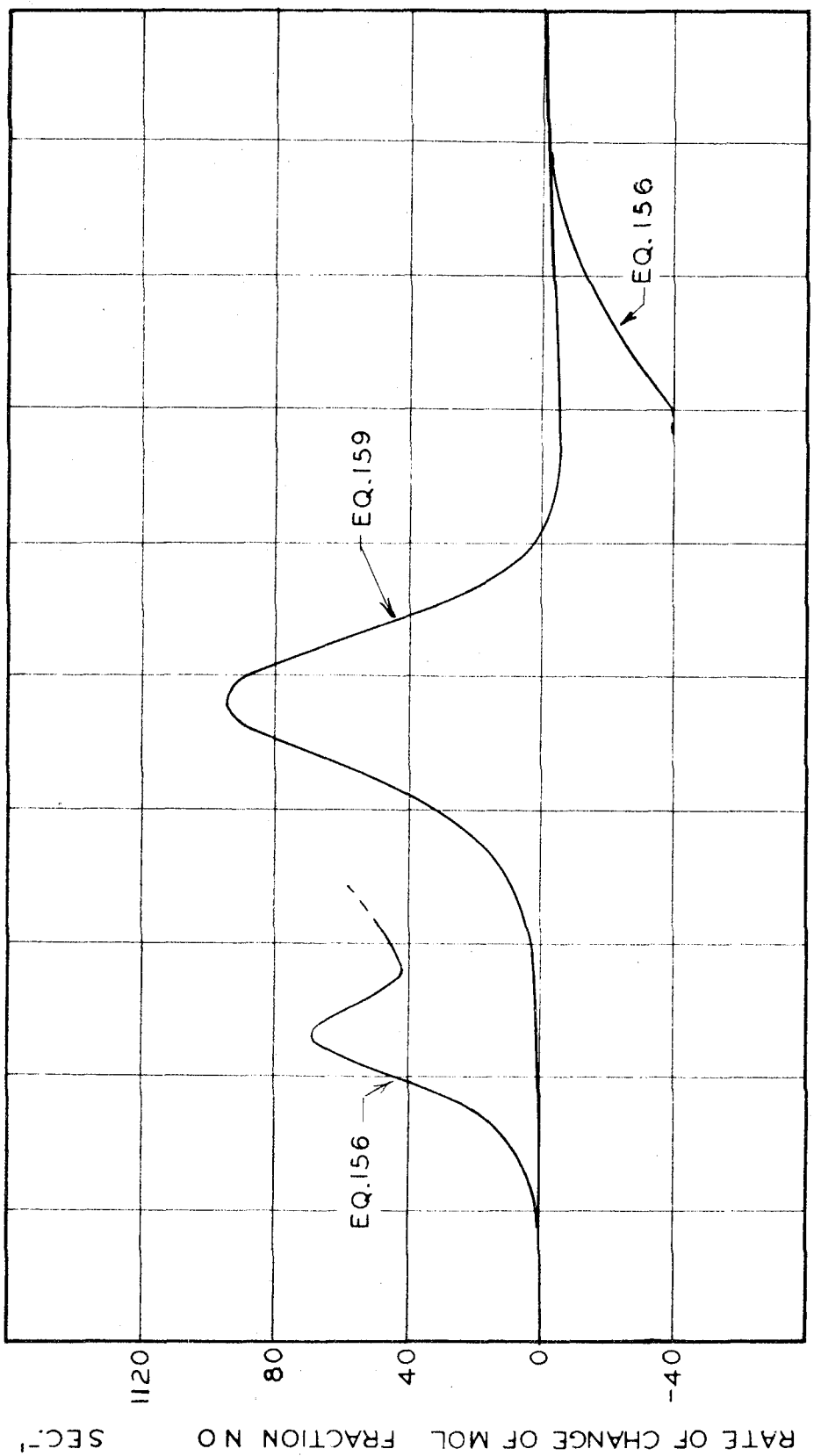

Figure 25. Predicted Rate vs. Time, Test 41

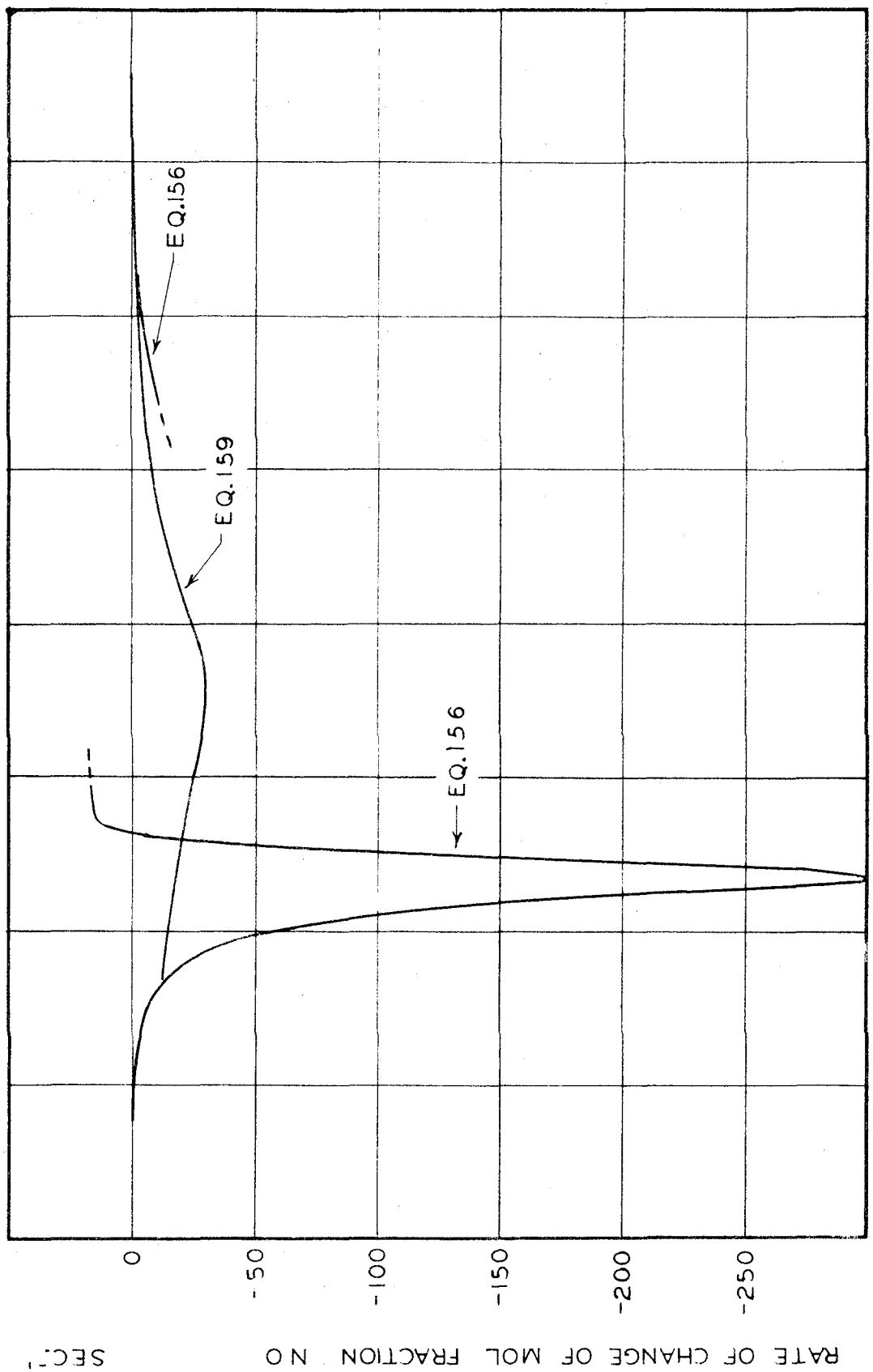

Figure 26. Predicted Rate vs. Time, Test 45

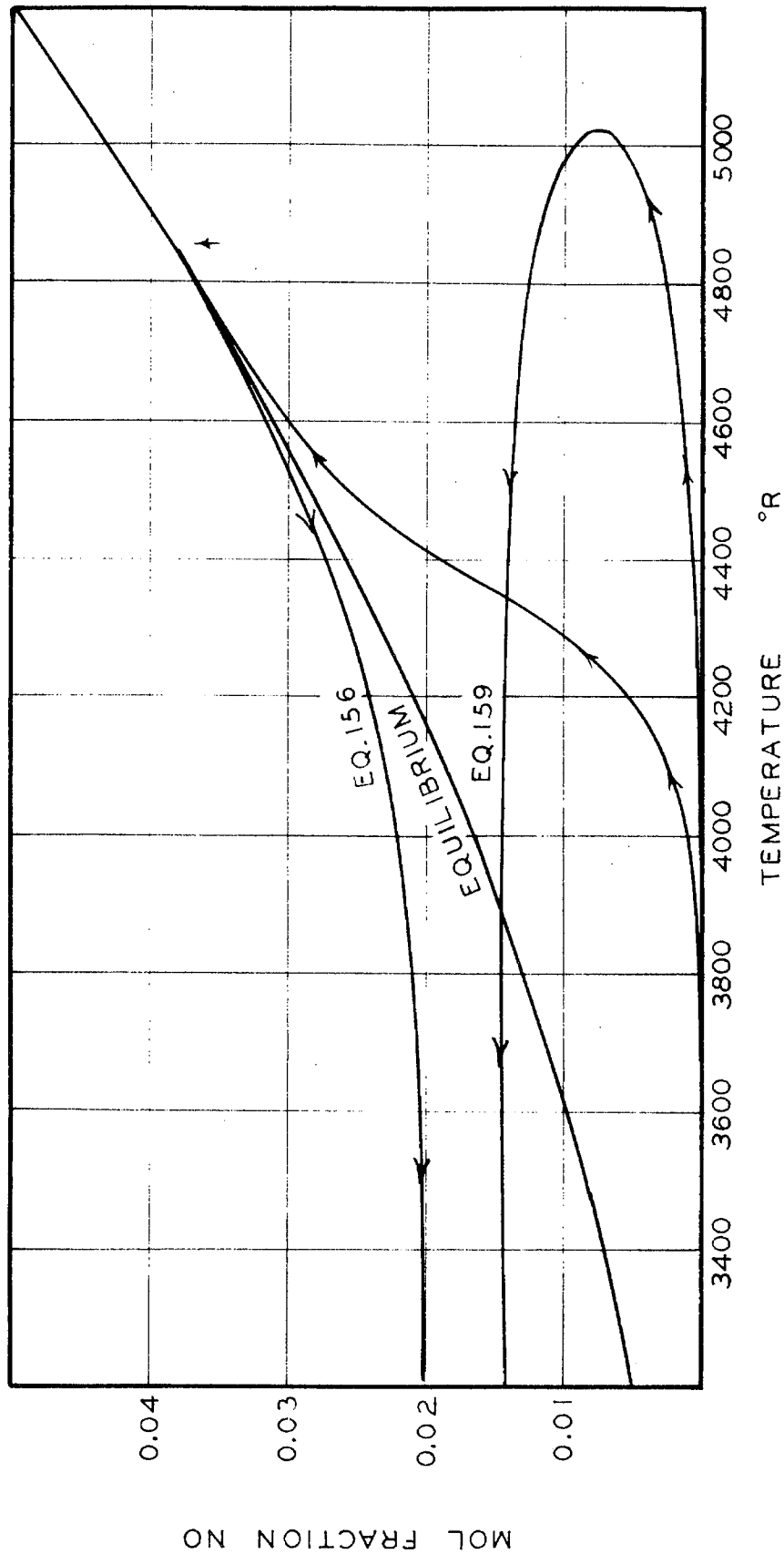

Figure 27. Predicted Composition vs. Temperature, Test 36

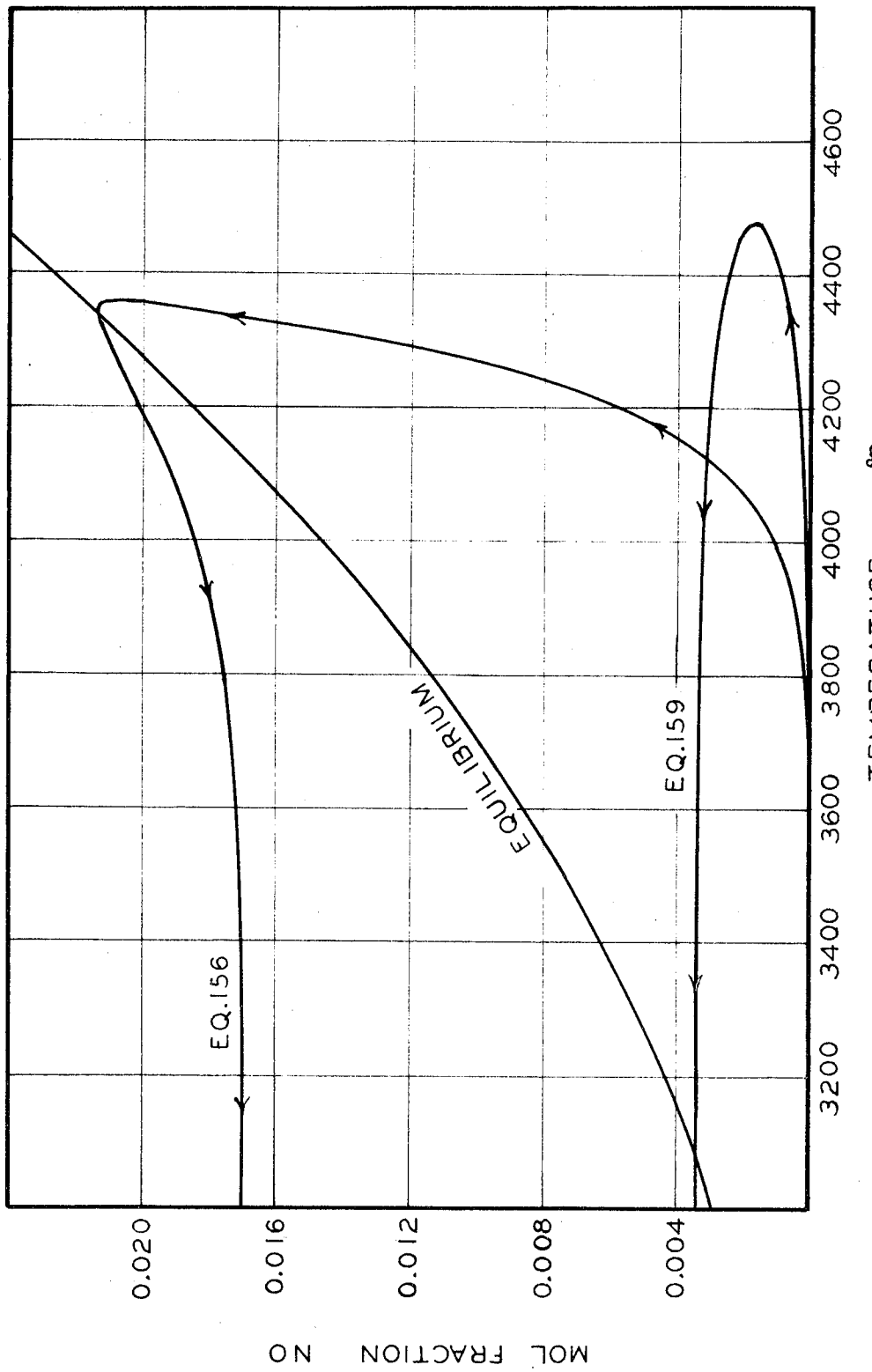

Figure 28. Predicted Composition vs. Temperature, Test 39

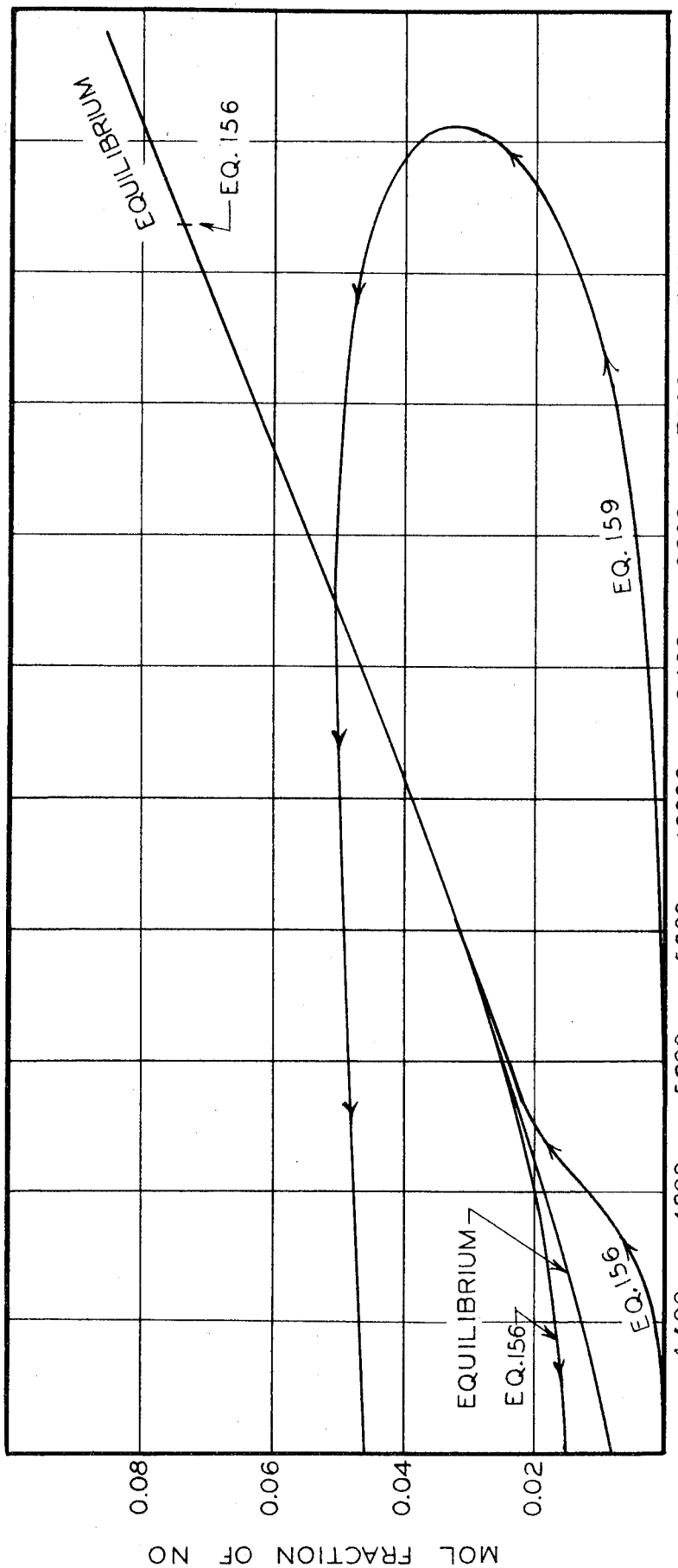

Figure 29. Predicted Composition vs. Temperature, Test 41

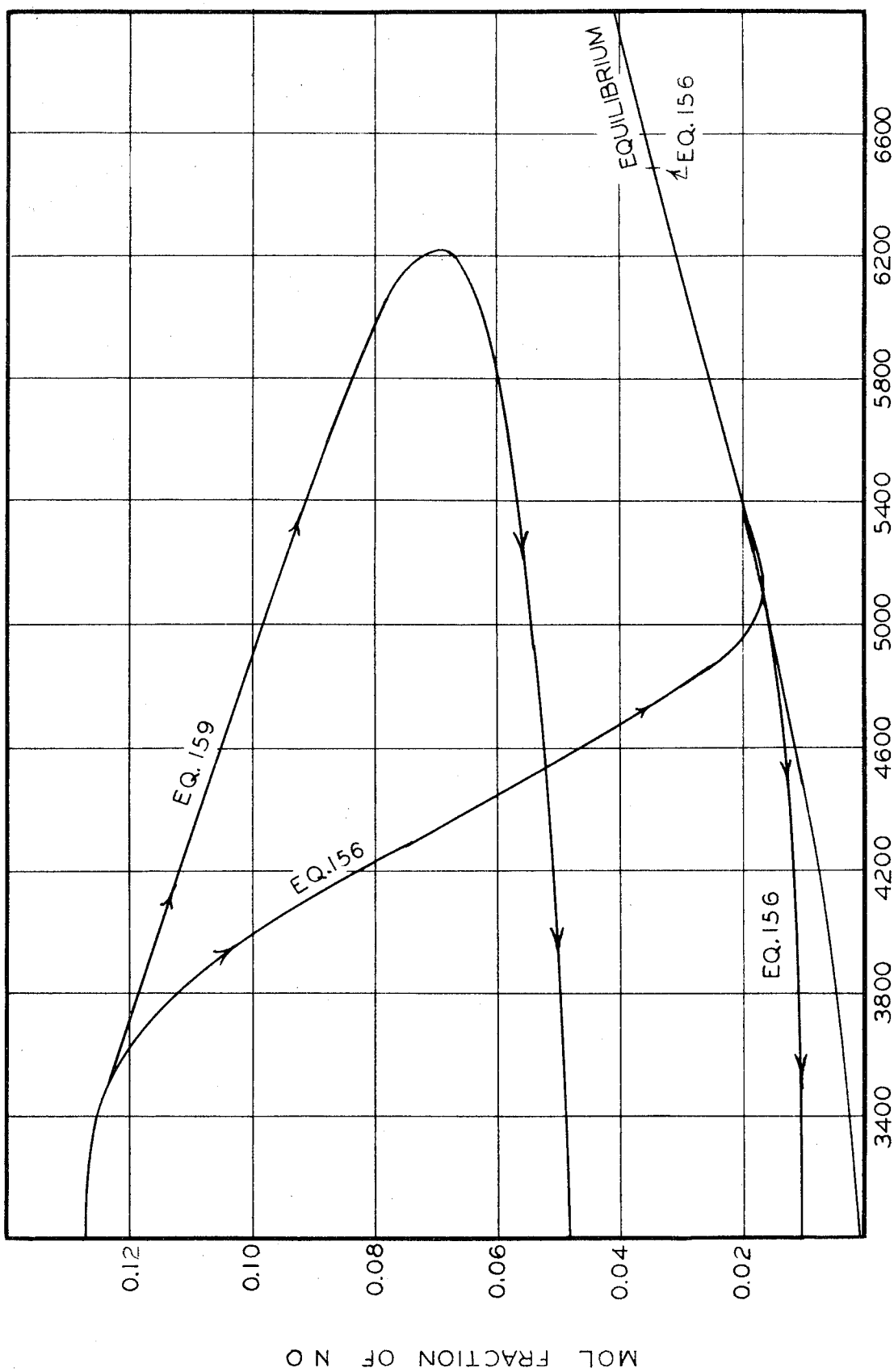

Figure 30. Predicted Composition vs. Temperature, Test 45

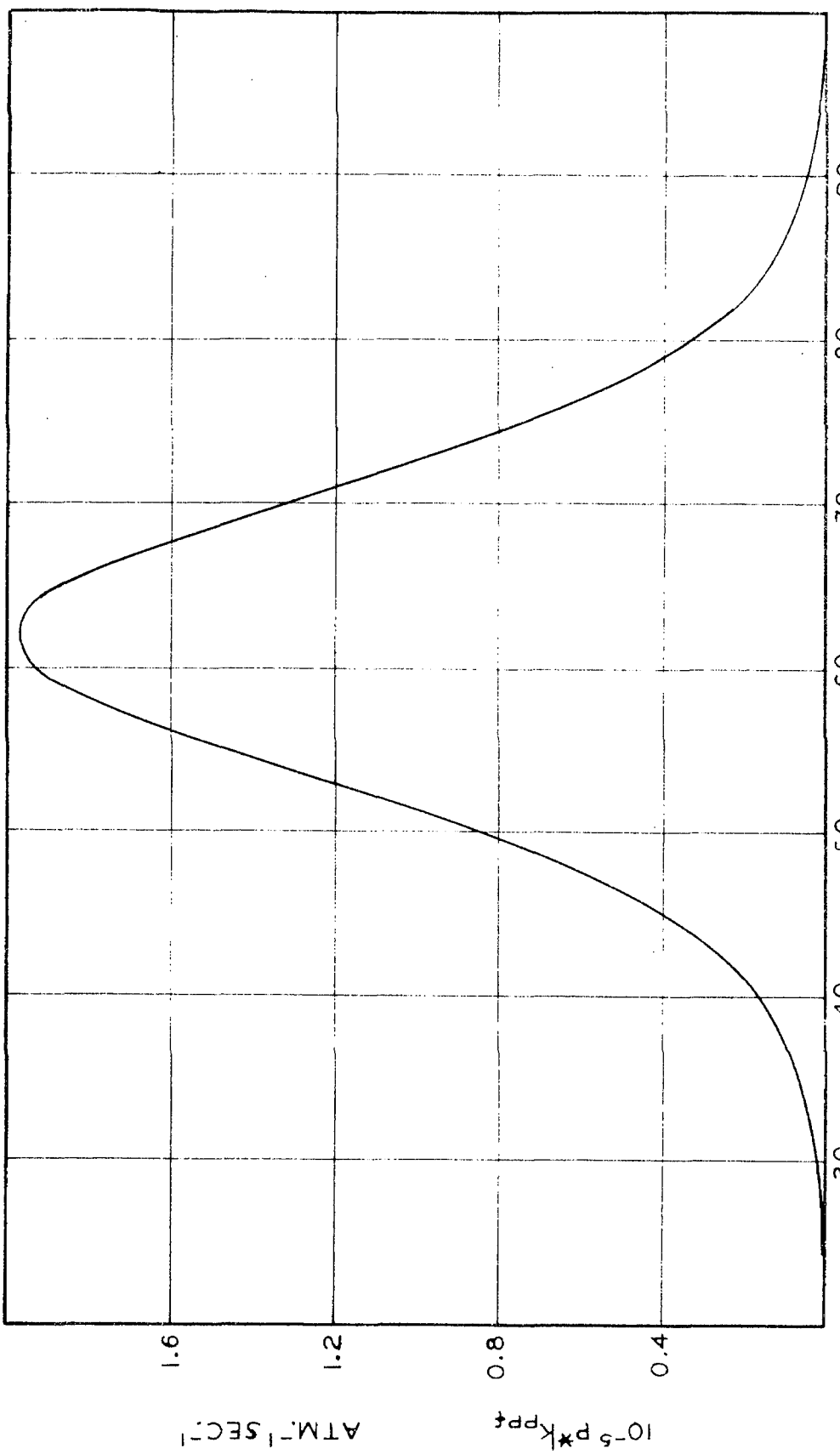

Figure 31. P*K_{pp_f} vs. Time for Test 36, from Table XIX

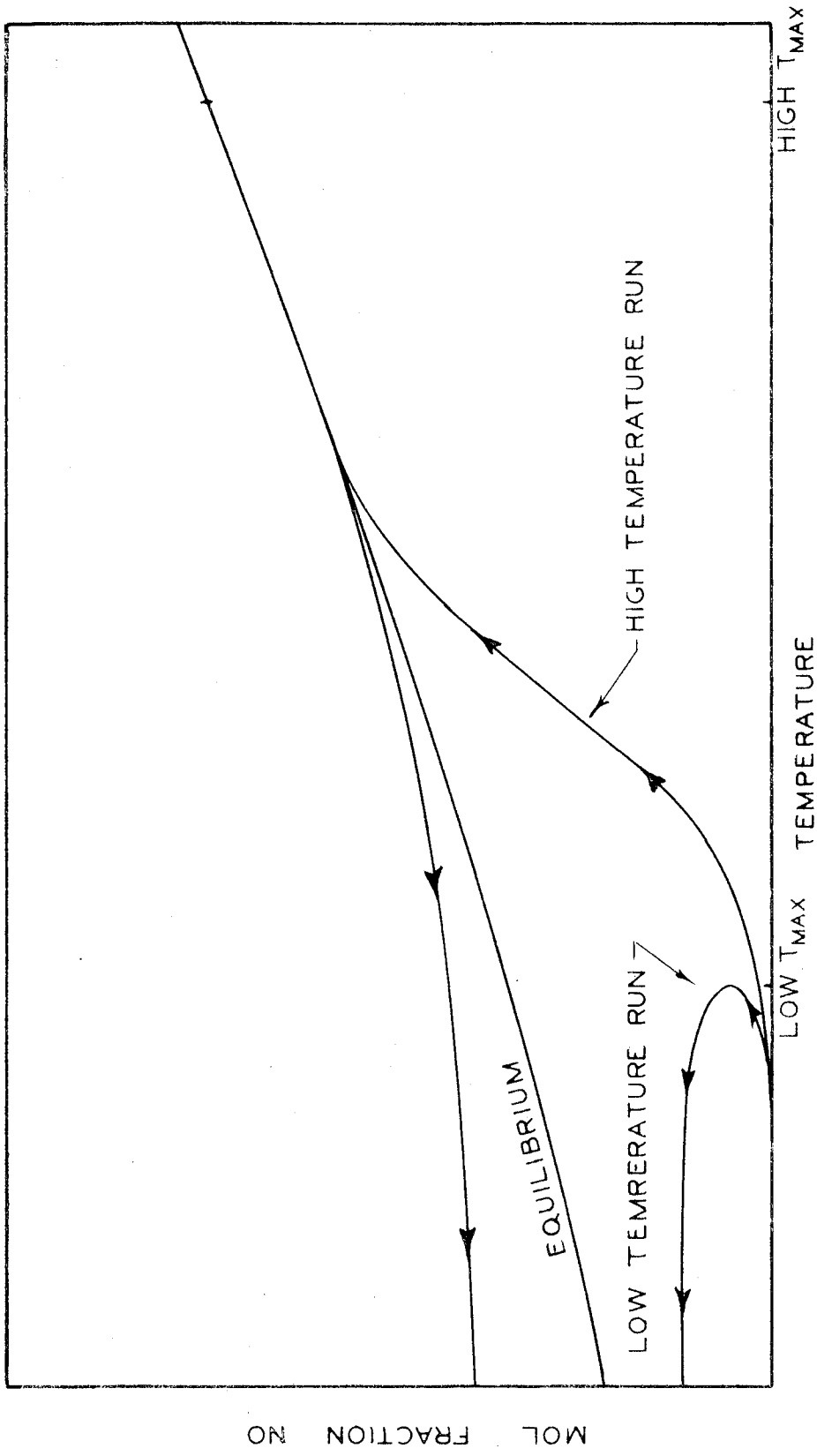

Figure 32. Mol Fraction of Nitric Oxide in Typical High Temperature Run and in Typical Low Temperature Run

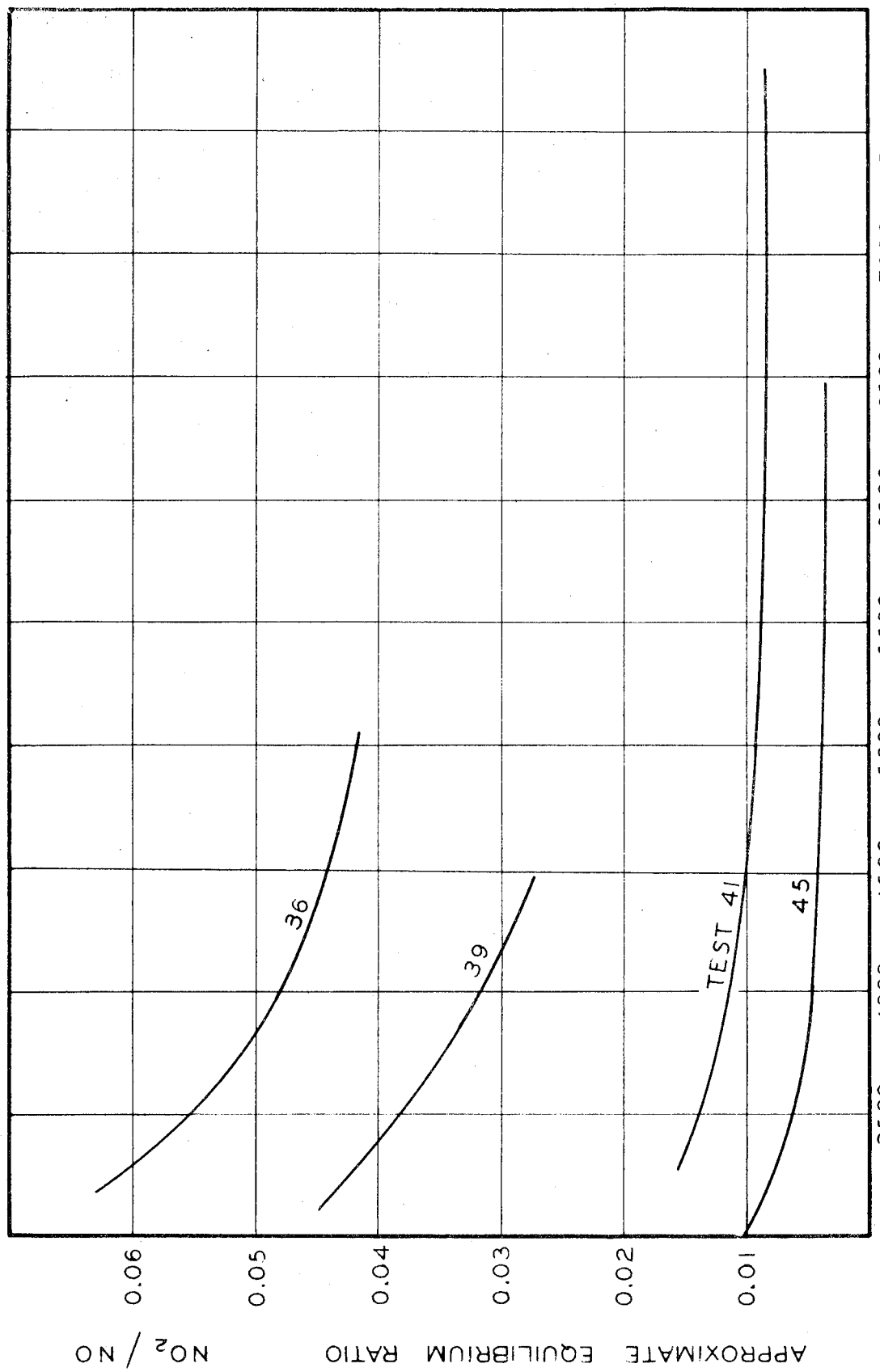

Figure 33. Approximate Molal Equilibrium Ratios of Nitrogen Dioxide to Nitric Oxide

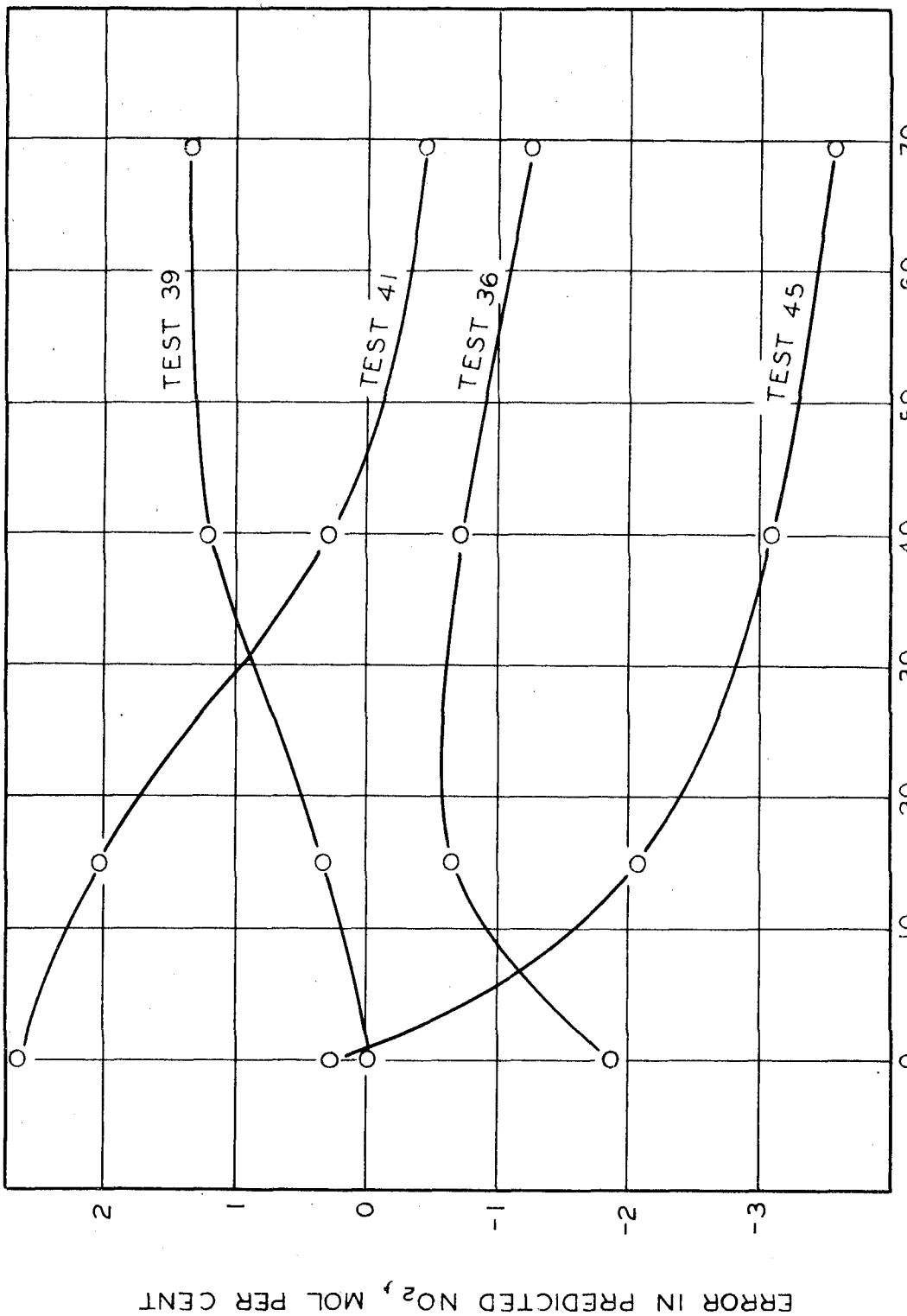

Figure 34. Errors in Predictions

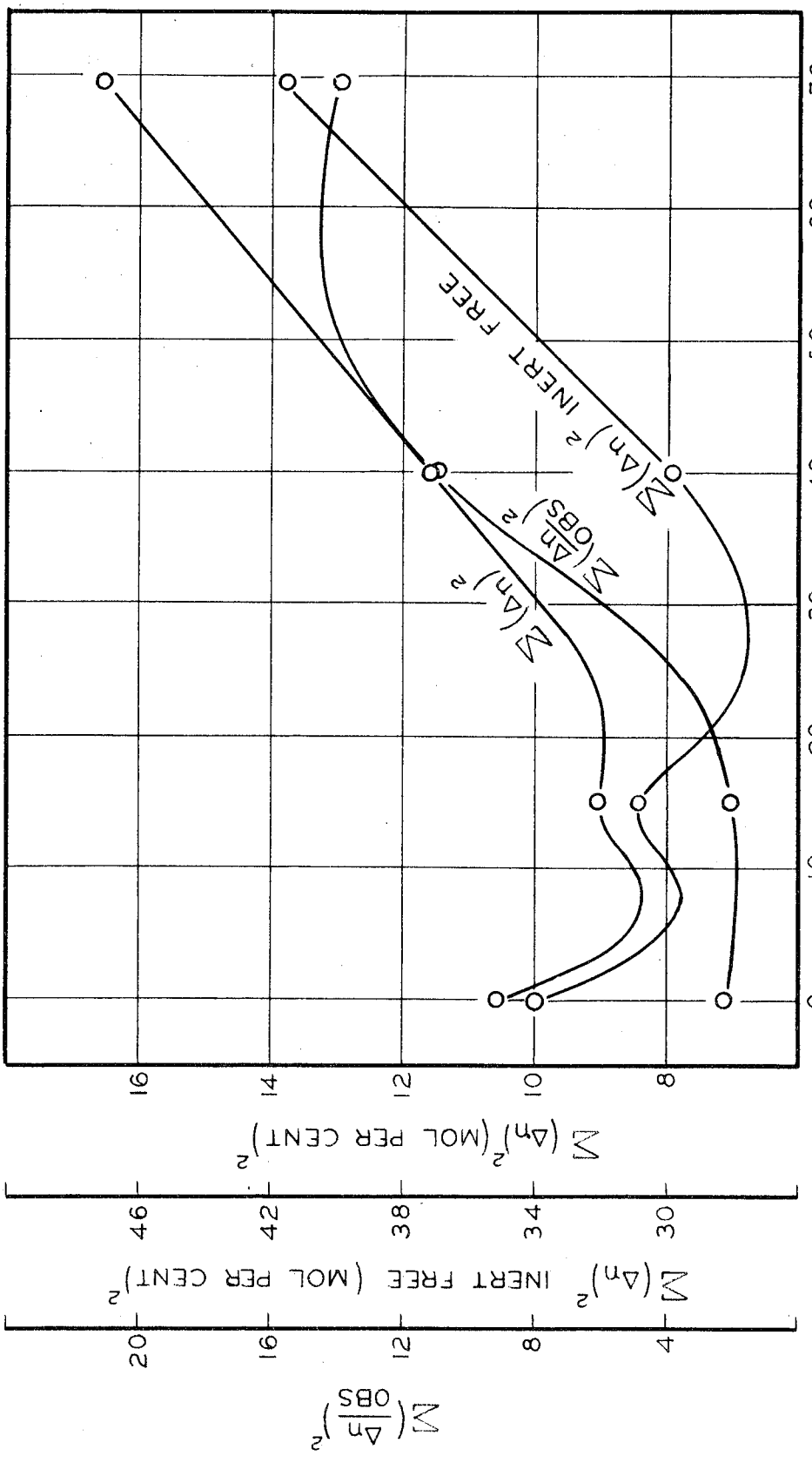

Figure 35. Error Parameters

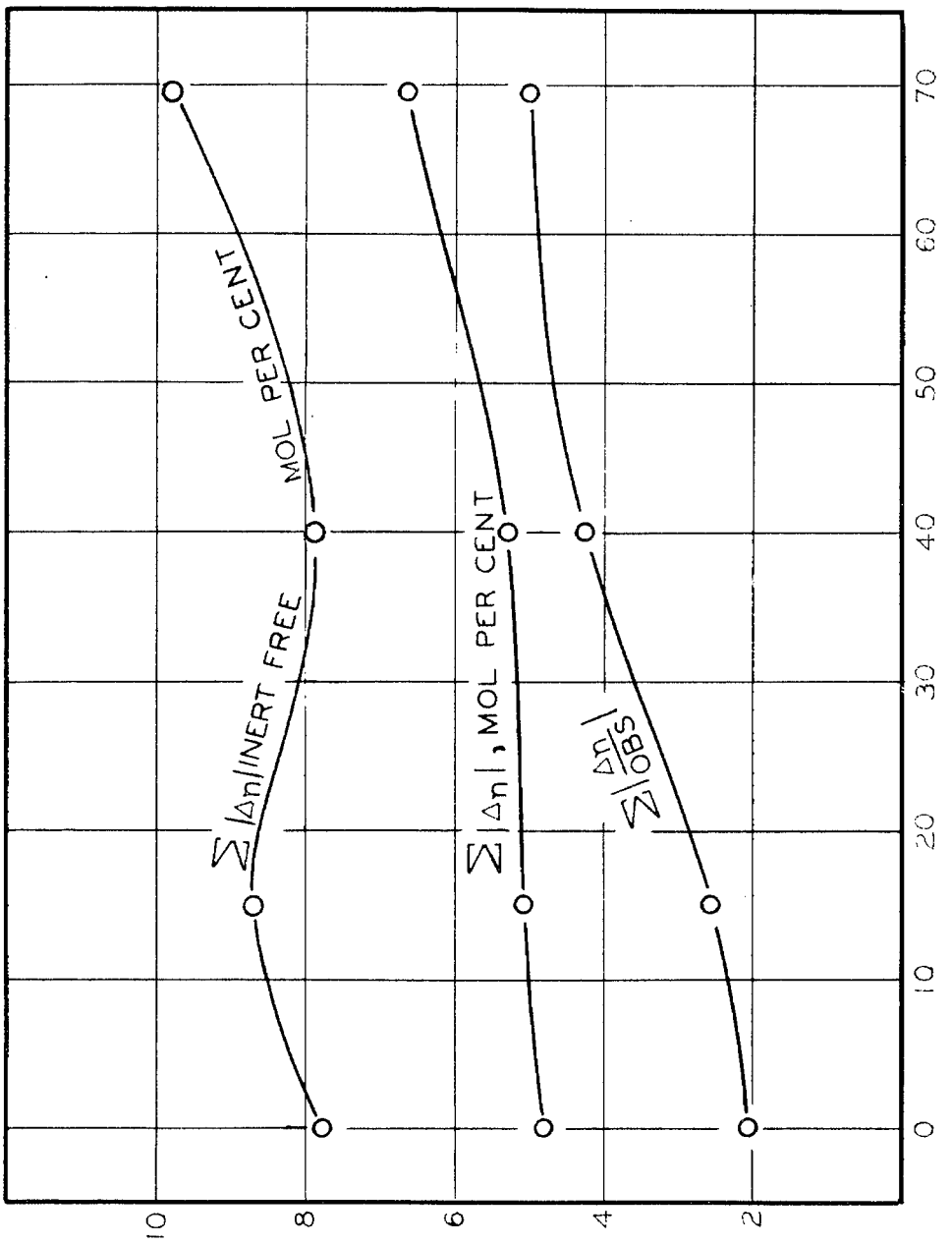

Figure 36. Error Parameters

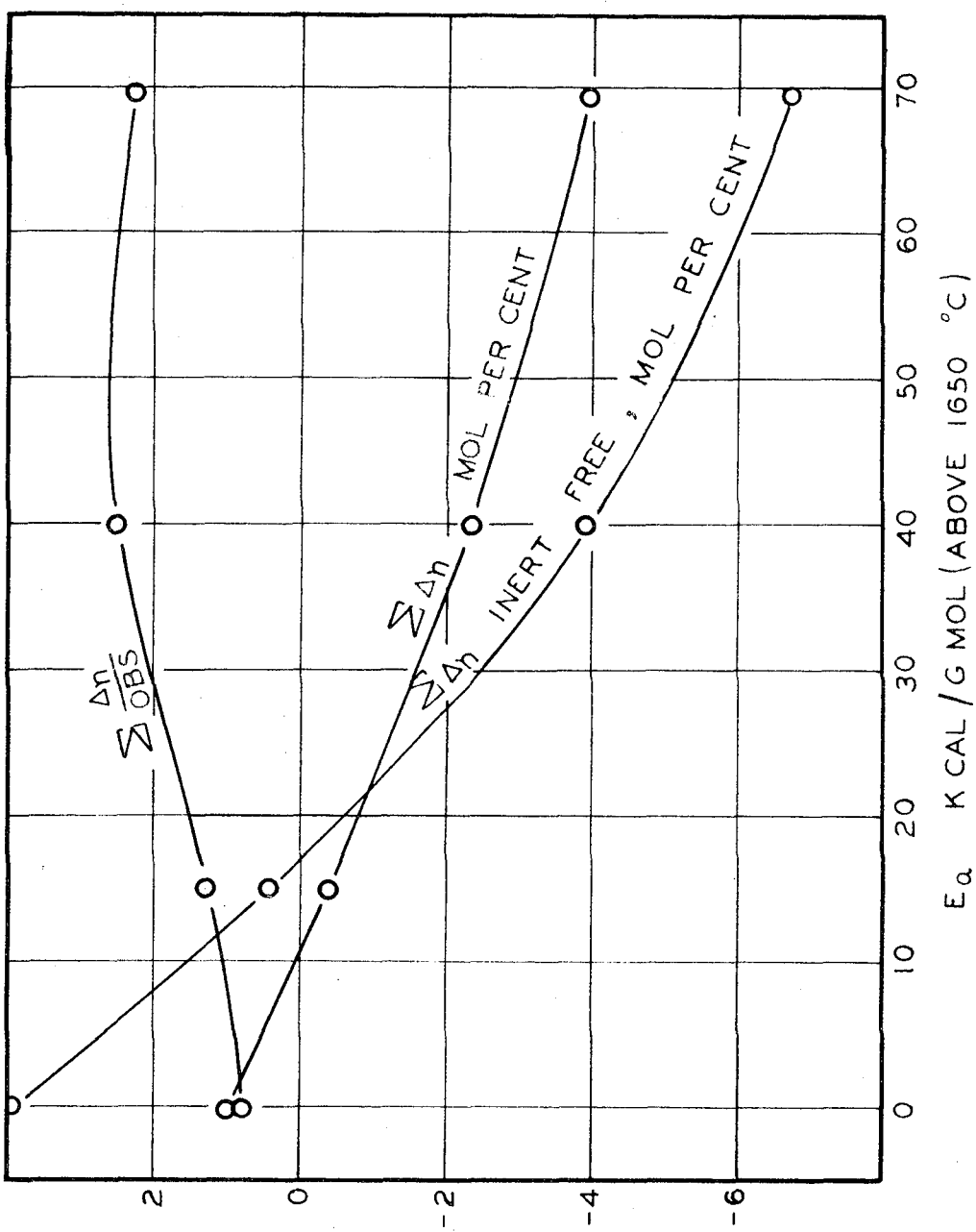

Figure 37. Error Parameters

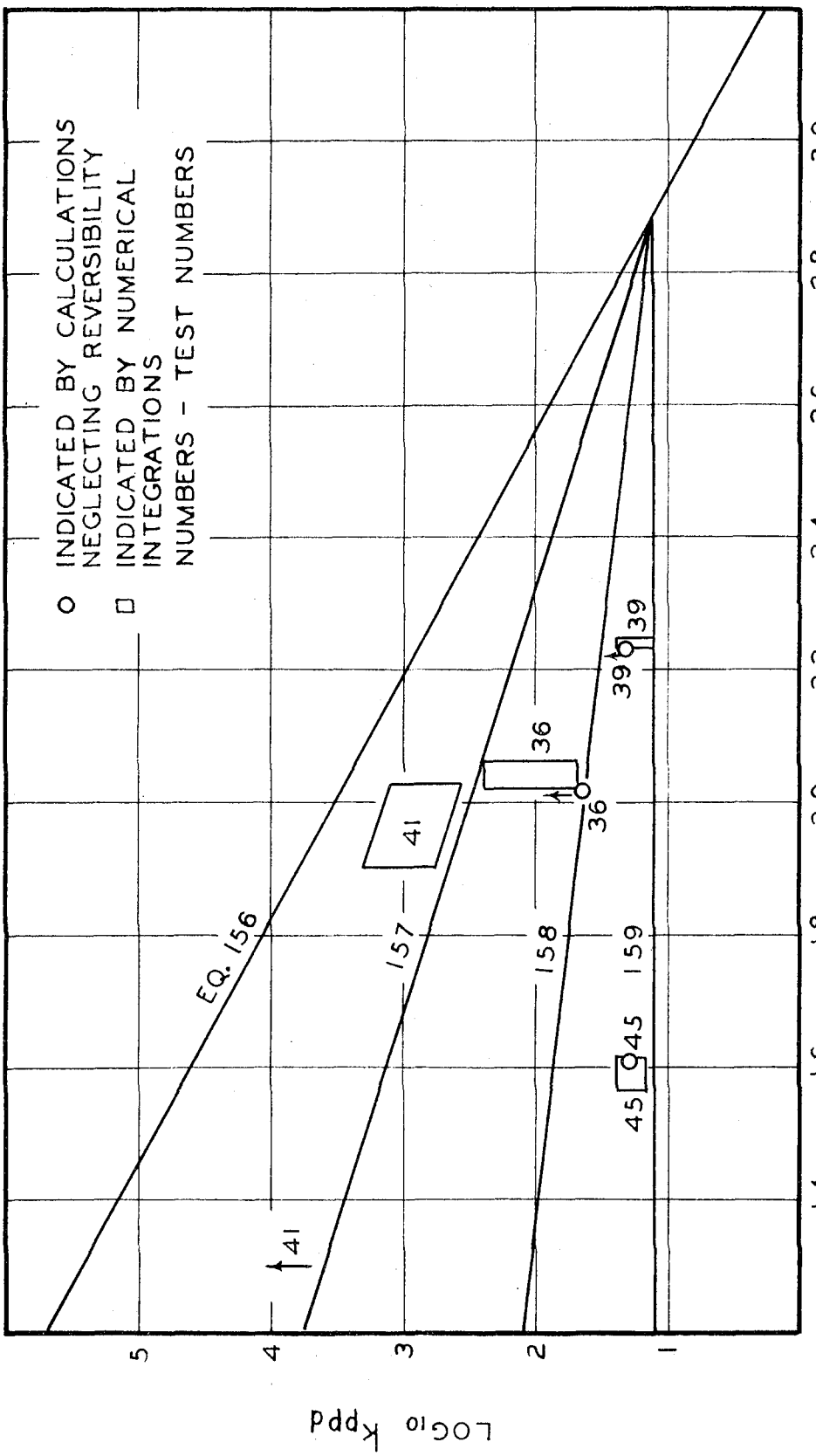

Figure 38. Indicated Rate Coefficients

APPENDIX I

Evaluation of Exponent for Polytropic Path

In order to simplify computations, it was assumed that the expansion of the high pressure air, which furnished kinetic energy to the piston, was adequately described by the polytropic path

$$PV^k = \text{constant} = c \quad . \tag{A-1}$$

In this appendix, all properties refer to the air, unless otherwise specified.

The work done on the piston by the expanding air was evaluated as

$$\underline{W} = \int P d\underline{V} \quad . \tag{A-2}$$

Since leakage was neglected, this may also be written as

$$\underline{W} = m \int P dV \quad . \tag{A-3}$$

Effective values of k were evaluated by equating the work done by the expanding air, as calculated from equation A-1, with that calculated from data on the real gas, air, assuming isentropic expansion.

Combination of equations A-1 and A-3 gives

$$\underline{W} = mc \int_{V_0}^{V} V^{-k} dV \quad . \tag{A-4}$$

Evaluation of the integral term results in

$$\underline{W} = \frac{mc}{1-k}\left(V^{1-k} - V_0^{1-k}\right) \quad . \tag{A-5}$$

It will be convenient to substitute the initial values in equation A-1 to evaluate c. Substitution of the result in equation A-5 gives

$$W = \frac{m P_0 V_0^k}{1-k}\left(V^{1-k} - V_0^{1-k}\right) \quad , \tag{A-6}$$

which may be rearranged to

$$W = \frac{m P_0 V_0}{1-k}\left\{\left(\frac{V}{V_0}\right)^{1-k} - 1\right\} \quad . \tag{A-7}$$

In view of the assumption of no leakage,

$$\frac{V}{V_0} = \frac{\underline{V}}{\underline{V}_0} \quad . \tag{A-8}$$

The behavior of the piston during most of its travel is of no great importance. It is of principal interest to evaluate the kinetic energy of the piston near the bottom of the first downstroke, in the region corresponding to high tem-

perature in the sample. A representative value of $\frac{V}{V_o}$ corresponding to the maximum expansion of the air was chosen as 21.3.

For an initial temperature of 540° R (80.3° F), which is representative of the actual conditions of the runs, and for various assumed initial pressures, equation A-3 was solved for the work done by the air in expanding to 21.3 times its initial volume, along the assumed isentropic path. Corresponding values of pressure and temperature along the path were obtained from the tabulated data of Williams.[1] The volumetric behavior was established from the tabulated virial coefficients of Hall and Ibele.[2] From these data, corresponding values of pressure and volume along the isentropic path were computed, and the ratio $\frac{W}{m}$ was evaluated by graphical integration. For this purpose, the equation was most convenient if cast in the form

$$\frac{W}{m} = \int P V \, d(\ln V) \qquad \text{(A-9)}$$

Equation A-7 was also solved for $\frac{W}{m}$, in terms of k, for the expansion ratio of 21.3. The initial specific volume corresponding to a temperature of 540° R and to the various nominal pressures were computed from the data of

---

[1] Williams, V. C., A. I. Ch. E. Trans., 39, 93-111 (1943).

[2] Hall, N. A., and Ibele, W. E., Trans. ASME, 76, 1039-56 (1954).

Hall and Ibele.

By equating the values of $\frac{W}{m}$ from equation A-7 to those from the graphical integrations, k was evaluated for each nominal initial pressure, and for the expansion ratio of 21.3.

To check the influence of the arbitrary expansion ratio, values of k were also computed for an expansion ratio of 13.5. They were nearly identical with those for the ratio 21.3. This is natural, since most of the work is expended early in the expansion, and beyond a certain point, further increase in $\frac{V}{V_o}$ has little influence on the computed value of k.

The values of k obtained are shown in Figure A-1, as a function of the nominal initial pressure. In treating data from an experimental run, the value of k was read from the curve, at the initial pressure of the run. No account was taken of departures of the initial temperature from 540° R, or of the expansion ratio from 21.3.

Effect of Error in Effective k.

Substitution of equation A-8 and the relation

$$m V_o = \underline{V}_o \qquad \text{(A-10)}$$

in equation A-7 gives

$$\underline{W} = \frac{P_o \underline{V}_o}{1-k}\left\{\left(\frac{\underline{V}}{\underline{V}_o}\right)^{1-k} - 1\right\} , \qquad \text{(A-11)}$$

or

$$\underline{W} = \frac{P_o \underline{V}_o}{k-1}\left\{1 - \left(\frac{\underline{V}_o}{\underline{V}}\right)^{k-1}\right\} . \qquad \text{(A-12)}$$

Taking logarithms,

$$\ln \underline{W} = \ln P_o + \ln \underline{V}_o - \ln(k-1) + \ln\left\{1 - \left(\frac{\underline{V}_o}{\underline{V}}\right)^{k-1}\right\} \quad . \tag{A-13}$$

Differentiation of both sides of equation A-13 with respect to ln(k-1) gives

$$\frac{d \ln \underline{W}}{d \ln(k-1)} = -1 + \left\{\frac{k-1}{1 - \left(\frac{\underline{V}_o}{\underline{V}}\right)^{k-1}}\right\}\left\{\left(\frac{\underline{V}_o}{\underline{V}}\right)^{k-1} \ln\left(\frac{\underline{V}}{\underline{V}_o}\right)\right\} \quad . \tag{A-14}$$

An estimate of the uncertainty in the work, in the region of most interest, may be obtained by the substitution of typical numerical values into equation A-14. Substituting 21.3 for $\frac{\underline{V}}{\underline{V}_o}$ and 0.44 for k-1,

$$\frac{d \ln \underline{W}}{d \ln(k-1)} = -0.53 \quad . \tag{A-15}$$

Thus the relative uncertainty in the work done by the expanding air is roughly half the relative uncertainty in the effective value of k-1. It is clear that the value of k employed need not be very precise.

Also, until much more refined analysis of the behavior

of other features of the overall problem is available, it will not be worth while to attempt more accurate treatment of the air than is given by the use of equations A-1 and A-7, together with the effective k values of Figure A-1.

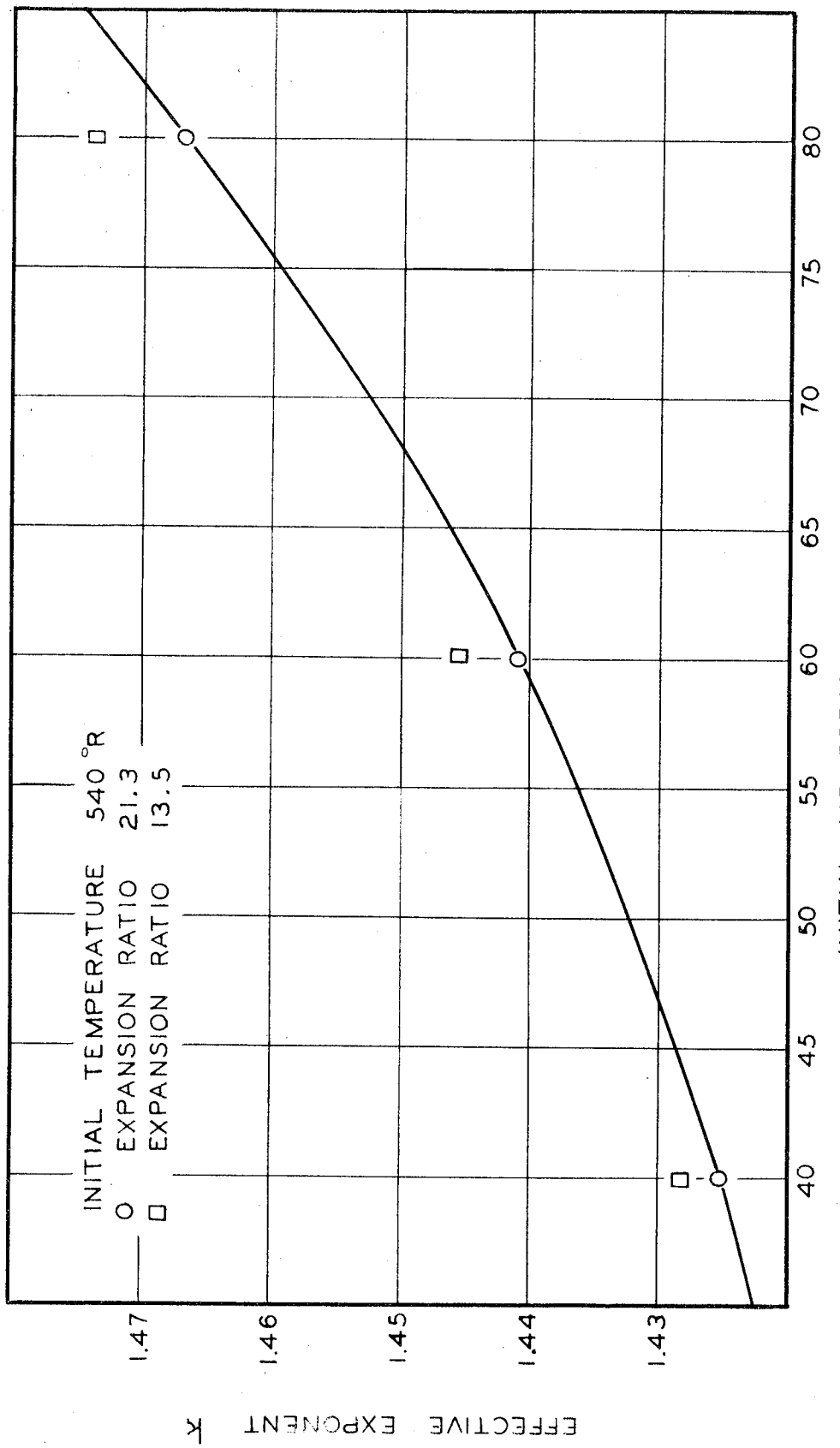

Figure A-1. Effective Exponent for Polytropic Path for Air

APPENDIX II

Differential equations describing the motion of the piston may be written from consideration of the forces acting upon it, as with equations 22 and 69, and equations involving the piston velocity may be obtained by integration, as with equations 68, 83, and 84.

The velocity equations may also be obtained by application of the principle of conservation of energy. This approach is less cumbersome, particularly if motion subsequent to the first downstroke is of interest.

The assumptions of no leakage, no heat transfer, and no chemical reaction are retained. Neglecting energy associated with gross motion or elevation of the sample gas and driving air, we may write an energy conservation equation for the system of interest as follows:

(potential energy gained by piston) + (A-16)
(kinetic energy gained by piston) + (energy gained by "surroundings" due to action of frictional drag on piston) + (energy gained by gas in sample chamber) + (energy gained by driving air) = 0

Using nomenclature as in the text, and making the same assumptions regarding properties of the sample gas and driving air, the terms may be expressed as follows:

potential energy gained by piston = $-\omega_p x$; (A-17)

kinetic energy gained by piston = $m_p \frac{U^2}{2}$; (A-18)

energy gained by sample gas = $-\int_{\underline{V}_{B_o}}^{\underline{V}_B} P_B \, d\underline{V}_B$; (A-19)

energy gained by air = $-\int_{\underline{V}_{A_o}}^{\underline{V}_A} P_A \, d\underline{V}_A$; (A-20)

energy transferred to "surroundings" by action of friction = $\int_o^{l'} F \, dl$ (A-21)

This energy will be evidenced by an increase in the temperature of the cylinder, the O-rings, and the metal piston itself; from the viewpoint of the system of interest, it is lost.

Substituting appropriate symbols for the verbal expressions of equation A-16, we have

$$-w_p x + m_p \frac{U^2}{2} + \int_o^{l'} F \, dl - \int_{\underline{V}_{B_o}}^{\underline{V}_B} P_B \, d\underline{V}_B - \int_{\underline{V}_{A_o}}^{\underline{V}_A} P_A \, d\underline{V}_A = 0 \quad . \tag{A-22}$$

The right hand side of equation A-19 may be evaluated as it was for equation 64,

$$-\int_{\underline{V}_{B_o}}^{\underline{V}_B} P_B \, d\underline{V}_B = P_{B_o} \underline{V}_{B_o} \frac{\Psi}{R} \quad . \tag{A-23}$$

As in the steps leading to equation 64,

$$-\int_{V_{A_o}}^{V_A} P_A \, dV_A = \frac{P_{A_o} V_{B_o}}{k-1} \left\{ \beta^k (1+\beta-V^*)^{1-k} - \beta \right\} . \qquad \text{(A-24)}$$

Substitution of equations A-23 and A-24 in A-22 gives

$$-\omega_p x + m_p \frac{v^2}{2} + \int_o^l F \, dl + P_{B_o} V_{B_o} \frac{\psi}{R} \qquad \text{(A-25)}$$

$$+ \frac{P_{A_o} V_{B_o}}{k-1} \left\{ \beta^k (1+\beta-V^*)^{1-k} - \beta \right\} = 0 .$$

Substituting appropriate relations from equations 57, 66, and 67 in A-25 and dividing by $\frac{V_{B_o}}{A}$ we have

$$\omega_p (V^* - 1) + \frac{m_p V_{B_o}}{2A} v^{*2} + \frac{A}{V_{B_o}} \int_o^l F \, dl \qquad \text{(A-26)}$$

$$+ \frac{A P_{A_o}}{k-1} \left\{ \beta^k (1+\beta-V^*)^{1-k} - \beta \right\} + A P_{B_o} \frac{\psi}{R} = 0 .$$

It seems fairly clear that, for any point in the n^{th} downward stroke,

$$\int_o^l dl = x + 2 \sum_{i=1}^{n-1} x_{D_i} - 2 \sum_{i=1}^{n-1} x_{U_i} , \qquad \text{(A-27)}$$

and for any point in the n^{th} upstroke,

$$\int_o^l dl = -x + 2 \sum_{i=1}^{n} x_{D_i} - 2 \sum_{i=1}^{n-1} x_{U_i} . \qquad \text{(A-28)}$$

Substitution of equation 57 and either A-27 or A-28 in A-26 results in equations identical to 83 or 84 respectively.

APPENDIX III

The defined functions ϕ and Ψ were tabulated for the pure compounds of interest, on the basis of a standard initial temperature of 77° F. In this appendix, equations will be given for the small corrections necessary when the initial temperature of a sample differs from the standard value.

The Function ϕ

By definition, equation 40,

$$\phi(T) = \frac{1}{\ln T^*} \int_0^{\ln T^*} \tilde{C}_v \, d\ln T^* \quad . \tag{A-29}$$

Since by definition, equation 36,

$$T^* = \frac{T}{T_o} \quad , \tag{A-30}$$

the definition of ϕ may also be written

$$\phi(T) = \frac{1}{\ln T_o - \ln T} \int_{T=T_o}^{T} \tilde{C}_v \, d\ln T \quad . \tag{A-31}$$

The standard initial temperature will be designated T_{o_s} and the corresponding value of ϕ as ϕ_s . Applying the definition of ϕ to the standard initial temperature,

$$\phi_s(T) = \frac{1}{\ln T - \ln T_{o_s}} \int_{T=T_{o_s}}^{T} \tilde{C}_v \, d\ln T \qquad \text{(A-32)}$$

Equation A-31 may be broken into parts as

$$\phi(T) = \frac{1}{\ln T - \ln T_o} \int_{T=T_o}^{T_{o_s}} \tilde{C}_v \, d\ln T \qquad \text{(A-33)}$$

$$+ \frac{1}{\ln T - \ln T_o} \int_{T=T_{o_s}}^{T} \tilde{C}_v \, d\ln T \; .$$

Equations A-32 and A-33 may be combined to give

$$\phi(T) = \frac{1}{\ln T - \ln T_o} \int_{T=T_o}^{T_{o_s}} \tilde{C}_v \, d\ln T \qquad \text{(A-34)}$$

$$+ \frac{\ln T - \ln T_{o_s}}{\ln T - \ln T_o} \phi_s(T) \; .$$

Reversing the limits of the remaining integral and changing its sign

$$\phi(T) = \frac{1}{\ln T_o - \ln T} \int_{T=T_{o_s}}^{T_o} \tilde{C}_v \, d\ln T + \frac{\ln T - \ln T_{o_s}}{\ln T - \ln T_o} \phi_s(T) \; . \qquad \text{(A-35)}$$

Again making use of equation A-32, the last relation may be written

$$\phi(T) = \frac{\ln T_o - \ln T_{o_s}}{\ln T_o - \ln T}\,\phi_s(T_o) + \frac{\ln T - \ln T_{o_s}}{\ln T - \ln T_o}\,\phi_s(T) \qquad \text{(A-36)}$$

or

$$\phi(T) = \frac{\ln T_{o_s} - \ln T_o}{\ln T - \ln T_o}\,\phi_s(T_o) + \frac{\ln T - \ln T_{o_s}}{\ln T - \ln T_o}\,\phi_s(T) \,. \qquad \text{(A-37)}$$

Evaluation of $\phi(T)$ by means of equation A-36 or A-37, taking $\phi_s(T_o)$ and $\phi_s(T)$ from the tabulated values, is fairly simple, and far easier than computing $\phi(T)$ directly from the defining equation and tabulated values of $\tilde{C}_v$.

The Function Ψ .

By its definition, equation 69,

$$\Psi(T) = \int_{T^*=1}^{T^*} \tilde{C}_v \, d T^* \quad ; \qquad \text{(A-38)}$$

this may, using equation A-30, be written as

$$\Psi(T) = \frac{1}{T_o} \int_{T=T_o}^{T} \tilde{C}_v \, d T \quad . \qquad \text{(A-39)}$$

Application of equation A-39 from the standard initial temperature gives

$$\Psi_s(T) = \frac{1}{T_{o_s}} \int_{T=T_{o_s}}^{T} \tilde{C}_v \, dT \quad . \tag{A-40}$$

Equation A-39 may be broken up into

$$\Psi(T) = \frac{1}{T_o} \left\{ \int_{T_o}^{T_{o_s}} \tilde{C}_v \, dT + \int_{T_{o_s}}^{T} \tilde{C}_v \, dT \right\} \tag{A-41}$$

which by use of equation A-40 may be written

$$\Psi(T) = \frac{T_{o_s}}{T_o} \left\{ - \Psi_s(T_o) + \Psi_s(T) \right\} \tag{A-42}$$

or

$$\Psi(T) = \frac{T_{o_s}}{T_o} \Psi_s(T) - \frac{T_{o_s}}{T_o} \Psi_s(T_o) \tag{A-43}$$

The use of equation A-43 and the tabulated values is much easier than computation of Ψ from its defining equation.

PART II

ISOBARIC HEAT CAPACITIES AT BUBBLE POINT OF PSEUDOCUMENE AND OF n-HEPTANE

which are less inhibited by carbon black than are diaroyl peroxide cures.

Acceleration. Polyester cures catalyzed with benzoyl and chlorine-substituted benzoyl peroxides (diaroyl peroxides), in combination with aromatic amines or resorcinol, are accelerated by carbon black. Increasing the carbon black concentration increases rate of cure in these systems. *tert*-Butyl perbenzoate (an aroyl-alkyl peroxide) cures, which are slightly inhibited by carbon black in systems without promoters, are also inhibited by carbon black in mixtures promoted by aromatic amines. Increasing the carbon loading in these cures, with or without aromatic amines as promoters, decreases cure rate. Di-*tert*-butyl peroxide (a dialkyl peroxide) is very strongly inhibited by carbon black in promoted systems, with the inhibition increasing with higher carbon loading.

These accelerating and inhibiting effects may be due to the peroxides being adsorbed in varying degrees on the carbon surface. Aromatic peroxides would be expected to be adsorbed to a greater extent than alkyl peroxides. In a diaroyl peroxide–aromatic amine–carbon black system both the peroxide and amine, therefore, are strongly adsorbed on the carbon surface. The high adsorption of peroxide and amine on the carbon surface produces decomposition at an extremely rapid rate which is far beyond the rate at which the carbon surface can inactivate the radicals formed. In addition, the adsorbed amine may decrease the termination reaction by blocking reactive sites on the carbon surface—the net effect is an accelerated cure. If lauryl mercaptan, an aliphatic promoter, is added to resin-carbon–aroyl peroxide mixtures, inhibition is severe indicating that adsorption of promoter as well as peroxide is essential for acceleration with carbon black.

With *tert*-butyl perbenzoate and particularly di-*tert*-butyl peroxide the specific adsorption of the peroxide is much lower. The aromatic amine is, nevertheless, adsorbed on the carbon surface which effectively reduces the concentration of amine in the system. Increasing the carbon black loading at constant amine concentration decreases the effective concentration of amine. The rate of free radical formation is, therefore, much lower than in the benzoyl peroxide systems. The rate of termination on the carbon surface of the free radicals formed by thermal decomposition and the amine reaction is still sufficient to inhibit cure. In such cases cure rate decreases as carbon black loading increases.

CONCLUSIONS

1. Practical curing systems are described for carbon black–polyester resin mixtures.
2. Carbon black in these systems prolongs the shelf life of catalyzed resins but accelerates the polymerization when promoter is added. This combination of properties, should interest the fabricators of these resins.
3. Qualitative mechanisms of these carbon black–peroxide interactions are presented.

LITERATURE CITED

(1) Braden, M., Fletcher, W. P., and McSweeney, G. P., *Trans. Inst. Rubber Ind.*, 30, 44 (1954).
(2) Garten, V. A., and Sutherland, G. K., "Nature of Chemisorption Mechanisms in Rubber Reinforcement," presented at 3rd Rubber Technology Conference, London, June 22–25, 1954.
(3) Kolthoff, I. M., Gutmacher, R. G., and Kahn, A., *J. Phys. & Colloid Chem.*, 55, 1240 (1951).
(4) Nichols, F. S., and Bliss, C. H., *Modern Plastics*, 29, 124 (May 1952).
(5) Rhodes, F. H., and Goldsmith, H. E., IND. ENG. CHEM., 18, 566 (1926).
(6) Sweitzer, C. W., *Rubber Age (N. Y.)*, 72, 55 (1952).
(7) Sweitzer, C. W., and Lyon, F., IND. ENG. CHEM., 44, 125 (1952).
(8) Tobolsky, A. V., and Mesrobian, R. B., "Organic Peroxides," Interscience, New York, 1954.
(9) Watson, W. F., "Interaction of Rubber and Fillers during Cold Mixing," presented at 3rd Rubber Technology Conference, London, June 22–25, 1954.

RECEIVED for review January 18, 1955. ACCEPTED June 15, 1955. Division of Paint, Plastics, and Printing Ink Chemistry, 126th Meeting, ACS, New York, September 14, 1954.

Isobaric Heat Capacities at Bubble Point

Two Trimethylbenzenes and *n*-Heptane

P. F. HELFREY, D. A. HEISER, AND B. H. SAGE
California Institute of Technology, Pasadena, Calif.

LIMITED experimental data are available for the heat capacity of 1,3,5-trimethylbenzene (*10, 19, 21*), but there do not appear to be any recent heat capacity measurements relating to 1,2,4-trimethylbenzene at temperatures above 70° F. (*19*). However, as part of an early investigation, Schiff (*19*) reported heat capacities for this compound at temperatures below 70° F. The critical constants of both the trimethylbenzenes were measured by Altschul (*1*). In addition, the critical temperature of 1,3,5-trimethylbenzene was determined by Prud'homme (*16*). Mair (*11*) reported the index of refraction and density of these trimethylbenzenes, and Smith and coworkers (*24, 25*) determined the vapor pressure and the index of refraction of 1,2,4-trimethylbenzene at relatively lower temperatures.

Because of the absence or limited availability of heat capacity data above room temperature for these trimethylbenzenes, the isobaric heat capacities of these compounds were measured at temperatures from 80° to 220° F. In addition, measurements were made at temperatures from 70° to 220° F. of the heat capacity of *n*-heptane, which has been selected by the Fourth Conference on Calorimetry (*4*) as one of the reference substances for calorimetric work. The heat capacity of *n*-heptane was studied by Parks (*13*), and critically chosen values were reported by Ginnings (*7*). Beattie and coworkers (*23*) determined the critical constants and Smith (*22*) the vapor pressure of this compound. Rossini (*17*) summarized the properties of these three hydrocarbons and his values were used in establishing a measure of the purity of these compounds.

MATERIALS

The 1,2 4-trimethylbenzene was obtained from Project 44 of the American Petroleum Institute at the Ohio State University and was reported to contain less than 0.006 mole % of impurities. The specific weight was 54.4263 pounds per cubic foot at 77° F., and the refractive index as measured with the D-lines of sodium at 77° F. was 1.5024. These values may be compared with a specific weight of 54.4250 pounds per cubic foot and an index of refraction of 1.50237 under the same conditions reported by Rossini (*17*). The 1,3,5-trimethylbenzene was reported by Project 44 to contain 0.0022 mole fraction of impurities. The

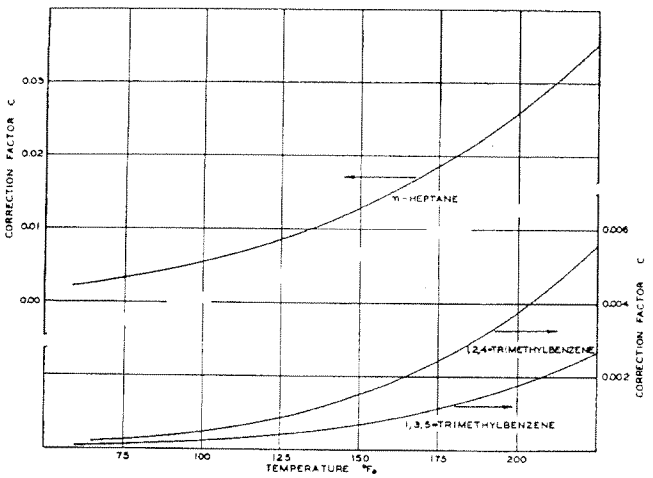

Figure 1. Volumetric corrections

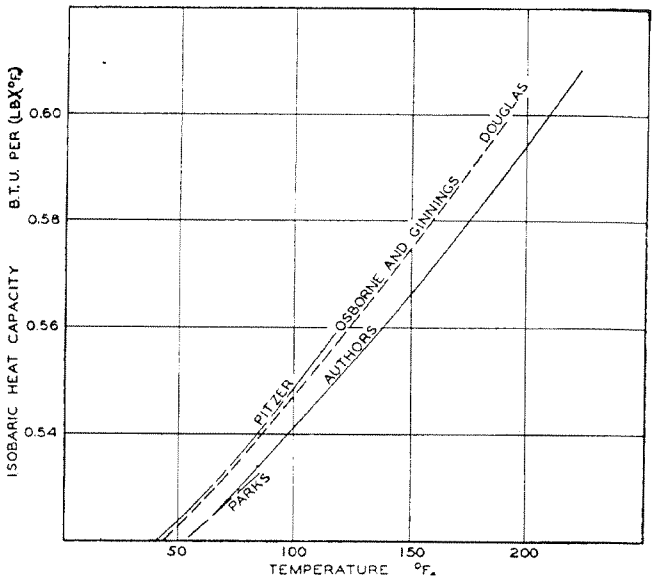

Figure 2. Comparison of experimental results for *n*-heptane

small size of the sample available precluded confirming measurements of physical properties of this sample.

The *n*-heptane used in this work was supplied by the National Bureau of Standards which determined its purity by freezing-point experiments and found it to contain 0.013 mole fraction of material other than *n*-heptane. After deaeration this material had a specific weight of 42.4194 pounds per cubic foot at 77° F. and an index of refraction at that temperature of 1.3852 relative to the D-lines of sodium. These values compare with 42.4207 cubic feet per pound for the specific weight and an index of refraction of 1.38511 under the same conditions reported by Rossini (*17*) for an air saturated sample.

METHODS AND APPARATUS

Experimental measurements of the heat capacity were made under isochoric conditions in the two-phase gas-liquid region in a calorimeter which has been described in some detail (*2*, *3*, *5*, *18*, *20*). A known quantity of energy was added electrically to the calorimeter and contents, and the resulting change in temperature of the system after the attainment of equilibrium was determined. This procedure was repeated throughout the temperature interval of the investigation. No changes were made from the experimental techniques that were used in the study of other hydrocarbons (*2*, *5*).

A series of measurements such as has been described was made with two different quantities of the sample of each of the three compounds investigated. The isobaric heat capacity was related to the quantities measured by means of the following equation:

$$C_{P,b} = \frac{\frac{q_1}{dT} - \frac{q_2}{dT}}{m_1 - m_2}\left(\frac{V_d - V_b}{V_d}\right) + T \left(\frac{\partial V}{\partial T}\right)_{P,b} \frac{dP''}{dT} + T\frac{dP''}{dT}\left(\frac{V_d \frac{dV_b}{dT} - V_b \frac{dV_d}{dT}}{V_d}\right) \quad (1)$$

$$\frac{V_b}{V_d}\left[C_{P,d} - T\left(\frac{\partial V}{\partial T}\right)_{P,d}\frac{dP''}{dT}\right] = \frac{\frac{q_1}{dT} - \frac{q_2}{dT}}{(m_1 - m_2)(1 - c)}$$

In the second equality of Equation 1, the volumetric corrections were reduced to a single quantity, c. This correction term was established from the volumetric data available by the methods outlined by Auerbach (*2*) and Connolly (*5*). The magnitude of this correction term is shown in Figure 1. In most of the measurements except those on *n*-heptane the volumetric correction was less than 0.3% of isochoric heat capacity. As a result of the small magnitude of the volumetric correction term it was not necessary to establish these quantities with high accuracy. The law of corresponding states was employed in most cases to establish the volumetric behavior of the gas phase whereas the available experimental data were used to determine the vapor pressure and the specific volume of the liquid phase as a function of temperature. The heat capacity of the gas phase was established from the Rossini values (*17*) for the heat capacity of the ideal gas. Uncertainties in the determination of the volumetric correction shown in Figure 1 for each compound introduced less than 0.1% uncertainty in the reported values of the heat capacities.

RESULTS

Measurements were made on *n*-heptane as a reference substance and data were obtained from two different quantities of this compound. From these measurements, quadratic equations were fitted to the experimental data (*8*) by least squares techniques. The results of these calculations indicated a standard deviation of about 2.1% of the average difference between the heat capacities of the calorimeter and contents in each set of measurements. This large an uncertainty resulted from the relatively small sample of *n*-heptane available for measurement.

A summary of the experimental data obtained for *n*-heptane is recorded in a part of Table I. The results are in good agreement with the measurements of Parks and coworkers (*14*) at lower temperatures. The values are about 1% below the data reported by Ginnings (*7*, *12*) for *n*-heptane at the lower temperatures and nearly 2% below at the higher temperatures. They also are below the critically chosen values reported by Douglas and coworkers (*6*). The results of the measurements on *n*-heptane are shown in Figure 2. For comparison the data of Parks (*14*) and Pitzer (*15*) and the critically chosen values of Douglas (*6*) were included. These comparative measurements for *n*-heptane indicate that the heat capacity studies that have been made with the instrument used in this investigation may have yielded results as much as 1% below the most probable value. Throughout this series of measurements (*5*, *20*) good agreement was obtained with the earlier studies of Parks and

Table I. Isobaric Heat Capacities at Bubble Point for Two Trimethylbenzenes and *n*-Heptane

Temperature, ° F.	*n*-Heptane $\frac{q_1}{dT} - \frac{q_2}{dT}$ / $m_1 - m_2$	*n*-Heptane $C_{P,b}$ B.t.u./(lb.) (° F.)	1,2,4-Trimethylbenzene $\frac{q_1}{dT} - \frac{q_2}{dT}$ / $m_1 - m_2$	1,2,4-Trimethylbenzene $C_{P,b}$ B.t.u./(lb.) (° F.)	1,3,5-Trimethylbenzene $\frac{q_1}{dT} - \frac{q_2}{dT}$ / $m_1 - m_2$	1,3,5-Trimethylbenzene $C_{P,b}$ B.t.u./(lb.) (° F.)
70	0.5256	0.5271	0.4140	0.4141	0.3941	0.3941
80	0.5299	0.5318	0.4180	0.4181	0.4002	0.4003
90	0.5342	0.5366	0.4219	0.4221	0.4064	0.4065
100	0.5385	0.5414	0.4260	0.4262	0.4126	0.4126
110	0.5427	0.5463	0.4301	0.4304	0.4187	0.4188
120	0.5469	0.5512	0.4343	0.4347	0.4249	0.4250
130	0.5511	0.5562	0.4386	0.4391	0.4310	0.4312
140	0.5552	0.5613	0.4430	0.4436	0.4372	0.4374
150	0.5592	0.5665	0.4475	0.4482	0.4433	0.4436
160	0.5633	0.5718	0.4520	0.4529	0.4495	0.4499
170	0.5673	0.5773	0.4567	0.4577	0.4557	0.4561
180	0.5712	0.5828	0.4614	0.4626	0.4618	0.4624
190	0.5751	0.5886	0.4662	0.4677	0.4680	0.4687
200	0.5790	0.5945	0.4711	0.4728	0.4741	0.4750
210	0.5829	0.6006	0.4760	0.4781	0.4803	0.4813
220	0.5867	0.6069	0.4811	0.4836	0.4864	0.4877

coworkers (*13*, *14*). The results for all compounds reported are based on experimental measurements and did not involve any correction associated with calibration of the calorimeter with material of known heat capacities.

Similar measurements (*8*) were made for the two trimethylbenzenes. In the case of 1,2,4-trimethylbenzene a standard deviation of 0.00242 B.t.u. per ° F. was found in the experimental measurements on the two samples. This deviation corresponded to 1.2% of the heat capacity of this compound. These measurements are recorded in a part of Table I. Similar information is presented in a part of this table for 1,3,5-trimethylbenzene. In this instance the standard deviation corresponded to 0.006 B.t.u. per ° F. which was equivalent to approximately 2.5% of the heat capacity of 1,3,5-trimethylbenzene. The larger uncertainty for the latter compound resulted from the smaller sample available.

A comparison of the experimental measurements for 1,2,4-trimethylbenzene with the measurements of Huffman (*9*) is shown in Figure 3. In this instance, the heat capacities reported here are approximately 0.9% below the values reported by Huffman (*9*) at the lower temperatures. Since this deviation is of the same order as the standard deviation of the present data this discrepancy is not significant. A similar comparison is shown in Figure 4 for 1,3,5-trimethylbenzene. The early values of Schiff (*19*) and Kurbatov (*10*) have been included. Here again the present data are somewhat below the Schiff and the Kurbatov measurements.

ACKNOWLEDGMENT

The financial assistance of the California Research Corp. made this investigation possible. The calorimeter employed was developed as a part of the early activities of Project 37 of the American Petroleum Institute, which kindly gave permission to use the instrument. W. N. Lacey reviewed the manuscript, and Patricia Moen assisted in its preparation.

NOMENCLATURE

- c = volumetric correction factor
- C_p = isobaric heat capacity, B.t.u. per (pound) (° F.)
- d = differential operator
- m = weight of material in calorimeter, pounds
- P = pressure, pounds per square inch absolute
- q = heat associated with infinitesimal change in state, B.t.u.
- T = thermodynamic temperature, ° R.
- V = specific volume, cubic feet per pound
- ∂ = partial differential operator

Subscripts

- b = bubble point
- d = dew point
- 1, 2 = conditions with different quantities of sample in calorimeter

Superscript

- $''$ = two-phase state

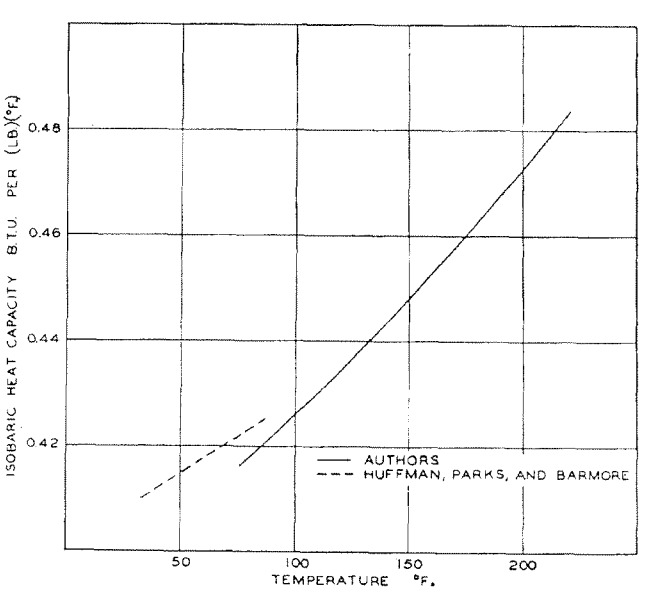

Figure 3. Heat capacities of 1,2,4-trimethylbenzene

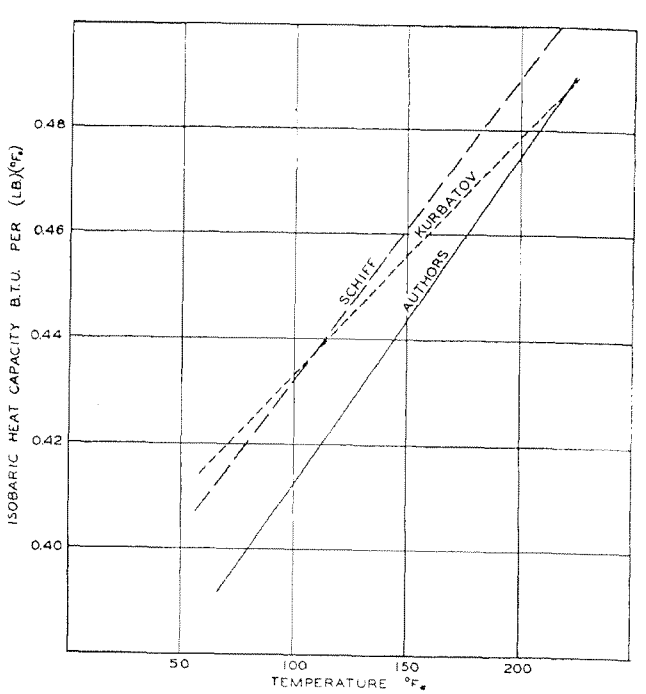

Figure 4. Heat capacities of 1,3,5-trimethylbenzene

LITERATURE CITED

(1) Altschul, M., *Z. physik. Chem.*, **11**, 590 (1893).
(2) Auerbach, C. E., Sage, B. H., and Lacey, W. N., IND. ENG. CHEM., **42**, 110 (1950).
(3) Budenholzer, R. A., Sage, B. H., and Lacey, W. N., IND. ENG. CHEM., **35**, 1214 (1943).
(4) *Chem. Eng. News*, **27**, 2772 (1949).
(5) Connolly, T. J., Sage, B. H., and Lacey, W. N., IND. ENG. CHEM., **43**, 946 (1951).
(6) Douglas, T. B., Furukawa, G. T., McCoskey, R. E., and Ball, A. F., *J. Research, Natl. Bur. Standards*, **53**, 139 (1954).
(7) Ginnings, D. C., and Furukawa, G. T., *J. Am. Chem. Soc.*, **75**, 522 (1953).
(8) Helfrey, P. F., Heiser, D. A., and Sage, B. H., Washington, D. C., Am. Doc. Inst., Doc. No. 4599 (1954).
(9) Huffman, H. M., Parks, G. S., and Barmore, M., *J. Am. Chem. Soc.*, **53**, 3876 (1931).
(10) Kurbatov, V. Ya., *J. Gen. Chem. (U.S.S.R.)*, **17**, 1999 (1947).
(11) Mair, B. J., *J. Research, Natl. Bur. Standards*, **11**, 665 (1933).
(12) Osborne, N. S., and Ginnings, D. C., *J. Research, Natl. Bur. Standards*, **39**, 453 (1947).
(13) Parks, G. S., *J. Am. Chem. Soc.*, **52**, 1035 (1930).
(14) Parks, G. S., Huffman, H. M., and Thomas, S. B., *Ibid.*, **52** 1032.
(15) Pitzer, K. S., *Ibid.*, **62**, 1224 (1940).
(16) Prud'homme, M., *J. Chim. Phys.*, **18**, 270, 307 (1920).
(17) Rossini, F. D., "Selected Values of Properties of Hydrocarbons," National Bureau of Standards, Washington 25, D. C., 1947.
(18) Sage, B. H., Evans, H. D., and Lacey, W. N., IND. ENG. CHEM., **31**, 763 (1939).
(19) Schiff, R., *Ann.*, **234**, 300 (1888).
(20) Schlinger, W. G., and Sage, B. H., IND. ENG. CHEM., **44**, 2454 (1952).
(21) Shanholtzer, O. G., thesis, Univ. of Missouri, Columbia, Mo., 1941.
(22) Smith, E. R., *J. Research, Natl. Bur. Standards*, **24**, 229 (1940).
(23) Smith, L. B., Beattie, J. A., and Kay, W. C., *J. Am. Chem. Soc.*, **59**, 1587 (1937).
(24) Smith, L. I., and Cass, O. W., *J. Am. Chem. Soc.*, **54**, 1603 (1932).
(25) Smith, L. I., and Lund, A. P., *Ibid.*, **52**, 4144 (1930).

RECEIVED for review January 7, 1955. ACCEPTED May 19, 1955
A more detailed form of this paper (or extended version, or material supplementary to this article) has been deposited as Document No. 4599 with the ADI Auxiliary Publications Project, Photoduplication Service, Library of Congress, Washington 25, D. C. A copy may be secured by citing the document number and by remitting $1.25 for photoprints or $1.25 for 35-mm. microfilm. Advance payment is required. Make checks or money orders payable to Chief, Photoduplication Service, Library of Congress.

Effects of Radiation on Organopolysiloxanes

E. L. WARRICK, *Mellon Institute, Pittsburgh 13, Pa.*

THE original purpose of this study was to evaluate organopolysiloxane elastomers and resins as materials of construction around radiation sources of high intensity. It soon was clear that vulcanization of organopolysiloxane elastomers by radiation gave rubbers of superior high temperature performance. Ultimately the effects of radiation from four different sources were noted. In most respects the results were parallel to those reported recently for a number of organic polymers (*8, 10*); the greatest differences were in the precise nature of the chemical effects. However, the same equivalence of energy, regardless of source, was observed with dimethylpolysiloxanes as with organic polymers. The few phenomena already observed on radiating dimethylpolysiloxanes (*2, 9*) with two types of source were confirmed.

The radiation used in this work was secondary radiation including neutrons produced from cyclotron-accelerated deuterons, gamma rays from cobalt-60, electrons from a high voltage electrostatic source, and x-rays from conventional targets.

Samples were placed inside a water cooled copper cup in the primary cyclotron beam, where the 14.5 m.e.v. deuterons produced secondary radiation from the cup. A. J. Allen, director of the cyclotron at the University of Pittsburgh, cooperated in making these exposures.

The samples which received gamma radiation from cobalt-60 were exposed within a cylindrical source of 1470 curies, where they received 500,000 roentgens per hour as certified by the agency making the exposures. The exposures were made by S. I. Taimuty of the Stanford Research Institute using a cobalt-60 source provided by the United States Atomic Energy Commission under contract No. AT (04-3)-52.

The electron-irradiated samples were exposed to 2-m.e.v. electrons from a van der Graaf generator operating at 246-μa. current to yield 2 Mrep (million roentgen equivalent physical) per pass under the beam. Some of the radiation exposures carried out at the plant of the High Voltage Engineering Corp., Boston, Mass., were facilitated by arrangements made by the Westinghouse Electric and Manufacturing Corp. for the use of the radiation source.

Samples receiving x-ray exposure were subject to the full beam no more than 2 inches from the tube. In this case a number of different targets were used through the courtesy of L. E. Alexander and Alvin Cohen, Departments of Chemical Physics and Glass Science, Mellon Institute.

CYCLOTRON RADIATION

Experiments with the secondary radiation produced by the 14.5-m.e.v. deuteron beam within the water-cooled copper cup were less satisfying quantitatively than all the other experiments. It was impossible to make any reasonable measurement or even any estimate of the intensity of the radiation used. However, these experiments were first, chronologically, and demonstrated two points clearly.

Comparative measures of the effects of the secondary radiation, gamma, electrons, and neutrons, on a number of commercial silicone rubbers showed the phenomenon to be similar to aging at high temperatures. Moreover, the nature of the process was shown to be one of cross linking equivalent to a normal vulcanization.

Samples of Silastic 152 (Dow Corning Corp.), a simple formulation of dimethylpolysiloxane, roughly 20 volume % of a finely divided silica as the major filler (25 to 30 mμ), and an organic peroxide as vulcanizing agent, both as press vulcanized and after oven aging 24 hours at 250° C., were exposed in the water-cooled

Table I. Effect of Cyclotron Radiation on Elongation

	% Elongation	
	As cured	Aged
Before radiation	587	309
Radiated stack		
Top	225	165
Second	315	185
Third	350	200
Bottom	350	165

PROPOSITIONS

1. The rise in temperature of a thin disk in the bottom of the cylinder has been measured, as an index of the heat lost from samples in the ballistic piston apparatus. Investigations using a series of such disks, with surfaces varying from highly polished to black, would be of value in estimating the relative importance of radiation.

2. The formulation of the second law of thermodynamics employed by Lacey and Sage (1), $TdS = q + j$, presents certain difficulties. Effort should be devoted to clarifying the meaning of T for cases in which j is not zero.

3. The boiling point of a heterogeneous mixture of immiscible liquids is usually taken to be the temperature at which the sum of the vapor pressures of the separate liquids is equal to the applied pressure (2,3).

This principle is applied to the separation of homogeneous mixtures having heat sensitive components, by the addition of another, non-miscible, component (4,5).

To avoid considerable superheating, the heterogeneous system should be agitated in such fashion as to promote mixing of the phases and formation of extensive liquid-liquid interfacial area. A qualitative analysis of the transport phenomena involved predicts that bubble formation will occur at or near a liquid-liquid interface. A simple demonstration experiment is proposed, which shows that bubble formation takes place as expected, and that considerable superheating is possible in a quiescent system.

4. Kayser (6) has proposed that the technique of "descriptive dimensional analysis" sheds light on the physical phenomena involved in heat, momentum, and mass transfer, and on the interrelation of the respective coefficients k, , and D.

The physical interpretations offered do not follow from the arguments adduced. An extension of the device of descriptive restrictions on the quantities involved offers one means of avoiding the errors in his interpretations.

5. In using graphical integration to evaluate the work done by the adiabatic expansion of a real gas, the equation

$$W = \int PV\, d(\ln V)$$

is more satisfactory than the form

$$W = \int P\, dV ,$$

since the relative variation in the function to be plotted is much less.

6. Variable volume PVT cells, in which the volume is changed by addition or withdrawal of known amounts of mercury, may be used to study some systems which would react with mercury, by confining the samples in thin plastic bags. This procedure would undoubtedly result in some loss of accuracy, but would be useful for exploratory studies.

7. For the evaluation of reaction rate constants from data taken from laboratory flow reactors, Hougen and Watson (7) suggest equations based on the integral equation

$$\frac{V_r}{F} = \int_0^{x_A} \frac{dx_A}{r}$$

A slight modification is proposed, in which the equations are based on the form

$$\int_0^{V_r} r\, dV_r = F_o\, x_A ,$$

where F_o is a hypothetical equivalent feed rate. This procedure has the advantage that zero values of r can be handled graphically, and all of the experimental data utilized in evaluating reaction velocity coefficients.

8. The installation of an additional blinker signal on automobiles is proposed. This device would be used to signal the motorist's intention to yield the right of way.

9. In the calculations reported in this thesis, only one chemical reaction was considered. Among those neglected was dissociation of NO into the atomic species N and O. The results of certain of the "decomposition" runs may be used to suggest rough upper limits to the rate of this dissociation or to the rates of recombination of the atomic species into N_2 and O_2.

10. The logarithmic mean is encountered in many problems of engineering interest, and is often approximated by the arithmetic mean. Since the geometric mean is more readily obtained in rapid slide-rule calculations, it is of interest that the geometric mean is a better approximation to the logarithmic mean than is the arithmetic mean.

11. Leaky exhaust valves may contribute to an increase in the concentration of oxides of nitrogen in automobile exhausts.

12. It is proposed that the institution of "Finals Week" be abolished, and that an additional week of regular course work would be of more benefit to the students.

NOMENCLATURE

D	diffusion coefficient defined by Fick diffusion equation.
F	feed to reactor, mols per unit time.
j	friction, infinitesimal.
k	thermal conductivity.
P	pressure.
q	heat, infinitesimal.
r	rate of chemical reaction, mols per unit time per unit volume.
S	entropy.
T	temperature, absolute scale.
V	specific volume.
V_r	volume of flow reactor.
W	work, specific.
x_A	mols of component A converted per mol of feed.
μ	viscosity.
$\int$	line integral; integral along particular path.

REFERENCES

1. Lacey, W. N., and Sage, B. H., Thermodynamics of One Component Systems, Issued in mimeographed form, California Institute of Technology, 1947.

2. MacDougall, F. H., Physical Chemistry, p. 379, Macmillan, New York (1948).

3. Daniels, F., Outlines of Physical Chemistry, p. 216, John Wiley & Sons, New York (1948).

4. Lucas, H. J., and Pressman, D., Principles and Practice in Organic Chemistry, pp. 118-21, John Wiley & Sons, New York (1949).

5. Robinson, C. S., and Gilliland, E. R., Elements of Fractional Distillation, 4th ed., pp. 85, 119, 134, 396, McGraw-Hill Book Co., Inc., New York (1950).

6. Kayser, R. F., Ind. Eng. Chem., 45, 2634-6 (1953).

7. Hougen, O. A., and Watson, K. M., Chemical Process Principles, p. 854, John Wiley & Sons, New York (1947).